

University of Nottingham
UK | CHINA | MALAYSIA

The antagonistic role of rhizosphere and endophytic fungi from feral and cultivated date palms on wilt causing fungi in Oman.

Raja Al Mutasim H. Al Busaidi

Thesis submitted to The University of Nottingham

(UK) for the degree of Doctor of Philosophy

July 2024


بسم الله الرحمن الرحيم

Abstract

Date palm is one of the major crops grown in Oman. Date palm wilt, caused by the soil borne pathogen *Ceratocystis radicicola*, is a disease that is spreading rapidly. In this study, endophytic and rhizosphere fungi have been isolated from roots and rhizosphere soil of cultivated and feral date palm from different locations. Rhizosphere soil was analysed for minerals, total organic carbon (TOC) and total inorganic carbon (TIC). DNA was extracted from soil and fungal diversity was determined using Illumina MiSeq sequencing. Results showed that fungal diversity between feral and cultivated date palms was not significantly different. However, the fungal diversity was significantly different between locations; for example, Swaiq location 1 showed a unique fungal diversity. A correlation network clustering and a Principal Component Analysis (PCA) was done between Operational Taxonomic Units (OTUs) and soil minerals that showed 13 clusters with clusters 4 and 5 having highest OTUs with feral date palm. The influence of different soil parameters between feral and cultivated systems revealed no outcome on the fungal diversity.

The isolated fungi were tested for antagonistic effect on date palm pathogens *Ceratocystis radicicola* and *Fusarium solani* by dual culture. Two fungi showed an antagonistic effect with prominent inhibition zones for both date palm pathogens. The DNA was extracted from the antagonistic fungi and sequenced using ITS1 and ITS4 primers, and were identified as *Talaromyces* sp. from cultivated date palm roots and *Aspergillus terreus* from rhizosphere soil of cultivated date palm. In addition, sequencing resulted in identification of 3 new

species of *Talaromyces*. A phylogenetic tree was constructed with ITS sequences and ITS-RPB2 and revealed that the isolates are new species of *Talaromyces* Section *Trachyspermi*. This study is the first report of the potential new *Talaromyces* species. An electrolyte leakage bioassay was carried out on the culture filtrates of the antagonistic fungi where EC and pH of the pathogen was recorded. *Aspergillus terreus* caused more significant changes than *Talaromyces* sp.

SEM imaging of the inhibition zones from dual cultures with *A. terreus* and *Talaromyces* sp. with the pathogens *C. radicicola* and *F. solani*, showed the antagonistic effect, where *Talaromyces* spp. effected *C. radicicola* spores by formation of chains or a net-like structure around the spores resulting in their shrinkage. The effect of *A. terreus* was through its spores clumping on the hyphae of *C. radicicola* and the hyphae of *A. terreus* covering the hyphae of *C. radicicola* causing it to shrivel. For *F. solani*, *Talaromyces* spp. spores and hyphae bound to the hyphae of *F. solani* causing them to shrivel. In contrast, *Aspergillus terreus* resulted in wrinkled spores and distorted hyphae of *F. solani*, with evident tissue degradation.

This study showed the potential of investigating the rhizosphere and endophytic fungi of date palms especially the feral palms as an insight on the biodiversity of these micro communities. Also, new biocontrol agents could be detected and investigated on various plant pathogens, using dual culture, SEM imaging and electrolyte leakage to provide further evidence on the efficacy of these isolates.

Acknowledgements

First of all, I thank the Al Mighty God for giving me Strength and Guidance and Blessings throughout this journey.

I dedicate this study to my Father and my recently deceased Mother for their dream and encouragement and support for me to obtain my PhD degree.

I dedicate this study for my loving Husband Salahdeen and children Mazin and Melia. My gratitude for their love, support, encouragement and above all their patience during my absence in busy days has no right words to fulfill it. Thank you.

Thank you to all my extended family for their support and encouragement.

I acknowledge my supervisors, Prof. Matthew Dickinson and Prof. Abdullah Al Sadi, for their continuous support, encouragement and guidance. Their patience with my questions and emails. Thank you.

My lab technician, Ms. Waffa Al Hatali and staff from SQU: Ms. Zainb Al Bulushi, Mr. Issa Al Mahmoli and last but not least Ms. Badriya Al Shaili. You were the support network that the success of this study had relied on. Thank you.

Table of Content

	Title	Page
Chapter 1	Date Palm Wilt, Antagonistic Endophytic Fungi and Fungal Diversity.	16
1	Introduction	16
1.1	Date Palm in Oman	16
1.2	Date Palm Wilt Disease	17
1.3	*Ceratocystis* species	17
1.4	*Fusarium* species	18
1.5	Rhizosphere and endophytic fungi	22
1.6	Antagonistic rhizosphere and endophytic fungi	25
1.7	Fungal diversity of Date Palm	27
1.8	Mi Seq analysis	29
2	Study Impact and Aims	33
3	Research Objectives	34
Chapter 2	Investigation of fungal diversity through Illumina Mi Seq of rhizosphere fungi and the chemical analysis of the soil from feral and cultivated Date Palm in Oman	35
2.1	Introduction	35
2.2	Materials and Methods	40
2.2.1	Soil and root sampling from three locations	40
2.2.2	Soil chemical analysis	41
2.2.3	Extraction of Fungal DNA from Soil	49
2.2.4	Illumina MiSeq analysis	51
2.2.5	Bioinformatics	60
2.2.6	Statistical Analysis by Correlation between Operational Taxonomic Units (OTU), Soil Minerals, Cultivation Practices and Location	54
2.3	Results	55
2.3.1	Soil chemical analysis	55
2.3.2	Bioinformatics	60
2.4	Discussion	80
Chapter 3	Evaluation of antagonistic role of endophytic fungi against Date Palm pathogens: *Ceratocystis radicicola* and *Fusarium solani* via dual culture screening and identification of the eminent antagonistic fungi by morphology and molecular methods.	84
3.1	Introduction	84
3.2	Materials and Methods	90
3.2.1	Isolation and Selection of endophyte	90
3.2.2	Molecular identification of the antagonist endophytic fungi	92

3.2.3	Morphological and Molecular Analysis of Three Potential New *Talaromyces* species.	93
3.3	Results	97
3.3.1	Endophyte antagonism	97
3.3.2	Molecular identification of the antagonist endophytic fungi	109
3.3.3	Morphological and Molecular Analysis of Three Potential New *Talaromyces* species	112
3.4	Discussion	124
Chapter 4	Scanning Electron Microscopy imaging of antagonistic effect of endophytic fungi *Aspergillus terrus* and *Talaromyces* sp on *Ceratocystis radicicola* and *Fusarium solani* and Effect of culture filtrate of the antagonistic fungi to on electrolyte leakage of *Ceratocystis radicicola* and *Fusarium solani*.	129
4.1	Introduction	129
4.2	Materials and Methods	132
4.2.1	Scanning electron microscopy imaging	132
4.2.2	Culture filtrate effect of the antagonistic *Aspergillus terrus* and *Talaromyces* sp. fungi on electrolyte leakage on *Ceratocystis radicicola* and *Fusarium solani*	133
4.3	Results	134
4.3.1	Scanning Electron Microscopy imaging	134
4.3.2	Culture filtrate effect of the antagonistic *Aspergillus terrus* and *Talaromyces* sp. fungi on electrolyte leakage on *Ceratocystis radicicola* and *Fusarium solani*	143
4.4	Discussion	147
Chapter 5	General Discussion	151
References		158
Annex 1	Sample collection and labelling per Area	166
Annex 2	Soil Chemical Analysis Raw Data (ND is for Not Detected)	167
Annex 3	Extraction of DNA of Soil Borne Fungi Directly from Soil (Modified from Volossiouk et al. (1995))	170
Annex 4	Microbiome Analysis Report	171
Annex5	Maximum Likelihood tutorial, for Maximum Parsimony and Bayesian Inference phylogeny	173
Annex 6	Colony Diameter of *Talaromyces* spp. with different media Average colony dimeter per plate and Total average colony diameter for all replicates	183
Annex 7	Electrolyte leakage (mV) and pH measurement	186

List of Figures

	Title	Page
Figure 1	Map of Oman showing governorates distribution.	20
Figure 2	Diseased Date Palm showing yellowing of fronds and weakened growth. A) First symptoms B) Symptoms just before death C) Death of Date Palm, image taken before uprooting.	21
Figure 3	The inducing factors of the rhizosphere microbial communites and models how they were selected from soil by the root exudates and their rhizosphere competence. Berg et al. (2009).	24
Figure 4	Feral Date Palm growing in the wadi (vally) in State of Samail. First location for root and rhizosphere soil sampling. The uncut offshoots under the stem and dry older fronds not pruned are evident.	43
Figure 5	Feral Date Palm growing in the wadi (vally) in State of Samail. Third location for root and rhizosphere soil sampling .Evidence of over growth, un atended date palms with uncut offshoots under the stem and dry older fronds not pruned.	44
Figure 6	Cultivated Date Palm growing in a farm in State of Samail. Second location for root and rhizosphere soil sampling.Typical traditional farming with intercropping and flood irrigation.Absence of offshoots under the date palm and fronds maintained shows proper cultivation practices.	45
Figure 7	Cultivated Date Palm growing in a farm in State of Samail. Fourth location for root and rhizosphere soil sampling. Typical traditional farming with intercropping and flood irrigation.	46
Figure 8	Cultivated Date Palm growing in a farm in State of Swaiq. First location for root and rhizosphere soil sampling.Modern cultivation with no intercropping, spacing between palm and double basin for irrigation with drip system.	47
Figure 9	Cultivated Date Palm growing in a farm in State of Swaiq. Second location for root and rhizosphere soil sampling. Modern cultivation with no intercropping, spacing between date palms and double basin for irrigation with drip system	48
Figure 10	Rarefraction plot for Species Richness (rare) of Fungal community between all groups (locations and cultivation type). Sub sampling from 500 – 20000 reads between all groups with no significant differences between cultivation type and location in fungal diversity.	61
Figure 11	Shannon diversity of fungal community between all groups (locations and cultivation type). No significant differences in the range between 2.5 to 3.9 for Group 1 and Group 8 respectively in fungal diversity levels	62
Figure 12	Richness Estimate (Chao 1) of fungal community between all groups (locations and cultivation type). The diversity level ranging between a minimum of 418 for Group 1 to a maximum of 497 for Group 4. With no significant differences in fungal diversity levels regardless of cultivation type or location.	63

Figure 13	Relative abundance of fungal community by Phylum level between locations and cultivation types. The three most common Phyla between all the groups were: Ascomycota, Basidiomycota and an unclassified phylum. No significant differences between all groups regardless of the location or cultivation type. The highest Ascomycota was detected in Group 1, whereas the lowest was recorded for Group 5.	66
Figure 14	Relative abundance of fungal community by Class level between all locations and cultivation types. The common classes were: Sordariomycetes, Agaricomycetes and Dothideomycetes respectively. With no significant differences between all groups regardless of location or cultivation type. The highest Sordariomycetes detected in Group 1 and the lowest was recorded for Group 5.	67
Figure 15	Relative abundance of fungal community by Genus level between all locations and cultivation types. The common Genera were: Agaricales, Hypocreales and Cortinariaceae respectively. With no significant differences between cultivation types. As for locations shows no difference between them. However, Swaiq (Group 1) shows a significant difference from all the other locations with common Genus being: Sarocladium, Agaricales and Cladosporium respectively	68
Figure 16	Relative abundance of fungal community by Species level between all locations and cultivation types. The common Species are: Agaricales and Hypocerealis then second comes Cortinariaceae followed by Sordariomycetes and Agaricomycetes. No significant differences between cultivation types. As for locations no significant difference between them. However, Swaiq (Group 1) shows a significant difference from all the other locations having the most common Species : Sarocladium, Hypocerealis and Agaricales respectively.	69
Figure 17	Bray Curtis of fungal community between all groups (locations and cultivation type). The fungal diversity is affected by location shown by the clustering of Hoqian locations (Group 3 and 4) and Samail (Group 5-8) with one location from Swaiq (Group 2).Whereas the second location from Swaiq (Group 1) is clustered alone and away from all the other locations. However, fungal diversity is not affected by cultivation types.	71
Figure 18	Principal Coordinate Analysis Un Weighted UniFrac of fungal community between all groups (locations and cultivation type) shows clustering between all groups indicating that the fungal diversity is not affected by cultivation type or location.	72
Figure 19	Principal Coordinate Analysis Weighted UniFrac of fungal community between all groups (locations and cultivation type). Here the fungal diversity is affected by location with evidence of simple separation in clustering. Hoqain (Group 3 and 4) and Samail (Group 5, 7 and 8) are clustered separately, whereas Swaiq (Group1 and 2) is clustered with one location in Samail (Group 6). Also fungal diversity is not affected by cultivation types.	73
Figure 20	Correlation Network Clustering of Operation Taxonomic Units (OTU) at Species between all groups (location and cultivation	76

	type). Markov Clustering (MCL) =1.01. Figure generated using Graphia software ($r \leq 0.8$).	
Figure 21	Operation Taxonomic Units (OTU) from Cluster 4 of the Correlation Network Clustering at Species level between all groups (location and cultivation type).Where highest OTU of cluster 5 are the samples from Feral location of Group 4-5 compared to Group 1-3 and Group 7 and8.	77
Figure 22	Operation Taxonomic Units (OTU) from Cluster 5 of the Correlation Network Clustering at Species level between all groups (location and cultivation type).Where highest OTU of cluster 5 are the samples from Feral location of Group 5 and 6 compared to the other Groups.	78
Figure 23	Multivariate Principal Analysis (PCA) between Operational Taxonomic Units (OTU) MCL for all groups and total soil minerals. Markov Clustering (MCL) =1.01 Key Cluster 13 is not indicated. Figure generated using Graphia software.	79
Figure 24	Dual culture. A: *Ceratocystis radicicola* (left) with a mix of *Trichderma harzanium* and *T. lixii* (right) antagonism effect is not clear, *T. harzanium* and *T. lixii* are growing over *C. radicicola* which seem restricted. B: *C. radicicola* pure culture C: Mixed culture of *T. harzanium* and *T. lixii.*	99
Figure 25	Dual Culture. A: *Trichderma harzanium* and *T.lixii* pure culture B: *Fusarium solani* pure culture. C,D and E: Dual culture of mix of *T. harzanium* and *T. lixii* (left) with *F. solani* (right) showing clear over growth of *Trichoderma* on *F. solani*, where its growth remains without disruption with clear red pigmentation on the perimeters of *F. solani*.	100
Figure 26	Dual culture. A: *Penicillium griseofulvum* pure culture with clear dispersal of the colonies B: *P. griseofulvum* (on the left) with *Ceratocystis radicicola* (on the right) showing good antagonism effect and inhibition zone C: Dual culture of Penicillium griseofulvum (on the left) with *C. radicicola* (on the right) showing restriced growth of *C.radicicola* without a clear inhibition zone D: *C. radicicola* pure culture.	101
Figure 27	Dual Culture. A: *Penicillium griseofulvum* pure culture B: *Fusarium solani* pure culture C: *P.griseofulvum* (left) with *F. solani* (right) showing antagonism effect and clear and wide inhibition zone and red\ orange pigmentation only on the far edges of the inhibition zone. D: *P. griseofulvum* (left) with *F. solani* (right) showing antagonism effect and smaller inhibition zone and red\ orange pigmentation spread in most of the inhibition zone E: *P. griseofulvum* (left) with *F. solani* (right) showing restriced growth with no clear or minmal inhibition zone, but higher red/ orange pigmentation	102
Figure 28	Dual culture. A: *Aspergillus terreus* pure culture B: *Fusarium solani* . C, D and E: *A. terreus* (left) with *F. solani* (right) showing good antagonism effect and inhibition zone with a deep yellow pigmentation.	103
Figure 29	Dual culture. A: *Ceratocystis radicicola* (left) with *Aspergillus terreus* (right) showing good antagonism effect and inhibition zone Due to the fast growth of the *C. radicicola* the growth of *A.terreus*	104

	looks restricted and the inhibition zone was narrow 30 days after inoculation. B: *C. radicicola* pure culture C: *A. terreus* pure culture	
Figure 30	A pure isolate of *Talaromyces* species from the initial direct culture from date palm roots. It was isolated from Samil location 1 of cultivated date palm (sample S15). Evident uniform growth and production of red pigment (azaphilone polyketide).	105
Figure 31	Dual culture. A: *Talaromyces* species pure culture B: *Ceratocystis radicicola* pure culture. C and D: *C. radicicola* (left) with mixed *Talaromyces* species a and b (right) showing antagonism effect and clear inhibition zone with red pigmentation from *Talaromyces* . Due to the fast growth of the *C. radicicola* the growth of *Talaromyces* was dispersed but the inhibition zone was clear 30 days after inoculation. E: *C. radicicola* (left) with mixed *Talaromyces* species (right) shows the *Talaromyces* species b with very dispersed and quick growth, inhibition zone not clear and patches of mild red pigmentation.	106
Figure 32	Dual culture. A: Pure culture of mixed *Talaromyces* species with 3 colonies in the center and dispersed smaller colonies of *Talaromyces* b on the edges of the petri dish B: *Fusarium solani* pure culture. C,D,and E: *F. solani* (left) with mixed *Talaromyces* species (right) showing good antagonism effect and inhibition zone with strong red pigmentation	107
Figure 33	Cultures of C11a isolates (top plate anterior , lower plate reverse) from left to right respectively are YESA,MEA, CDA,CMA medium incubated at 25°C for 7 days. YESA : Colony average diameter 180 mm, white mycelia, velvety texture, dense spores, conidia en masse dark and dull green slightly blueish grey on the edges, red soluble pigment, color on reverse dark red. MEA: Colony average diameter 178 mm, white mycelia, velvety texture, dense spores, conidia en masse dark and dull green, yellowish exudate, red soluble pigment, moderate color on reverse dark red. CDA: Colony average diameter 148 mm, white to beige mycelia, sparse spores, yellowish red soluble pigment, color on reverse orange red at the center of colony. CMA: Colony average diameter 180 mm, white mycelia, velvety texture, dense spores, conidia en masse dark and dull green, red soluble pigment, color on reverse dark red.	114
Figure 34	Cultures of C11b isolates (top plate anterior , lower plate reverse) from left to right respectively are YESA,MEA, CDA,CMA medium incubated at 25°C for 7 days. YESA: Colony average diameter 193 mm, white mycelia, velvety texture, dense spores, conidia en masse dark and dull green slightly blueish grey on the edges, red soluble pigment, color on reverse dark red. MEA: Colony average diameter 189 mm, white mycelia, velvety texture, dense spores, conidia en masse dark and dull green, yellowish exudate, red soluble pigment, moderate color on reverse dark red. CDA : Colony average diameter 91 mm, white to beige mycelia, sparse dark and dull green spores, yellowish orange soluble pigment, color on reverse orange red and red at the center of colony.CMA : Colony average diameter 120 mm, few white mycelia, velvety texture, moderate dense spores, conidia en masse dark and dull green, red soluble pigment, color on reverse dark red.	115

Figure 35	Cultures of C12b isolates (top plate anterior , lower plate reverse) from left to right respectively are YESA,MEA, CDA,CMA medium incubated at 25°C for 7 days YESA: Colony average diameter 213 mm, white mycelia, velvety texture, dense spores, conidia en masse dark and dull green, red soluble pigment, color on reverse dark red colony has white interior edges. MEA: Colony average diameter 188 mm, white mycelia, velvety texture, dense spores, conidia en masse dark and dull green, yellow and reddish exudate, red soluble pigment, color on reverse dark red, some colonies with no pigment. CDA 25°C dark 7 days: Colony average diameter 99 mm, white to beige mycelia, sparse spores, yellowish red soluble pigment, color on reverse orange red at the center of the colony. CMA: Colony average diameter 133 mm, white mycelia, velvety texture, dense spores, conidia en masse dark and dull green at center only, red soluble pigment, color on reverse dark red, some colonies without pigment.	116
Figure 36	Cultures of C11a isolates anterior (No reverse) from left to right respectively are C11a , C12a and C12b in OA medium incubated at 25°C for 7 days. Isolate C11a: Colony average diameter 170 mm, white mycelia, velvety texture, dense spores, conidia en masse dark and dull green, soluble pigment absent, no observation on reverse due to dense media. Isolate C11b: Colony average diameter 193 mm, white mycelia, velvety texture, dense spores, conidia en masse dark and dull green, soluble pigment absent, no observation on reverse due to dense media. Isolate C12b: Colony average diameter 192 mm, white mycelia, velvety texture, dense spores, conidia en masse dark and dull green, soluble pigment absent, no observation on reverse due to dense media.	117
Figure 37	Cultures of isolates (top plate anterior , lower plate reverse) from left to right respectively are C11a , C11b and C12b in MEA medium incubated at 37°C for 7 days. Isolate C11ab: Colony average diameter 153 mm, beige mycelia with light and dark red at the center of colony, sparse spores, no soluble pigment, color on reverse similar to top. Isolate C11b: Colony average diameter 178 mm, Colony average diameter 153 mm, beige mycelia with light and dark red at the center of colony, sparse spores, no soluble pigment, color on reverse similar to top. Isolate C12b: Colony average diameter 230 mm, Colony average diameter 153 mm, beige mycelia with light and dark red at the center of colony, sparse spores, no soluble pigment, color on reverse similar to top.	118
Figure 38	Maximum Likelihood tree from ITS5 sequence of *Talaromyces* isolate C11b, C12a and C12b reconstructed using RaxML. *Talaromyces* isolate C11b, C12a and C12b where potential new recognized species are shown in pink box in *Talaromyces* sect *Trachyspermi* with bootstrap value 100% in the nodes. Bar =0.08 substitutions per nucleotide position.	120

Figure 39	Imaging of positive PCR product of potential new species of *Talaromyces* species Samples1-6 amplified with large subunit of nuclear ribosomal DNA (28S) primer LROR/ LR5. 1.C11a 2.C11a* replicate 3.C11b 4. C11b* replicate 5. C12b 6.C12b* replicate 7. Negative. Sample 8-6 amplified with translation elongation factor 1-alpha (TEF-1a) primer EF1-983F/ EF1-1567R.8.C11a 9.C11a* replicate 10.C11b 11. C11b* replicate 12. C12b 13.C12b* replicate (absence of band may be due to pipetting error) 14. Negative. Sample 15-20 amplified with DNA-dependent RNA polymerase II subunit 2 (RPB2) primer bRPB2-6F/ bRPB2-7R. 15.C11a 16.C11a* replicate 17.C11b 18. C11b* replicate 19. C12b 20.C12b* replicate. 21. Negative L.0.1-10 kb 2 log ladder.	121
Figure 40	Imaging of positive PCR product of potential new species of *Talaromyces* species C12a. Samples1and2 amplified with large subunit of nuclear ribosomal DNA (28S) primer LROR/ LR5. 1.C12a 2.C12a* replicate 7a Negative. Sample 3and4 amplified with translation elongation factor 1-alpha (TEF-1a) primer EF1-983F/ EF1-1567R. 3.C12a 4. C112a* replicate 7b. Negative. Sample 5and6 amplified with DNA-dependent RNA polymerase II subunit 2 (RPB2) primer bRPB2-6F/ bRPB2-7R.5. C12a 6.C12a* replicate. 8.C11a 9.C11a* replicate 7c Negative L. 0.1-10 kb 2 log ladder.	122
Figure 41	Maximum Likelihood tree Comparing ITS-RPB2_36 all sections of *Talaromyces* isolate C11b, C12b reconstructed using RaxML. Talaromyces isolate C11b and C12b where potential new species depicted in the tan box with bootstrap value 100% in the nodes in *Talaromyces* sect *Trachyspermi*. Isolate C11a was recovered with a long branch, thus was excluded in the final analysis. Bar =0.07 substitutions per nucleotide position	123
Figure 42	*Ceratocystis radicicola* spore and hyphae from date palm wilt. SEM image from AlNaemi *et al* 2016	136
Figure 43	*Fusarium solani* spore hyphae and spore. SEM image from Hashem *et al* 2016	137
Figure 44	Scanning Electron Microscopy image of effect of antagonistic endophyte *Talaromyces* spp on *Ceratocystis* radicicola. A: *Talaromyces* spp chain of spores shown by arrow.Red circle shows the shrinkage of *C. radicicola* spore B: *Talaromyces* spp spores on *C. radicicola* spores. Red circle shows *C. radicicola* spore with partial shrinkage.	138
Figure 45	Scanning Electron Microscopy image of effect of antagonistic endophyte of *Aspergillus terreus* on *Ceratocystis radicicola* A: *Ceratocystis radicicola* hyphae shriveled as seen in red circle compared to smoothness of hyphae of *Aspergillus terreus* indicated by red B: Hypha of *Ceratocystis radicicola* shriveled as seen inside red circle and Aspergillus terreus spores are aatached to it.	139
Figure 46	Scanning Electron Microscopy image of antagonistic endophyte *Talaromyces* spp., effect on *Fusarium solani*. A: *Fusarium solani* hyphae shrivelled B: *Talaromyces* spp spores attached on shriveled hyphae of *Fusarium solani* as shown inside red circle.	140

Figure 47	Scanning Electron Microscopy image of effect of antagonistic endophyte *Aspergillus terreus* on *Fusarium solani*. A: Red circle shows *Fusarium solani* wrinkled , The red arrow points at the spores of *Aspergillus terreus* B: *Fusarium* solani shrivelled hyphae.	141
Figure 48	Close up image in the red circle showing the degeneration of the of *Fusarium solani* hypha by the spores of *Aspergillus terreus*. The red arrows point at the degenerated section and at the smoother section right below it.	142

List of Tables

	Table Title	Page
Table 1	Identified Fungal OTUs and their abundance from control and salt treated date palm roots based on ITS DNA sequences. Yaish et al. (2016).	29
Table 2	Sample collection and labelling per Area.	50
Table 3	PCR Reactions for Soil DNA Samples.	50
Table 4	Mean and STDEV of Total Nitrogen, Sodium, Phosphorus, Potassium and Protein from Soil per Location.	56
Table 5	Mean and STDEV of Total Magnesium, Calcium, Total Organic Carbon (TOC) and Total Inorganic Carbon (TIC) from Soil per Location.	58
Table 6	Mean and STDEV of Total Zinc, Copper Aluminum, Iron, Nickel and Chromium from Soil per Location.	59
Table 7	Media and incubation conditions used for identification of 3 *Talaromyces* spp.	95
Table 8	Media used for morphological identification of 3 Talaromyces spp	95
Table 9	PCR reaction used for each primer and its sequence.	97
Table 10	Average Growth Measurement (cm) from day 1-4 and Inhibition percentage of dual culture of *Ceratocystis radicicola* and *Fusarium solani* with *Talaromyces* species and *Aspergillus terreus*. Average Growth Measurement (cm) of each control.	108
Table 11	Sequence results, best Gene bank matches, strain, identity percentage, accession, variation /BP for isolates.	110
Table 12	Average colony diameter per media at 25°C dark 7 days for identification of 3 *Talaromyces* isolates.	113
Table 13	Electrolyte leakage (mV) and pH measurement for *Ceratocystis radicicola* and*Fusarium solani* after application of *Talaromyces* spp. culture filtrate CF at 0, 2 and 24 hours.	144
Table 14	Electrolyte leakage (mV) and pH measurement for *Ceratocystis radicicola* and *Fusarium solani* after application of *Aspergillus terreus* culture filtrate CF at 0, 1 and 24 hours.	1146

Chapter 1

Date palm wilt, antagonistic endophytic fungi and fungal diversity.

1. Introduction

1.1 Date palm in Oman

Oman is in the south-eastern part of the Arabian Peninsula (Fig. 1). Date palms (*Phoenix dactiylefra* L.), bananas, mango and citrus are the four most important fruit crops in the country in terms of production, with date palm being the most important crop in Oman and the Arabian Peninsula. Date palms occupy more than 80% of the area devoted for fruit production and approximately 50% of the agricultural land in Oman. The total number of cultivated date palms has reached over 7.5 million in farms and 900,000 around streets and urban areas (Oman Agricultural Census, 2012/2013). The estimated number of cultivars is around 325 types of which 32 are currently being DNA finger-printed (MAF Report, 2015). Approximately 200,000 tissue culture offshoots were distributed to farmers and to the Million Date Palm Plantation Project between 2011 and 2015. The total national production for 2020 was 369,000 tonnes (FAO, 2022), making Oman among the top 10 countries in date production in the world. Date palms are mainly grown in the northern part of the country (Fig. 1), with highest production in Al Batinah South governate mainly due to the wilayat (province) of Rustaq with an estimated date production of 34.53 thousand tonnes. This is followed by the governates of Dhakhiliya, Al Batinah North, South and North Sharqiya.

1.2 Date palm wilt disease

Several important diseases can affect date palms. In Oman, date palm wilt is increasingly becoming the major constraint for date palm cultivation (Al-Raisi *et al.*, 2011; Al-Sadi *et al.*, 2012b). Affected date palms show weakened growth, yellowing of older fronds and then death of the highly affected palms (Fig. 2). Al-Raisi *et al*. (2011) had first reported that *Ceratocystis radicicola* is associated with date palm wilt diseases in Oman. However, a limited-scale study in 2012 reported association of other pathogens with date palm wilt in some wilayats (provinces) in Oman (Al-Sadi *et al.*, 2012b) along with *Ceratocystis* spp. These additional pathogens were *Fusarium* spp., *Lasiodiplodia* spp. with some other pathogens. Furthermore, during a follow up survey by Al Sadi in 2014, isolations revealed association of *Fusarium oxysporum* and *F. solani* with several date palms developing wilt symptoms (unpublished).

1.3 *Ceratocystis* species

Ceratocystis was initially identified in 1890 with species such as *C. fimbriata* as a potato pathogen (de Beer *et al.*, 2014). Its phylum is Ascomycota and Sordariomycetes (Carbera *et al.*, 2016). According to Carbera *et al*. (2016) *Ceratocystis* is homothallic; i.e., it has developed a system by which it shifts between sexual (self-fertile) and asexual (self-sterile) reproduction status. *Ceratocystis* spp. attack the vascular system either through a wound or through root anastomoses between neighboring trees (Carbera *et al*. (2016). After colonizing the sapwood followed by crown/branch dieback then the host is eventually killed. Leaf

symptoms include: leaf drop, poor development, chlorosis or other coloration and giving wilt appearance to the crown. Xylem discoloration is found either below a dying branch, main stem or if the infection is from the roots then at the base of the tree. Discoloration is a mixture of host response to infection and the pigmentation of the hyphae and spores of *Ceratocystis* spp. (Harrington., 2013). Host induced reaction by producing gels, tyloses and gums as occluding structures to restrict colonization of the vascular tissue, that leads to obstruction of water and nutrient. As a result the branch wilts and dies (Carbera *et al*., 2016).

1.4 *Fusarium* species

Fusarium spp. is considered a universal and diverse fungus. This genus includes non-pathogenic and pathogenic species that cause plant and human diseases (Roncero *et al.,* 2003; Hafizi *et al.,* 2013). Its multiple species target a wide range of crops plus it has the ability to develop into races that infect specific crops (Roncero *et al.,* 2003). As a soil borne pathogen, *Fusarium* can persevere and survive as propagules in the soil for decades until a suitable host is available, as is the case with *F. oxysporum* (Roncero *et al.,* 2003). An example is *F. oxysporum* f.sp. *albedinis* which induces Al Bayoud disease of date palm. It is amongst the most destructive diseases of date palm and has wiped out more than 12 million date palms in Morocco and Algeria. Differentiating *F. oxysporum* f.sp. *albedinis* from other *formae speciales* through morphological criteria is challenging due to variability in colony morphology within *F. oxysporum* f.sp. *albedinis* itself (Freeman *et al.,* 2000). According to Freeman *et al.* (2000), using molecular techniques and specific

primers for *F. oxysporum* f.sp. *albedinis* is a more efficient and reliable way to detect or differentiate between different *F. oxysporum formae speciales* isolates. Currently Al Bayoud disease has not been reported in Oman, nor *F. solani* which is associated with yellow disease of date palm in Iran (Mansoori and Kord, 2006). However, another destructive disease was reported in Oman in 2011 (AFDF, 2017) known as Panama Disease of banana caused by *F. oxysporum* f.sp. *cubense*, in which race 4 (TR4) was confirmed. This race is considered the most aggressive race (Ploetz, 2006; Ploetz *et al.,* 2015). This indicates that Oman has many factors that allow the establishment of *F. oxysporum formae speciales* pathogens. For example, a recent study showed the presence of *F. oxysporum* f.sp. *vasinfectum* as the pathogen for corm rot of Saffron (*Crocus sativus* L) (unpublished data).

Fusarium solani is also considered a pathogen for various crops. In a follow up survey in 2014 (Al-Sadi *et al.,* 2014), results showed that *Fusarium solani* was the most frequently isolated pathogen from roots of acid lime and bark and roots of sweet lime, followed by two species of *Lasiodiplodia*. The pathogenicity tests generated dieback and death of both acid lime and sweet lime. This was also verified the following year, where isolation from date palm yielded 30 *F. solani* isolates (Al-Sadi *et al.,* 2015). In Iraq, an extensive survey was carried out after reports of yellowing, drying then death of date palms (Alyasiri *et al.,* 2016). Results showed that the most frequently isolated fungus was *F. solani,* which was further verified by pathogenicity tests that gave the same symptoms of yellowing, wilt then death after 2 months.

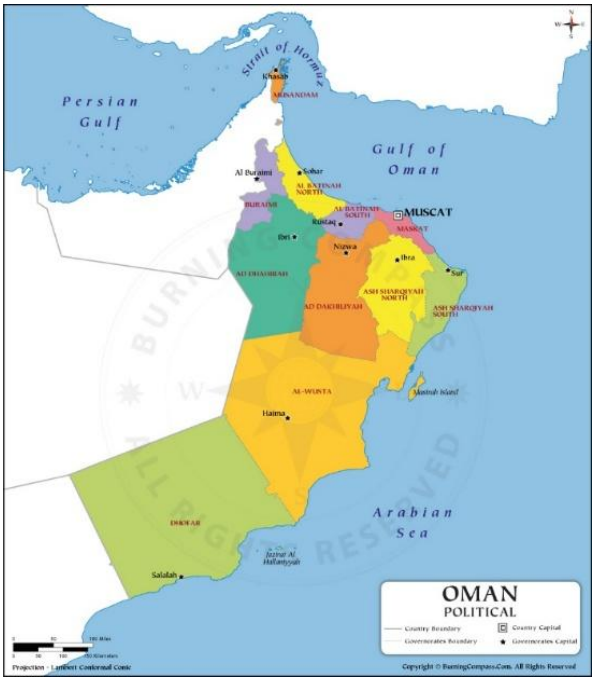


Figure 1: Map of Oman showing governerates distribution.

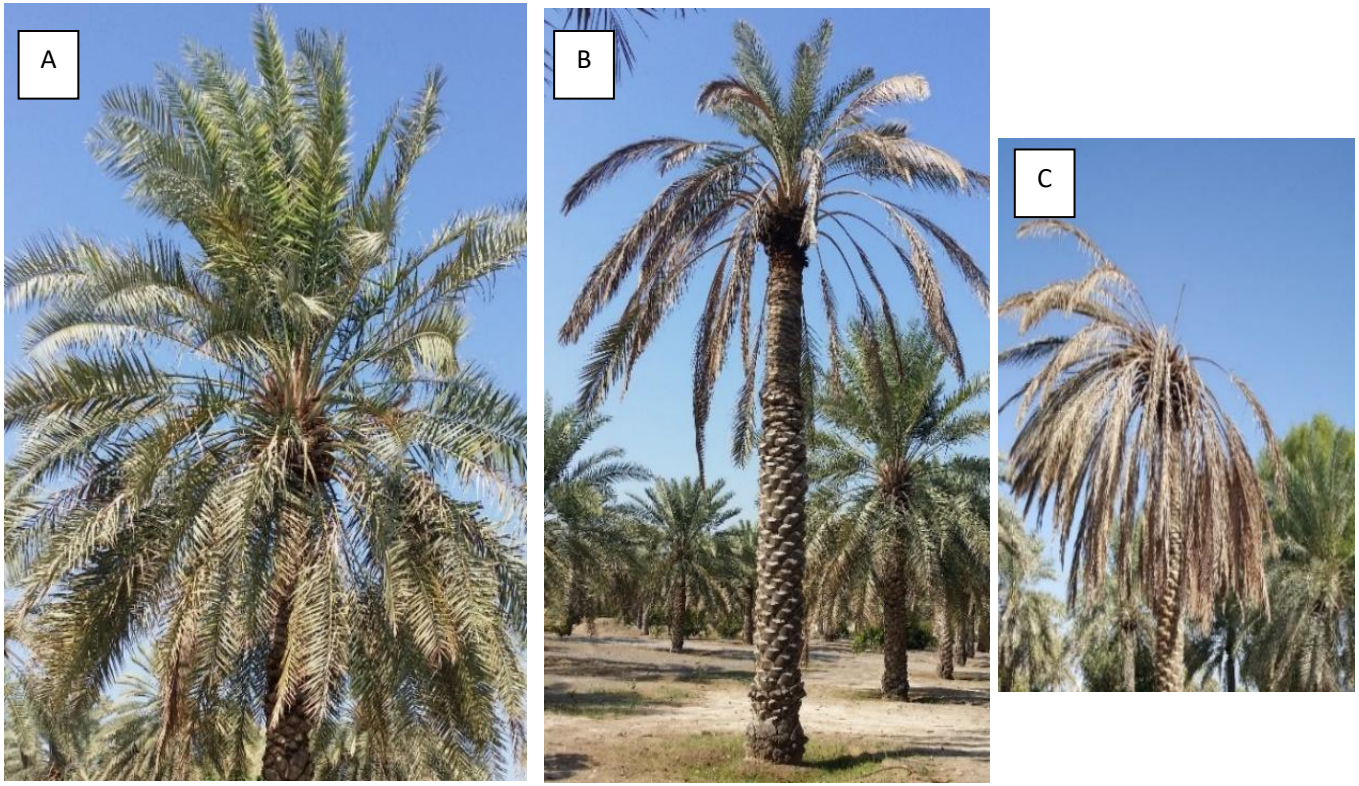


Figure 2: Diseased date palm showing yellowing of fronds and weakened growth. A) First symptoms B) Symptoms just before death C) Death of date palm, image taken before uprooting.

1.5 Rhizosphere and endophytic fungi

The term rhizosphere was first introduced in 1904 (Berg *et al.,* 2009). It is used to describe the soil zone around the plant root system that influences the chemistry of the soil through root exudates and thus the microflora activity and biomass. These microorganisms affect the plant health, nutrition and quality. Plant-microorganism interactions, whether in forest or agricultural systems, have an influential effect on retaining carbon from the air (carbon sequestration), several operations in the ecosystem and in nutrient cycles. The figure below (Fig. 3) illustrates the factors that influence the rhizosphere microbial flora and how they can be selected by root exudates and rhizosphere competence (Berg *et al.,* 2009). The influence on the microbial rhizosphere community is affected by two main factors: environmental, with biotic and abiotic components, and the interactions between the plant and microorganism. Biotic factors are determined by plant species, their developmental stage and overall health, along with human activity and animal grazers. Abiotic factors include soil quality, as in type and structure, application of pesticides or any other treatments to the soil, and finally geography and climate. The effect of the soil microbial communities on the rhizosphere microbial communities is determined by the root exudates and competence for colonization and growth, recognition, adherence and finally chemotoxins. Positive interactions include biocontrol agents, phytohormones, micronutrient availability and stress tolerance, whereas negative interactions are pathogenesis.

Plant species and cultivars have their impact on the specificity of the microbial populations. This allows for a variability and complexity in research tools. Not only

have the above-mentioned factors impacted microbial flora, but also soil characteristics and sampling methods: soil collected from the root surface as rhizosphere or the differentiated micro environment from soil attached to roots as rhizoplane are affected by soil type and the effect of moisture determining adhering amounts. Since root exudates differ at different growth stages, time of sampling contributes as another level of complexity (Berg *et al.,* 2009).

Endophytic fungi is a term used to describe fungi that colonize healthy plants without causing any symptoms (Stone *et al.,* 2004). This virtually covers all plant – fungal symbiotic relationships including mutualism, parasitism and commensalism. The main distinct feature that distinguishes an endophytic fungus is its ability to discreetly temporarily reduce its activity (i.e., growth and colonization) for an extended duration up until the host reaches a certain physical / maturation stage. Then their function is evident whether it's as a mutualistic fungus, a latent pathogen or as a saprobe associated closely with the plant but not interdependent of it. As Stone *et al*. (2004) state, the phrase "internal mycobiota" is specific to the host, plant part and tissue, but the microbe can also be present in the rhizosphere, especially for the endophytic fungi found internally in the root system.

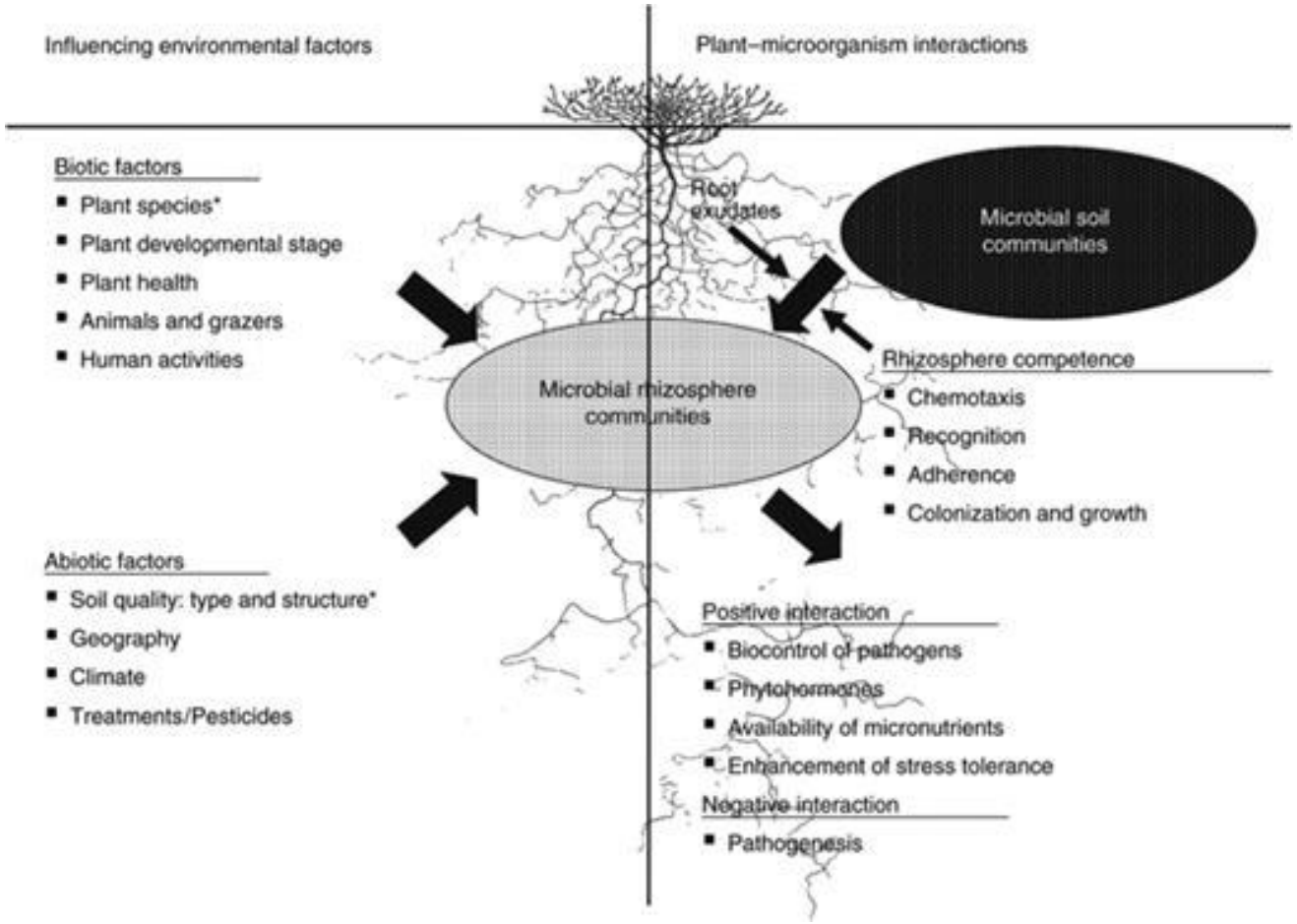


Figure 3: The inducing factors of the rhizosphere microbial communites and models for how they are selected from soil by the root exudates and their rhizosphere competence. Berg *et al.* (2009)**.**

1.6 Antagonistic rhizosphere and endophytic fungi

Antagonistic microorganisms are well studied and some are commercially produced and marketed as biological control agents against plant pathogens. These include bacteria and fungi. According to a review by Shrestha *et al.* (2014), microorganisms isolated form the rhizosphere have the potential of biological control against plant pathogens. The effect against the pathogens is through various mechanisms such as root colonization and nutrient competition, induced systemic resistance in the plant and antibiotic production. This review also stated that the most effective fungi against diseases caused by fungi and oomycetes were *Trichoderma* spp., endophytic *Fusarium* spp., and *Ganoderma* spp.

Trichoderma spp. are the most studied antagonistic fungi. Verma *et al.* (2007) noted that there are 100 phylogenetic classes of *Trichoderma*. Several studies have shown the antagonistic action of *Trichoderma* spp., for example against *Rhizoctonia solani* (Anees *et al.,* 2010; Goes *et al.,* 2002) and *Pythium aphanidermatum*, *Fusarium oxysporum* and *Alternaria alternata* (Sreeshama *et al.,* 2016). Their mode of action is through three strategies: production of metabolites, competition and mycoparasitism (Verma *et al.,* 2007). *Trichoderma* spp. are present in all soils around the world with different climatic conditions (Vinale *et al.,* 2008). This review shows the triangular interaction (plant –pathogen – *Trichoderma*) where it shows that it produces cell wall degrading enzymes in addition to antibiotics (Vinale *et al.,* 2008). In Oman, several species of *Trichoderma* have been identified as locally abundant and able to withstand high temperatures. Several studies have been carried out to study their antagonism against plant pathogens (Al Sadi *et al.,* 2015). One

study isolated two or more species from wilted date palm and focused on their effect on the wilt causing fungus *Ceratocystis* spp., which showed promising results (unpublished data MAF).

Recently, several papers have been published on other antagonistic endophytic fungi, in particular, species from *Aspergillus* and *Talaromyces*. The Ascomycota *Talaromyces* was initially identified in 1955 by Benjamin with a type species as *T. vermiculatis*. Its taxonomic tree is class Ascomycetes, order Eurotiales and family Trichocomaceae. *Penicillium,* specifically Biverticillate-Symmetrica is the prevalent anamorphic state. Bioactive compounds are generated by considerable numbers of *Talaromyces* species that range from talarodexins A and B that combat bacteria, talaroconvolutins that combat pathogenic human and plant fungi, Wortman lactones A-D, new compounds of azaphilones and luteusins A-D (Manoch and Dethoup, 2011). Halo (2019) showed the production of extracellular enzymes from *T. variabilis* that affected and suppressed growth of *Pythium aphanidermatum* in tomato and cucumber damping off. These were glucanases and cellulases that caused cellular leakage of the pathogen. In addition, siderophore compounds are produced that perhaps restrict availability of iron as a nutrient from the pathogen. Siderophores are secreted both by bacteria and fungi. Kazerooni *et al.* (2019) also demonstrated the antagonistic effect of *T. pinophilus* against *Pythium* and *Rhizoctonia* in cucumber damping off and Naraghi *et al.* (2010) showed the effect of *T. flavus* against *Verticillium* wilt of cucumber. Furthermore, *Talaromyces* was reported to affect diseases not only in annual crops as cucumber but also in perennial crops such as palms, as investigated by Goh *et al.* (2020) on Ganoderma basal stem

rot disease in oil palm. *Talaromyces* has been reported to have an antagonistic affect against a wide spectra of soil borne pathogenic fungi, including *Fusarium* spp., *Phytophthora* spp., *Alternaria* spp. and *Sclerotium* spp. (Manoch and Dethoup, 2011).

On the other hand, *Aspergillus* species have also been reported to have antagonistic affects by producing compounds against plant pathogens. Halo *et al*. (2018) investigated the effect of *A. terreus* against *P. aphanidermatum* on cucumber damping off by secreting glucanases and siderophores. Also, Al Shibli *et al*. (2019) showed the production of cellulase from *A. terreus* on the same damping off pathogen, with the difference being the source of isolate of *A. terreus.*

1.7 Fungal diversity of date palm

Fungal diversity is the determination of the variance in the fungal flora from any habitat whether it includes living or non-living substrates such as soil and water. As mentioned earlier, the fungal flora is specific to plant type among other factors. Several studies have been conducted to study the fungal diversity of date palm. In 2016, two studies were carried out on date palms in Oman. The first one by Kazerooni *et al.* (2016) investigated the fungal diversity by using 454-pyro sequencing for several crops (date palm, acid lime and cucumber) in semi oasis farm systems and organic farms systems. Rhizosphere soil was used. Operational Taxonomic Units (OTUs) are the basic unit in numerical taxonomy that indicate individuals, species or class and is used to classify groups of closely related individuals. The results showed that the highest OTUs were obtained from date palms in semi oasis farming systems, while the highest Shannon diversity estimate

was 2.50 also for date plam. The most dominant phylum was *Ascomycota* from all crops, followed by *Micrrosporidia*, *Basidiomycota* and *Chytridomycota*. As for the classes, the most common for all the crops were *Dothideomycetes*, *Microsporidetes* and *Sordariomycetes*. Finally, for the species for all the crops, *Cladosporium* and *Systenostrema* were reported. Another study later that year by Yaish *et al.* (2016) used date palm seedlings planted in date palm rhizosphere soil and irrigated with distilled water as control and treatments with saline solution increasing weekly from 50 mM to 300 mM. The study was mainly aimed to characterize the bacterial and fungal endophytes. The results showed that 24 OTUs were identified from both control and salinty treated date palm roots, as listed in Table 1. Two fungal species were significantly enriched in the roots of plants grown under treatments with normal or saline water. The fungal species were *Humicola fuscoatra,* which increased with the salt treatment and *Aspergillus niger*, which decreased with salt.

Table 1: Identified Fungal OTUs and their abundance from control and salt treated date palm roots based on ITS DNA sequences. Yaish *et al.* (2016).

Taxon name	Abundance		p-value	Taxon name	Abundance		*p*-value
	Control	NaCl			Control	NaCl	
Humicola fuscoatra	0	2043.7	0.04	*Fusarium oxysporum*	55	0	0.54
Aspergillus niger	1733.4	112	0.05	*Mortierella* sp.	26	0	0.54
Preussia sp.	15	640.4	0.12	*Ceratobasidium* sp.	143.4	1.4	0.55
Unclassified *Sordariomycetes*	40.4	0	0.17	*Rhizopycnis vagum*	10,290.4	16,236.4	0.62
Humicola sp.	0	33.7	0.19	*Fusarium* sp.	18	18.7	0.62
Fusarium solani	42	23.4	0.31	*Rhizopycnis vagum*	1	30	0.78
Meyerozyma caribbica	35.4	736.4	0.32	Unclassified *Sordariales*	37.4	0.4	0.79
Unclassified *Gnomoniaceae*	68	0	0.51	Unclassified *Pleosporales*	200	0.4	0.80
Unclassified *Sordariomycetes*	0	60.4	0.52	*Rhizopycnis vagum*	4	25.7	0.80
Unclassified *Sordariales*	73	0	0.53	*Haematonectria haematococca*	24.7	8	0.81
Aspergillus ochraceopetaliformis	154	0	0.53	*Fusarium solani*	6952	2983.7	0.92
Fusarium longipes	45.7	0	0.54	*Fusarium* sp.	331.4	124.7	0.93

1.8 Sequencing technologies

Sequencing of DNA is the procedure in which the arrangement of nucleotides in the DNA is determined. Early sequencing technologies were established by Fred Sanger and his associates in the 1970s, and became known as Sanger sequencing. This is a widespread technique that uses chain termination sequencing method (the di-deoxy chain termination technology). Limitations of this procedure are numerous and a few are mentioned here, including: 1) high cost; 2) the number of samples that can be analyzed in parallel is relatively low; 3) the fluorescent labelled DNA fragments require sieving separation media by gels/polymers; 4) larger sequences require cloning the DNA fragments into bacteria. Due to its several limitations, there has been extensive research to develop alternative methods, and the ones that hold a good potential are hybridization sequencing, parallel signature sequencing via ligation and cleavage and finally pyrosequencing.

Pyrosequencing is a technique developed in 2003 by the Royal Institute of Technology (KTH) as one of the primary alternative techniques to Sanger sequencing (Fakruddin *et al*., 2013). Lin *et al.* (2012) stated that in 2005, the 454 pyrosequencing approach was released, then bought by Roche in 2007 and this was considered the foremost and most lucrative Next Generation Sequencing (NGS) commercially available at the time. The summarized technical process can be accessed in detail in Lin *et al.* (2012) and Fakruddin *et al.* (2013). According to Fakruddin *et al*. (2013), there are several useful functions of pyrosequencing, including aiding in microbial identification and typing. In fungal detection and identification, this technology is considered an efficient tool, since the DNA fragment can be amplified by uniform primers that match the highly conserved region contained by the 18S rRNA gene. This subsequently allows amplification of a broad range of fungal species, and sequencing up to 40 bases in a sample can lead to accurate/precise identification. This is improved by repetitive sequencing of the amplicon where the data are identical for each sample. Fungal communities in the soil can be identified through an elevated complete DNA 454-Pyrosequencing, which can sequence the intricate fungal population without the requirement of initial cloning of the amplicon even at relatively low abundance (Ihrmark *et al*., 2012).

MiSeq Illumina is the sequencing by synthesis (SBS) method by Illumina (Ravi *et al.,* 2018). It has two stages for processing the amplification. First, by amplification of the genome region of interest. This is followed by the addition of the sequence adaptors of the sample with specific indices to the sample (Al Bulushi *et al.,* 2017).

According to Ravi *et al.* (2018), the main advantage that MiSeq has is its rapid library sequencing producing around 100 gigabase of data. It also has the ability to perform data analysis in one single integrated sequencing run. The MiSeq includes other features such as the on-board cluster generation and data analysis through its access to the Base Space®; which is the Illumina genomic analysis platform. This provides Insite/internet (cloud) real time-based, data uploading analysis tools and monitoring.

Illumina MiSeq sequencing technology has been successfully used to investigate and determine fungal diversity. Examples include the fungal diversity from plant parts, as is the case with the pumpkin powdery mildew (Zhang *et al.,* 2018) or from below the soil as in the rhizospheric fungal community for the Chinese medicinal plant *Panax notoginseng* (Miao *et al.,* 2016). It has also been used to determine the fluctuations in the microbial community/flora of disinfected soil (prior or during disinfection) that was infected with *Fusarim oxysporium* f.sp. *cubenese* the pathogen of Banana Panama disease (Huang *et al.*, 2015).

In a feature by Higgs (2024), titled 'The Latest Developments in Sequencing Technologies' it was stated that advances in sequencing technologies peaked between the years 2000-2010 for second or Next Generation Sequencing (NGS), which are sequencing methods using short-read technology, where Illumina is the most used technology today. Third Generation Sequencing using long-read methods, where long DNA fragments are sequenced, is also now used. This can allow coverage of repetitive DNA regions and potentially enables sequencing of a perfect genome. Initially, long-read technology lacked accuracy with some methods

reaching an error of 10%. Between 2022 and 2023, the accuracy was significantly improved which decreased the error comparable to short-read sequencing technology. The standard error for short-read technology was Q30 (1 error in 1000 bases). For major long-read technology it was Q30 for PacBio and Q28 for Oxford Nanopore. Some short-read technology achieved Q40 and beyond (1 error to 10,000 bases). The consortia T2T -Human Pangenome Reference and genome in a Bottle-project is aiming to achieve a Q100 (1 error in 10 billion bases).

For short-read sequence technology, Illumina dominates the market. According to an estimate in the last 10 years, 90% of world sequencing data has been generated on an Illumina machine. A 2022 estimate shows that this is expected to exceed the 90% level. This strength arises from the wide range offerings from high throughput instruments (Illumina NovaSeqX and PacBio Onso) to a lower cost instrument (iSeq).

1.9 Study impact and aims

Date palm is a key plant in arid and semi-arid regions, generally the Arabian Peninsula and especially in Oman. The substantial importance of date palm in Oman is linked to economics and cultural significance linked to heritage and religion. The vast number of grown cultivars and extensive climatic adaptation contributes to its importance, such that it is planted all over the adverse topography and assortment of climatic zones found in Oman. Diseases and pests are major constraints of cultivation. Date palm wilt caused by the soil borne pathogen *Ceratocystis radicicola* is one of these constraints. The wilt is spreading to all cultivation areas regardless of environmental conditions, quality of water and soil fertility or cultural practices. Use of pesticides is limited due to their lack of efficacy with this aggressive pathogen and the harmful effect on humans and the environment. Therefore, several studies have investigated the use of antagonistic microbes from the rhizosphere of the local herbs, plants and agricultural crops as an alternative control strategy (Halo *et al.*, 2018; Karunasinghe *et al.*, 2020). Since this microbiota are adapted to the climate and several parameters such as soil and temperature, they have a higher potential of success to combat pathogens or strengthen the plants resistance. In Oman, no previous studies have included feral date palms, which is a promising new domain of exploration. Tapping into this area for rhizosphere studies and comparisons to cultivated palms could lead to interesting and important findings.

The major aim of this doctoral study is to investigate the fungal diversity under the impact of different date palm growth conditions in different geographical locations.

The second aim is to identify and investigate fungi from the date palms rhizosphere and roots potential as antagonistic fungi against date palm pathogens: *Ceratocystis radicicola* and *Fusarium solani*. It is expected to give insight on any correlations or differences between feral and farming systems in view of fungal diversity and soil properties. Discovery of potential beneficial fungal antagonists will have positive outcomes and is research worth developing for date palm wilt management.

1.10 Research objectives

The main objectives of this study are as follows:

i. Characterize fungi associated with feral and cultivated date palms in Oman using culture-based methods as well as next generation sequencing.

ii. Compare the fungal diversity from roots and rhizosphere of date palms that grow as feral versus cultivated date palms grown in farms.

iii. Quantify the different types of fungal species/antagonists in date palms and the effect of farming systems on fungal diversity (increase or decrease the proportion of beneficial fungi).

iv. Analyze the soil parameters between feral and farming systems and their role in affecting the fungal diversity.

v. Identify the role of antagonistic fungi in the rhizosphere on date wilt causing fungi.

Chapter 2

Investigation of fungal diversity through Illumina MiSeq of rhizosphere fungi and the chemical analysis of the soil from feral and cultivated date palm in Oman

2.1 Introduction

Date palm has been grown in several arid regions, mainly in West Asia and North Africa, since ancient times (Yahyai *et al.,* 2015). In Oman, date palms are the most important cultivated agricultural crop, considering the volume of production. Other important crops include bananas, mangoes, and citrus. Cultural methods used for date palm cultivation in most governorates still follow the traditional methods, which include the use of organic manure, intercropping and flood irrigation. Some commercial farms have opted for bubbler irrigation soil fertilization with commercial fertilizers (Yahyai *et al.,* 2015). Some date palms are 'unaccountable' given that they grow in valleys or in high altitudes in the mountains or anywhere as long as there is a source of water. These date palms grow from fruit/seeds washed down from floods after heavy rain or thrown by campers to the animals. In addition, they may have been unattended date palms that originated from cultivated ones with no evidence of induced pollination or fertilization and the presence of uncut offshoots along the stem or at the base. Gros Ballthazard *et al.* (2016) termed these date palms as feral. Both studies of Gros Ballthazard *et al.* (2016 and 2017) were the only investigations carried out to identify wild from feral date palms using seed samples collected from 30 countries, in which some samples from Oman were identified as wild.

The soil around the root system contains abundant microorganisms ranging from nematodes, protozoa and algae to fungi, bacteria and viruses. The type, abundance, and activity of the microorganisms are determined in part by the exudates produced by the roots. Regardless of the system (forest, agricultural systems etc.) the plant-microorganism interaction has an influential effect on several operations in the ecosystem and nutrient cycles such as carbon sequestration (i.e. retaining carbon from the air).

In this study, fungal diversity of date palms in cultivated and feral systems has been investigated. There are limited previous studies in this field, such as by Al-Sadi *et al.* (2012b; 2013), Kazeeroni *et al.* (2016) and Al Bulushi *et al.* (2017). These studies investigated cultivated date palms, stored dates and other crops. Another study by Yaish *et al.* (2016) investigated the effect of salinity on endophytic microbiomes on date palms grown under controlled environments. A study in Tunisia has also investigated the fungal diversity in the internal tissue of leaves and roots (Ben Chobba *et al.,* 2013). No studies have been conducted to investigate the fungal diversity of the rhizosphere of feral date palms. Zhang *et al*. (2021) stressed that any agricultural practices, whether it's the use of chemical fertilizer or pesticide, will transform and change the plant biome composition and aid in selection of antimicrobial resistant bacteria.

Several methods have been used for estimating fungal diversity. Although culture-based techniques have been common in the past, they are limited by their ability to detect only non-obligate fungi. According to Ravi (2020), MiSeq is one of the new next-generation sequencing technologies (NGST) that was released in 2011. This

technique, along with other NGST, has helped elucidate fungal and bacterial diversities from different plant species and ecosystems, due to its ability to detect slow growing and obligate microorganisms. Zhang *et al*. (2021) added that the advances in high throughput sequencing technologies with the reduced costs allows us to understand and value the enormity and diversity of soil microorganisms. This in turn will lead to a better understanding of the dynamic interactions between the environment-plant-microbe axis that help promote plant growth under certain conditions by precision-application of these plant microbiomes. There are limitations to these sequencing technologies in conveying the correct taxonomy of the samples. This is due to obstacles of assigning species classification, since the technology utilises short reads only. Currently there are improvements being made in long read technology, but these were not available for use in the present study.

According to Praveen *et al.* (2009), soil nutrient status in arid regions will generally have low organic matter and humus or it's retrieved in a non-eroded mineral form. Low silt and clay content results in minimum nutrient retention and absorption. Coarse soil texture will have organic matter ranging between 0.05 and 2%, whereas organic matter in medium soil texture will range between 0.2 and 0.3%. Finally, organic matter in fine soil textures will range between 0.3 to 0.4 %. Higher clay content will result in higher organic matter.

Yang *et al.* (2016) showed that soil inorganic carbon is formed by two reactions of calcium carbonate and magnesium carbonate. Calcium carbonate is affected by CO_2 and calcium ion content in soil, pH and water. Inorganic carbon in soil in arid regions is related directly to type of land use. For example, in China, inorganic carbon was

higher in cropped land than in native or grass land. The relationship between soil organic and inorganic carbon can be either a strongly positive or negative correlation. Positive correlation is the high inorganic carbon reserves/stock in the soil due to high pH alkaline soils that contain ample calcium carbonate ($CaCO_2$) precipitations due to elevated Ca^{2+}/ Mg^{2+} ion content. This has been found in parts of China, Canada and the USA. Conversely, negative correlation is where the high inorganic carbon reserves/stock in the soil due to high CO_2 saturated soil surface from root respiration generate an acidic environment resulting in organic carbon. This was shown in the north of China. This difference is determined by two main factors. First are the climatic conditions i.e. precipitation and temperature. The second factor is the properties of the soil and how the land is managed as in crop system, organic amendments and fertilization. Soil properties, as in texture (coarse or fine), influence the direction of the effect, since calcium carbonate helps bonds the soil grains together as is the case in the loess soil. Also, the higher the fertility is the higher carbonate accumulation occurs in soil (Yang *et al.* 2016).

Nitrogen in soil is found in organic and inorganic forms where normally 95 to 98% is organic. In arid soils, 5-18% of nitrogen is inorganic and this can vary a great deal. Coarse soil textures will contain total nitrogen of 0.02-0.05%, medium around 0.042-0.056%, and in fine soils it will range between 0.06 to 0.065% (Praveen *et al.,* 2020). Protein content in soil is an indicator of biological and chemical quality that is linked to the general health status since it represents the largest pool of organically bound nitrogen in the soil (Hurisso *et al*., 2018). Organic nitrogen is

derived from plant biomass and root exudates, organic fertilizer application or soil microbiome immobilization of inorganic nitrogen (Naasko *et al*., 2023)

Total phosphorus content is 10-20% in organic form. Both total phosphorus and inorganic phosphorus in soil profiles in arid regions are found to be uneven/ irregular in distribution, since organic phosphorus decreases with depth. In arid regions, it was recorded that following a decent rainfall, response of crops to phosphorus fertilization was better (Praveen *et al.,* 2020). Rainfall has direct effects on the magnitude of phosphorus loss, since its intensity is considered the dominant factor in its erosion. Also, high intensity storms include high kinetic energy that has an effect on soil detachment and sealing. This leads to increased runoff rates and higher transport capacity of detached soil, which causes soil and nutrient loss (Ramos *et al*., 2022).

Microbes mobilize phosphorus. Arid regions have lower phosphorus solubilizing microorganisms, which varies with regions. The dominant microorganisms involved are bacteria: Actinomycetes and *Streptomyces* specifically have been reported to solubilize inorganic phosphorus. The second leading microorganisms are fungi, such as *Aspergillus*, *Penicillium* and *Trichoderma*. Due to competition with the soil native microflora, these phosphorus solubilizers will not perform well in the field (Praveen *et al.,* 2020).

The aims of this study were to investigate the difference in the fungal diversity between cultivated (regardless of whether traditional or non-traditional practices were used) and non-cultivated (feral) date palms. Will cultivation practices by growers have any influence on the rhizosphere fungal diversity of date palms? Will

feral date palm lacking care, fertilizer or pesticide application have any effect on fungal diversity? The second aims were to investigate the total soil minerals and whether there was a difference between cultivated and feral date palm and locations. This will provide a better understanding on the effect of cultivation practices, location and soil minerals on fungal diversity. As mentioned previously, a good rhizosphere microbiome promotes better growth and plant vigour and increases disease resistance.

2.2 Materials and Methods

2.2.1 Soil and root sampling from three locations

Three locations, Hoqain (H), Samail (S) and Swaiq (Q) were picked for the study: all of the locations provided farm sampling sites (H1, S3, S4, Q1 and Q2) (referred to as cultivated) and two of the locations provided wadi bank sampling sites (H2, S1 and S2) (referred to as feral). In total, there were 5 farm sampling sites and 3 feral sampling sites. Rhizosphere soil and roots were collected 20-30 cm from the date palm trunk at a depth of 30 cm. Four healthy date palms were sampled from each farm\wadi and considered as replicates (Annex 1). No wilt symptoms were observed at any of the locations (Figs 4-9).

The sampled soil was allowed to dry for 24 hours at room temperature, and sifted to remove debris and stones. The sifted soil was weighed (30 - 50 g) and placed in 50 ml sterile centrifuge tubes, labelled and stored in a -80°C -deep freezer. All the

samples were ground in liquid nitrogen to prevent overheating from friction. In total 48 samples were stored in 50 ml centrifuge tubes at -80°C until required for analysis.

2.2.2 Soil chemical analysis

The soil samples were analyzed for mineral content including heavy metals, nitrogen, protein and total organic carbon (TOC) and total inorganic carbon (TIC). Labeling is shown in Table 2. The mineral analysis was investigated as per a modified protocol of Howard *et al.* (2014) using the ICP-OES test method. The analysis was done at the Central Analytical and Applied Research Unit at Sultan Qaboos University, Muscat. The samples were weighed to 0.4-0.6 g in 100 ml beakers. Under a fume hood, nitric acid (trace analysis grade 68%) was added (just enough to cover the sample) then placed on a hot plate at 300°C to allow digestion for 10-20 minutes. The samples were transferred into plastic vials and filled up to the 100 ml mark with double distilled water. The vial was shaken to mix the contents. Then again under the fume hood, the sample was decanted onto filter paper (Whatman™ No. 41, ashless Dia.150 mm) and 11 ml filtrate was collected into a 20 ml sterile centrifuge tube. The filtrate was used to feed the ICP (Inductively Coupled Plasma) equipment for mineral analysis. The Walkley and Black method was used for total organic carbon (TOC) and total inorganic carbon (TIC).

The nitrogen and protein content was determined by the Kjeldehal method of digestion using a BÜCHI KjelMaster K375 and Kjel Sampler 376 System at the Department of Animal Science at College of Agriculture and Marine sciences, Sultan Qaboos University, Muscat. The soil samples were weighed to 0.5 g in tubes. Kjeltab (KSO_4 + Se) catalyst tablet (manufactured commercially) was added to each

sample tube. The sample tubes were placed in a fume hood where 10 ml of concentrated sulphuric acid was added. The digestion and reaction were allowed to proceed for approximately one hour or until the contents turned clear. They were then transferred to the Kjeldehal system to determine the nitrogen content. Nitrogen percentage (N%) per sample was calculated by the following formulae:

N% = (1.4 x Acid Molarity x (Titer value- Blank)) /Sample weight.

Where 1.4 = Value of nitrogen molecular weight in percentage.

Average nitrogen content contains about 16% of protein. Protein percentage (Protein %) was calculated by the following formulae:

Protein % = N% x 6.25

Where 6.25 = is 1/0.16 as conversion factor of nitrogen to protein.




Figure 4: Feral date palm growing in the wadi (vally) in State of Samail. First location for root and rhizosphere soil sampling. The uncut offshoots under the stem and dry older fronds not pruned are evident.



Figure 5: Feral date palm growing in the wadi (vally) in State of Samail. Third location for root and rhizosphere soil sampling .Evidence of over growth, unattended date palms with uncut offshoots under the stem and dry older fronds not pruned.



Figure 6: Cultivated date palm growing in a farm in State of Samail. Second location for root and rhizosphere soil sampling. Typical traditional farming with intercropping and flood irrigation.Absence of offshoots under the date palm and fronds maintained shows proper cultivation practices.



Figure 7: Cultivated date palm growing in a farm in State of Samail. Fourth location for root and rhizosphere soil sampling. Typical traditional farming with intercropping and flood irrigation.



Figure 8: Cultivated date palm growing in a farm in State of Swaiq. First location for root and rhizosphere soil sampling. Modern cultivation with no intercropping, spacing between palm and double basin for irrigation with drip system.



Figure 9: Cultivated date palm growing in a farm in State of Swaiq. Second location for root and rhizosphere soil sampling. Modern cultivation with no intercropping, spacing between date palms and double basin for irrigation with drip system.

2.2.3 Extraction of fungal DNA from soil

A modified Volossiouk *et al.* (1995) protocol was used for direct fungal DNA extraction from the ground samples (Annex 2), where 0.05 g of the sample was weighed into a 2 ml sterile Eppendorf tube (2 replicates per sample). Labelling was as shown in Table 2. To prepare skimmed milk powder, 0.1 g was weighed and added to 25 ml sterile distilled water (SDW). A 500 µl aliquot of skimmed milk solution was added and mixed well by a vortex. This is an effective carrier to reduce reaction-inhibiting contaminants and background signals. Also, the skimmed milk reduces the degradation and adsorption of nucleic acid to soil (Hoshino *et al.,* 2005). The tubes were incubated in a water bath at 60°C for 1 hour and inverted every 15 minutes. They were centrifuged at 4°C, 13000 x g for 10 minutes. The supernatant was transferred to a 1.5 ml sterile Eppendorf tube. SDS extraction buffer (500 µl) was added and mixed by inverting twice. One volume of phenol: chloroform: isoamyl alcohol (25:24:1) was added, centrifuged at 4°C, 13000 x g for 10 minutes. The supernatant was transferred to 1.5 ml sterile Eppendorf tube and 0.6 volume (400 µl) of cold isopropanol and 10 µl of sodium acetate (NaAc) were added. The mixture was incubated overnight at -20°C. As soon as tubes were removed from the freezer, they were centrifuged for 10 min at 13000 x g at 4°C. The supernatant was discarded and the pellet was washed with 400 µl 70% ethanol, then centrifuged for 4 min at 13000 x g at 4°C. The tubes were vacuum centrifuged at 60°C for 10 min. Finally, 100 µl deionized sterile distilled water was added. The quality and quantity of DNA was determined by Nanodrop 2000 spectrophotometer (Thermo scientific,

USA). Forty microliters in 1.5 ml Eppendorf tube were prepared for each sample (2 replicates per sample) for MiSeq analysis.

Table 2: Samples of rhizosphere soil and roots labelling as per location and type of cultivation.

Group	Sample codes	Type	Location
1	Q1, Q2, Q3	Cultivated	Swaiq
2	Q5, Q6, Q7, Q8	Cultivated	Swaiq
3	H1, H2, H3, H4	Cultivated	Hoqain
4	H5, H6, H8, H9	Feral	Hoqain
5	S1, S2, S3, S4	Feral	Samail
6	S5, S6, S7, S8	Feral	Samail
7	S9, S10, S11, S12	Cultivated	Samail
8	S13, S14, S15, S16	Cultivated	Samail

Table 3: PCR reaction conditions used for DNA extracted from soil samples.

	Reaction	Conditions	No. of Cycles
First PCR	Initial Denaturation	95 ° C for 5 min	-
	Denaturation	94 ° C for 30 sec	25
	Annealing	54 ° C for 40 sec	-
	Extension	72 ° C for 1 min	-
	Final Extension	72 ° C for 10 min	-
Second PCR	Initial Denaturation	95 ° C for 5 min	-
	Denaturation	94 ° C for 30 sec	10
	Annealing	54 ° C for 40 sec	-
	Extension	72 ° C for 1 min	-
	Final Extension	72 ° C for 10 min	-

2.2.4 Illumina MiSeq analysis

The soil microbial DNA was amplified and sequenced by Illumina MiSeq sequencing at the Research and Testing Laboratories (RTL) in Lubbock, Texas, USA. This was done by amplification of the 62 samples (2 replicates per each sample (31 samples)). Initially the genomic region of relevance was amplified, followed by augmenting sample - specific indices to the samples which are adaptors to facilitate the sequencing. The next step was using the Illumina i5 sequencing primer to construct the Forward primer (ITS1F) and the Reverse primer (ITS2aR) by Illumina i7 sequencing primer. The PCR was done twice. The first was performed by using a 25 µl reaction mix, which included 1 µl of the DNA template and 1 µl of the master mix (5 µM) which includes the Qiagen Hot Star Taq plus the primer (Qiagen, Valencia, California). The reaction conditions are shown in Table 2. The first PCR products were used with primers that were designed by Illumina Nextra for the second PCR run. The primers were Forward i5index and Reverse i7index. The amplification product was visualized and pooled equimolar. For each pool, the size selection was done in 2 rounds. Quantification was done by using the Quibit 2.0 fluorometer (Life Technologies). Subsequently, they were loaded onto a 2 x 300 flow cell at 10 pM in the Illumina MiSeq (Illumina, Inc, San Diego, California) (Al Bulushi *et al.*, 2017).

2.2.5 Bioinformatics

The bioinformatic data was done in Microbiome Analysis USA by Author: Matthew R. Fox M.S. shown in Annex 4.

The generated sequence data from the Illumina MiSeq underwent three different steps. The first was using USEARCH and UPARSE algorithms for de-noising to eliminate short and singleton sequences and any noisy reads. This was followed by chimera detection through UCHIME software in *de novo* mode, hence any chimeric sequences were removed. Any sequence errors were discarded and the leftover sequences were corrected per-base. Finally, for the diversity analysis, the UPARSE algorithm was used for all samples and compiled into the Operational Taxonomic Units (OTUs) at an identity of 97%. The global algorithm USEARCH was used for the sequences where they were aligned globally against a high quality ITS fungal gene sequence global database from GenBank, and compiled by the RTL for taxonomic classification. From multiple sequence alignment of OTUs, a phylogenetic tree was constructed (Newick format) using MUSCLE software to generate a Fast Tree. To classify the fungi at the suitable taxonomic level, the trimmed taxa was taken at a confidence account at every taxonomic level. Subsequently, individual analysis was performed to the sequences percentages assigned in every phylogenetic level for the pooled sample. This provided the relative abundance per sample. It was then filtered at a 97% similarity threshold.

The data were analyzed by the R software which generated a refraction curve plot of OTU versus sequence numbers. Fungal diversity was estimated by Richness and

Shannon Diversity indices and Bray-Curtis similarities. The analysis demonstrated the estimate of fungal diversity between cultivation types and locations by a refraction plot for species richness [rare]. Finally, the analysis of differences in fungal diversity between groups of samples was performed by using ADONIS functions (Permutational Multivariate Analysis of Variance (PERMANOVA) using Distance Matrices) (Al Bulushi *et al.*, 2017).

PERMANOVA is a statistical analysis initially influenced for implementation in ecological studies. In these studies, the variables consisted of abundant counts, coverage percentages, biomass or frequencies for extensive species counts. Therefore, PERMANOVA used geometric partitioning of multivariate variation in selected dissimilarity measure by given p-values through ANOVA (Analysis of Variance) design. Where appropriate, distribution-free permutation techniques were used. PERMANOVA is a semiparametric method initiated to perform classic partitioning similar to ANOVA but allowing estimated test and size of main effects, interaction terms, hierarchical structures and random components in mixed models, with "simultaneous retaining of important tough statistical properties of rank-based no parametric multivariate methods" (Anderson, 2017). This allows complex experimental designs and formal partitioning of multivariate data with a wider variety of contexts where there were different response variables than sampling units or severe non-normal data or nil /zero inflated or ordinal or qualitative (Anderson, 2017). Such was the case with our investigation of DNA sequences from large fungal populations.

2.2.6 Statistical analysis by correlation between Operational Taxonomic Units (OTUs), soil minerals, cultivation practices and location

Rarefaction plot (rare) is a method for changing differences in the size of metagenomic clone libraries across samples, facilitating the comparison of α diversity. The rarefaction curve is a graphical representation that illustrates the relationship between the number of individuals randomly selected from a sample and the corresponding number of species they represent. This method employs random sampling of sequences to construct the rarefaction curve while correlating the number of sampled sequences with the amount of Operational Taxonomic Units (OTUs) they represent. When sequencing data volume is enhanced, additional data would only yield a minimal increase in new OTUs, shown by a flat curve. Contrarywise, a steep curve indicates that further sequencing may still yield many new OTUs. Thus, generating a rarefaction curve proves useful in assessing the depth and adequacy of sequencing in a sample and is a critical tool for understanding species diversity within an ecosystem (CD Genomics, Zao Yi *et al.,* 2023). "The nonparametric Chao1 index [1] estimates total species richness with an equation that generates a ratio of the number of singletons squared divided by the number of doubletons multiplied by two. This value is then added to the number of observed species to generate a species richness prediction" (Deng *et al.,* 2024). The OTU data generated by the Bioinformatics was correlated with the data of soil minerals, protein, TOC, TIC with the cultivation and location. Microsoft Office Excel was used for correlation analysis. The graphs were generated using the data via Graphia

software to perform Principal Component Analysis (PCA) and JMP14 software for the Multivariate PCA.

2.3 Results:

2.3.1 Soil chemical analysis:

The full raw data analysis per sample are included in Annex 2. The following results are means with the standard deviation and one way ANOVA carried out using $P<0.05$. All mineral readings are total content and not available mineral for the date palm.

Total nitrogen, sodium, potassium, phosphorus and protein:

Nitrogen readings ranged between 0.070 - 0.238 % for feral samples (H2, S1, S2) while from cultivated samples (Q1, Q2, H1, S3 and S4) it showed a range from 0.08 - 0.3% (Table 4). The percentages were similar regardless of cultivation type. There was no significant difference within feral samples ($P< 0.05$), and no significant difference between cultivated and feral ($P< 0.05$) . However, a significant difference was shown within the location of Swaiq (Q1 and 2) ($P< 0.05$).

For the protein content, the highest reading was at S4 and lowest at S2 (Table 4). There was a significant difference between feral H1 and H2, cultivated S4 and all locations except H2.

For sodium, the highest reading was at S4 and lowest at H1 (Table 4). There was a significant difference between feral S1 and both H1 and H2. However, no significant difference was found between cultivated and feral.

For potassium, the highest reading was at S1 and lowest at H1 (Table 4). There was a significant difference between feral S1 and H1 and H2. However, no significant difference was found between cultivated and feral .

For phosphorus, the highest reading was at S4 and lowest at S1 (Table 4). There was a significant difference between feral S1 and H1 and H2. However, there was a significant difference between cultivated S4 and all locations.

Table 4: Mean and STDEV of total nitrogen, sodium, phosphorus, potassium and protein from soil from date palm rhizosphere per location**.**

	N (%)	NA (PPM)	P (PPM)	K (PPM)	PROTEIN (%)
Q1	0.084 ±0.013^{c}	1014.5 ±354.4^{a}	330.6 ±84.80^{cd}	877.01 ±430.03^{ab}	0.527 ±0.080^{c}
Q2	0.081 ±0.018^{c}	470.6 ±38.30^{bc}	204.1 ±27.40^{de}	514.65 ±71.90^{b}	0.506 ±0.109^{c}
H1	0.186 ±0.033^{b}	412.6 ±34.9^{c}	453.4 ±72.30^{bc}	482.64 ±7.30^{b}	01.162 ±0.203^{b}
H2	0.238 ±0.029^{ab}	680.7 ±85.2^{abc}	623.7 ±79.2^{b}	576.82 ±133.86 ^{b}	1.486 ±0.180^{ab}
S1	0.087 ±0.006^{c}	943.8 ±117.4^{ab}	63.2 ±6.3^{e}	1265.41 ±161.92^{a}	0.544 ±0.040^{c}
S2	0.070 ±0.011^{c}	996.1 ±264.7^{a}	91.1 ±22.0^{e}	1141.75 ±384.05^{ab}	0.436 ±0.070^{c}
S3	0.104 ±0.024^{c}	1189.8± 118.8^{a}	114.0 ±51.40^{de}	668.74 ±61.49^{ab}	0.652 ±0.150^{c}
S4	0.300 ±0.035^{a}	735.7±1 31.8^{abc}	881.2 ±153.9^{a}	849.53±16 0.13^{ab}	1.877 ±0.220^{a}

Means and Standard Deviation (±SD, n = 4) followed by same letter in a column are not significantly different (Tukey's test P< 0.05).

Total calcium, magnesium, total organic carbon (TOC) and total inorganic carbon (TIC)

For calcium, the highest reading was at H2 and lowest at Q2 (Table 5). There was a significant difference between feral locations. However, no significant difference was found between cultivated and feral.

For magnesium, the highest reading was at Q1 and lowest at S4 (Table 5). There was no significant difference between all feral locations. Also, there was a significant difference between cultivated and feral locations.

As for the TIC, the highest reading was at H1 and lowest at S2 (Table 5). There was a significant difference between feral S1 and H1 and H2. However, no significant difference was found between cultivated and feral .

TOC had the highest reading at S4 and lowest at S2 both feral (Table 5). There was a significant difference between feral S1 and H1 and H2. Also, there was a significant difference between feral S4 with all locations except for feral H2.

Other minerals and heavy metals

Iron and nickel both had the highest reading at Q1. Zinc, copper, aluminum, iron and chromium had highest readings at S4, S3, S2, S1 and Q1 respectively (Table 6). There was a significant difference in chromium between Q1 and all locations. However, there was no significant difference between cultivated and feral sites for zinc, copper, aluminum, iron and nickel.

Table 5: Mean and STDEV of total magnesium, calcium, total organic carbon (TOC) and total inorganic carbon (TIC) from soil of date palm rhizosphere per location**.**

	MG(PPM)	CA (PPM)	TOC (%)	TIC (%)
Q1	61086.4 ±4655.5^{a}	55323.1 ±3486.2^{b}	1.6 ±0.20^{c}	23.21 ±0.97^{bc}
Q2	51828.0 ±4301.3^{a}	31160.7 ±1422.4^{c}	1.27 ±0.21^{c}	17.98 ±1.01^{d}
H1	40759.2 ±4233.9^{bc}	68446.9 ±1660.7^{a}	2.84 ±0.51^{b}	28.81 ±1.14^{a}
H2	43678.8 ±5725.1^{bc}	70128.1 ±1256.7^{a}	3.59 ±0.43^{ab}	27.13 ±0.41^{ab}
S1	44862.5 ±4036.8^{bc}	48285.3 ±3373.6^{b}	1.18 ±0.07^{c}	19.13 ±0.82^{cd}
S2	49714.9 ±5321.9^{ab}	37233.4 ±2906.5^{c}	0.99 ±0.12^{c}	17.74 ±0.84^{d}
S3	49136.8 ±1503.0^{ab}	53894.4 ±2154.2^{b}	1.68 ±0.35^{c}	19.42 ±2.12^{cd}
S4	34834.0 ±6638.0^{c}	50003.7 ±6075.7^{b}	4.33 ±0.19^{a}	28.2 ±3.47^{a}

Means and Standard Deviation (±SD,n=4) followed by same letter in a column are not significantly different (Tukey's test P< 0.0).

Table 6: Mean and STDEV of total zinc, copper, aluminum, iron, nickel and chromium from soil of date palm rhizosphere per location**.**

	ZN (PPM)	CU (PPM)	AL (PPM)	FE (PPM)	NI (PPM)	CR (PPM)
Q1	28.52± 3.15^{bc}	47.18± 3.41^{cd}	6583.8± 824.6^{c}	14481± 1456.8^{ab}	455.66 ±36.48 ^{a}	127.41 ±13.26^{a}
Q2	20.27± 2.19^{c}	35.39± 5.35^{d}	6600.2± 748.4^{c}	11353.7± 1146.7^{abc}	422.21 ±32.34^{ab}	96.84 ±7.97^{b}
H1	36.18± 7.08^{ab}	46.67± 1.90^{cd}	5515.0± 651.0^{c}	9235.7± 1131.3^{c}	264.93 ±24.55^{cd}	59.74 ±7.10^{c}
H2	30.90± 4.09^{abc}	49.84± 4.63^{bcd}	5890.3± 1104.7^{c}	8963.3± 1821.6^{c}	275.39 ±38.21^{cd}	60.87 ±10.76^{c}
S1	22.19± 1.87^{c}	68.65± 7.49^{abc}	16440.7± 2208.4^{ab}	13718.4 ±1681.7^{abc}	336.12 ±25.89^{bc}	75.34 ±7.71^{bc}
S2	18.39± 2.09^{c}	74.43± 7.23^{ab}	19752.3± 3584.2^{a}	14883.8 ±2126.9^{a}	332.20 ±31.11^{bc}	81.18 ±9.44^{bc}
S3	23.49± 2.18^{bc}	78.64± 20.84^{a}	19668.3± 1880.2^{a}	15355.3 ±950.4^{a}	349.75 ±8.21^{bc}	80.84 ±4.20^{bc}
S4	42.65± 9.29^{a}	61.73± 6.87^{abcd}	13110.5± 2981.7^{b}	10003.3 ±2243.3^{bc}	188.53 ±42.86^{d}	58.83 ±14.47^{c}

Means and Standard Deviation (±SD,n=4) followed by same letter in a column are not significantly different (Tukey's test P< 0.0)

2.3.2 Bioinformatics

Fungal diversity estimates

The analysis demonstrated the estimate of fungal diversity between cultivation types and locations by a refraction plot for species richness [rare] (Fig. 10). Sub sampling was from 500 – 20000 reads between all groups. The data showed no significant differences in fungal diversity between cultivation type and location. As for Shannon diversity analysis between cultivation type and location, the graph (Fig. 11) illustrates no significant differences in fungal diversity levels that ranged between 2.5 to 3.9 for Group 1 (location Swaiq, cultivated date palm) and Group 8 (location Samail, cultivated date palm) respectively. Likewise, for the richness estimate [Chao 1] analysis (Fig. 12), the graph illustrates no significant differences in fungal diversity levels between cultivation type and location. The diversity level ranged between a minimum of 418 for Group 1 (location Swaiq, cultivated date palm) to a maximum of 497 for Group 4 (location Hoqain, feral date palm).

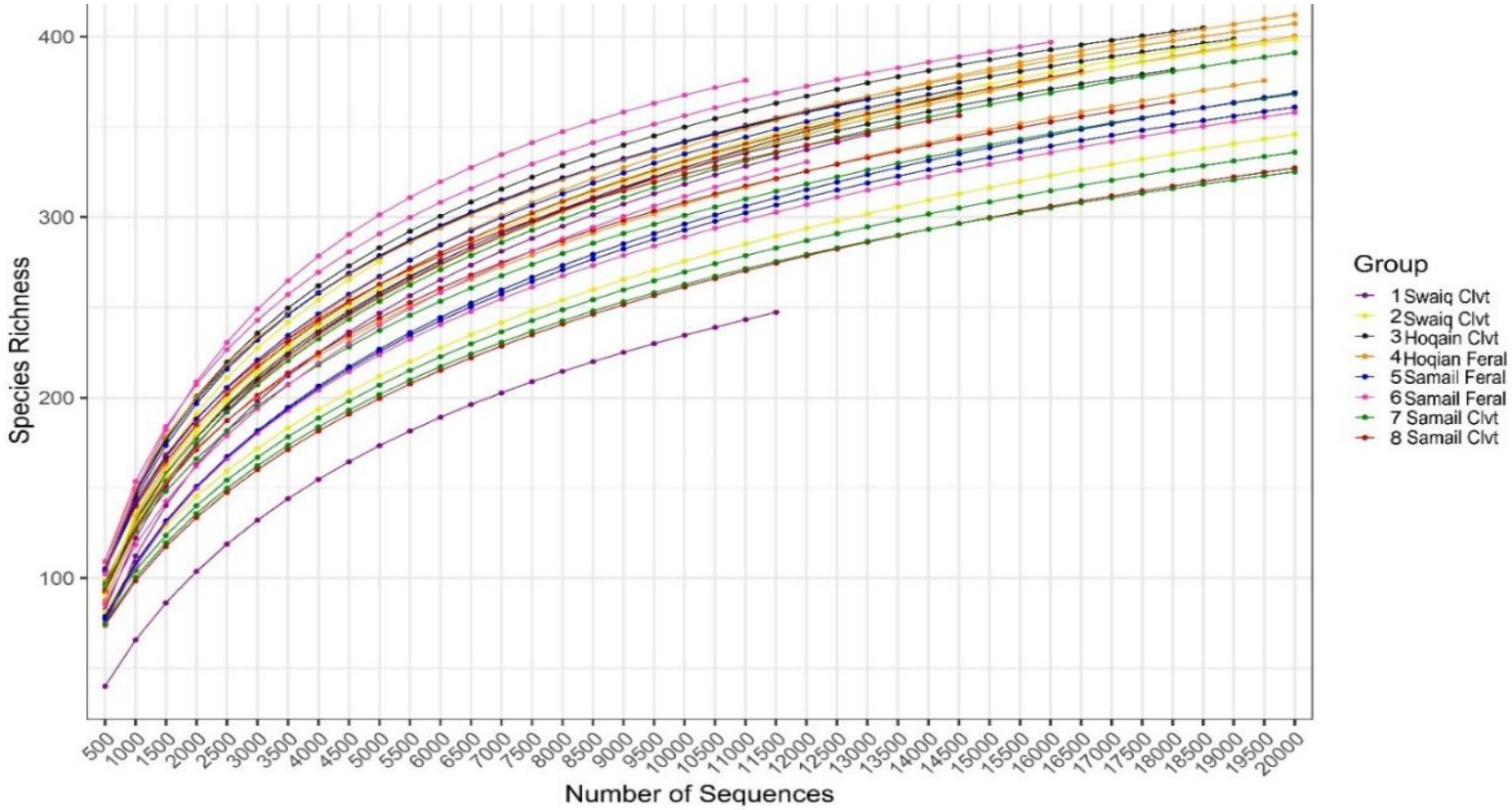


Fig 10: Rarefaction plot for species richness (rare) of fungal communities between all groups (locations and cultivation type). Sub sampling from 500 – 20000 reads between all groups with no significant differences between cultivation type and location in fungal diversity.

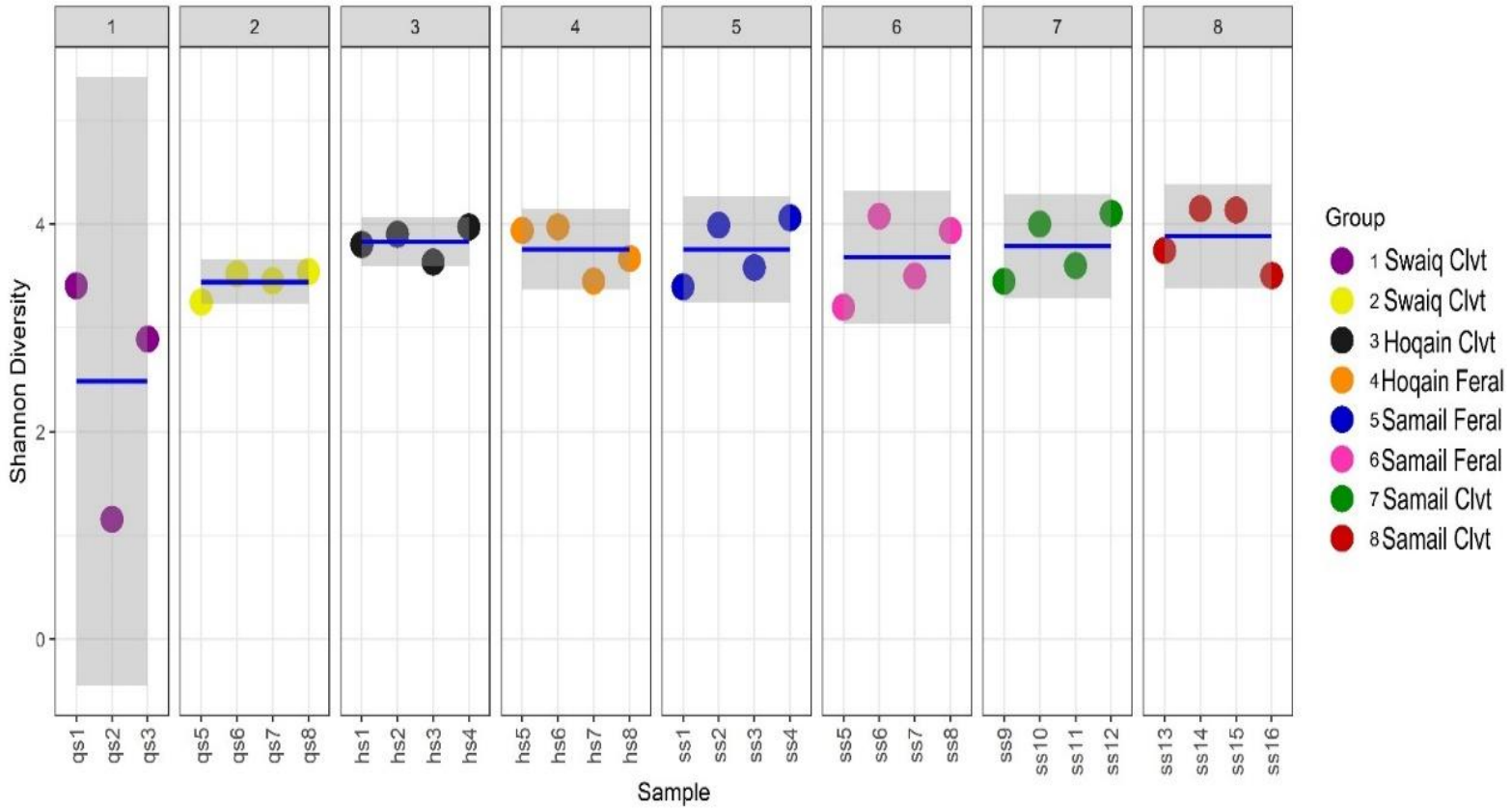


Fig 12: Shannon diversity of fungal communities between all groups (locations and cultivation type). There was no significant differences in the range between 2.5 to 3.9 for Group 1 and Group 8 respectively in fungal diversity levels.

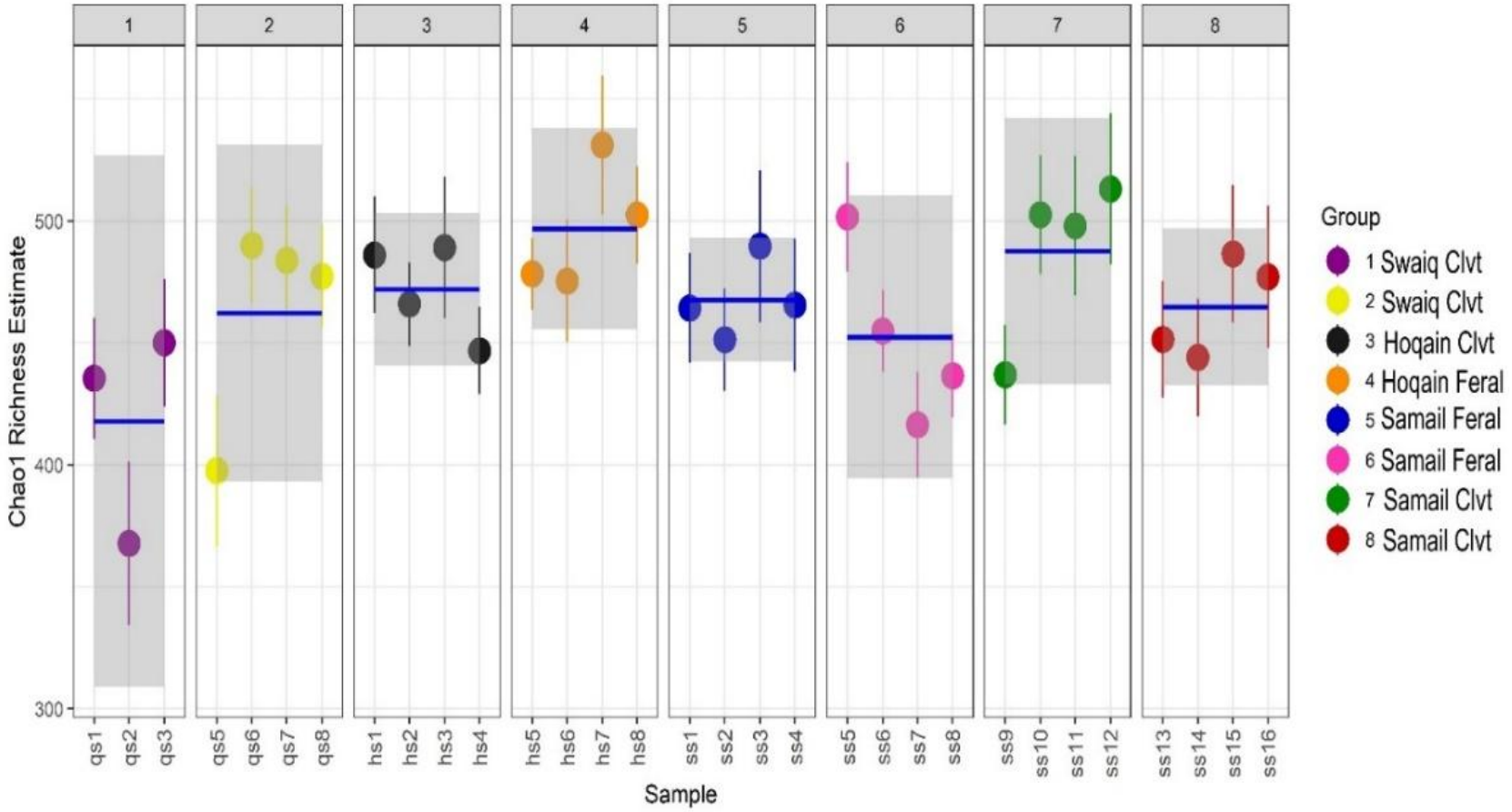


Fig 13: Richness Estimate (Chao 1) of fungal communities between all groups (locations and cultivation type). The diversity level ranging between a minimum of 418 for Group 1 to a maximum of 497 for Group 4. With no significant differences in fungal diversity levels regardless of cultivation type or location.

Dominant fungal groups in the rhizosphere of date palm roots

The three fundamental fungal phyla regardless of locations and cultivation type were Ascomycota and Basidiomycota and an unclassified group. Ascomycota made up around 85% while Basidiomycota made up around 10% of fungal reads. The unclassified group reads were less than 5 %.

Analysis of fungal community composition across cultivation types and locations

The fungal communities between all samples for all locations and cultivation types are illustrated in Fig. 13. There are no significant differences between all groups regardless of the location or cultivation type. The highest percentage of relative abundance of the fungal community by phylum was for Ascomycota detected in Group 1 (Swaiq location for cultivated date palm), whereas the lowest percentage recorded was for Group 5 (Samail location for the feral date palm). The relative abundance of the fungal community by class level (Fig. 14) shows the 3 common classes these were Sordariomycetes, Agaricomycetes and Dothideomycetes respectively. There were no significant differences between all groups regardless of location or cultivation type. The highest class was Sordariomycetes detected in group 1 (Swaiq location for cultivated date palm), whereas it was recorded as the lowest for Group 5 (Samail location for the feral date palm). As for the relative abundance of the fungal community by genera level (Fig. 15), it showed that the most common genera were *Sarocladium, Suillus, Humicola* and *Fusarium* respectively. There were no significant differences between cultivation types. As for

locations Hoqian and Samail and Group 2 in Swaiq, no differences were shown between them. Swaiq (Group 1) shows a significant difference from all the other locations. Its most common genera were *Sarocladium*, *Cladosporium* and *Penicillium* and *Meyerozyma* respectively. In Fig. 16, the relative abundance of the fungal communities by species level clearly illustrates that the most common species are *Sarocladium strictum*, *Humicola grisea* and *Aureobasidium pullulans*. There were no significant differences between cultivation types for species. As for locations Hoqian and Samail and Group 2 in Swaiq, no differences are shown between them, whilst Swaiq (Group 1) shows a significant difference from all the other locations. The most common species were *Sarocladium strictum*, *Meyerozyma guilliemondi*, and *Cladosporium* sp. respectively.

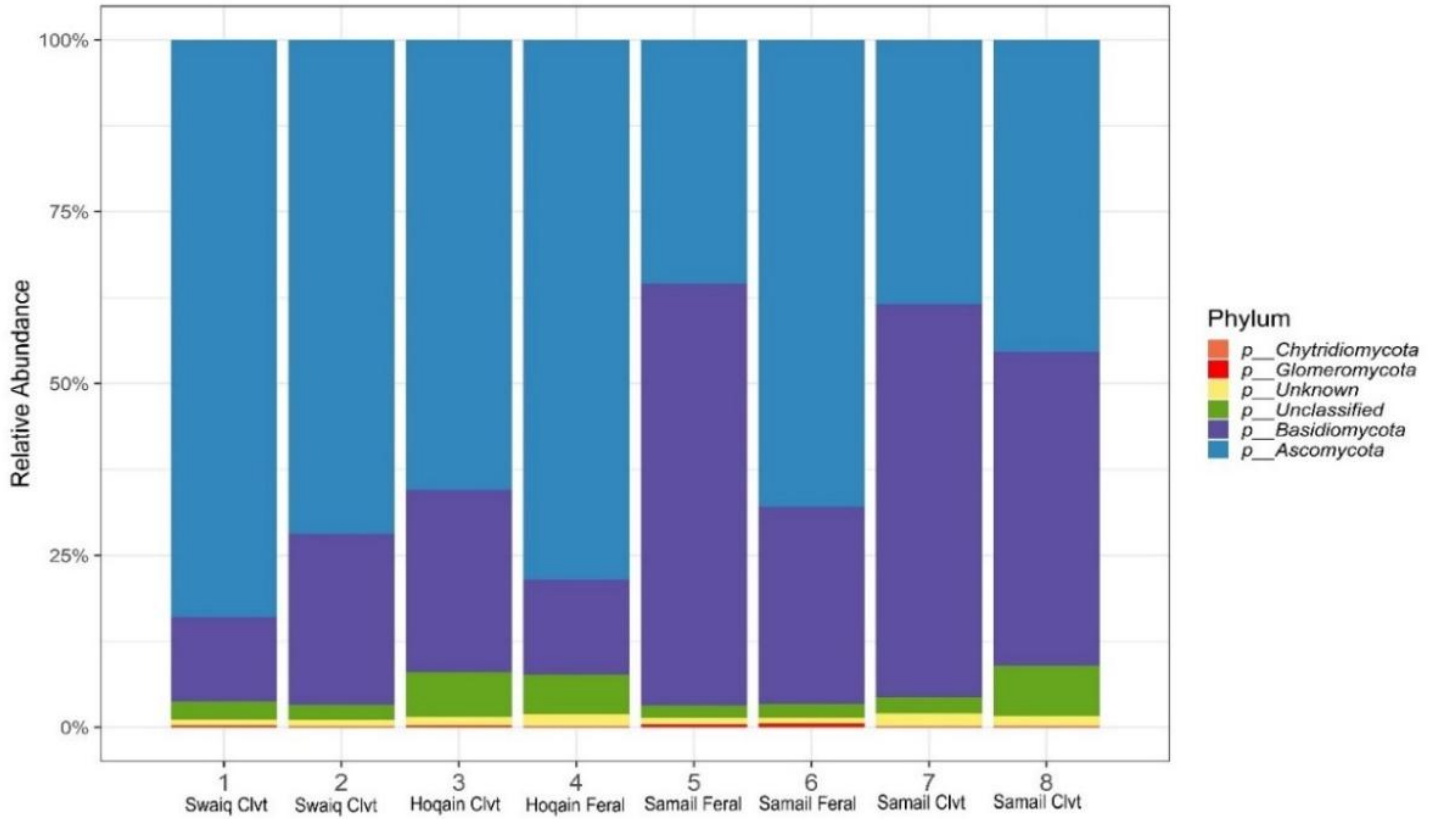


Fig 13: Relative abundance of fungal communities by Phylum level between locations and cultivation types. The three most common Phyla between all the groups were: Ascomycota, Basidiomycota and an unclassified phylum. No significant differences between all groups regardless of the location or cultivation type. The highest Ascomycota was detected in Group 1, whereas the lowest was recorded for Group 5.

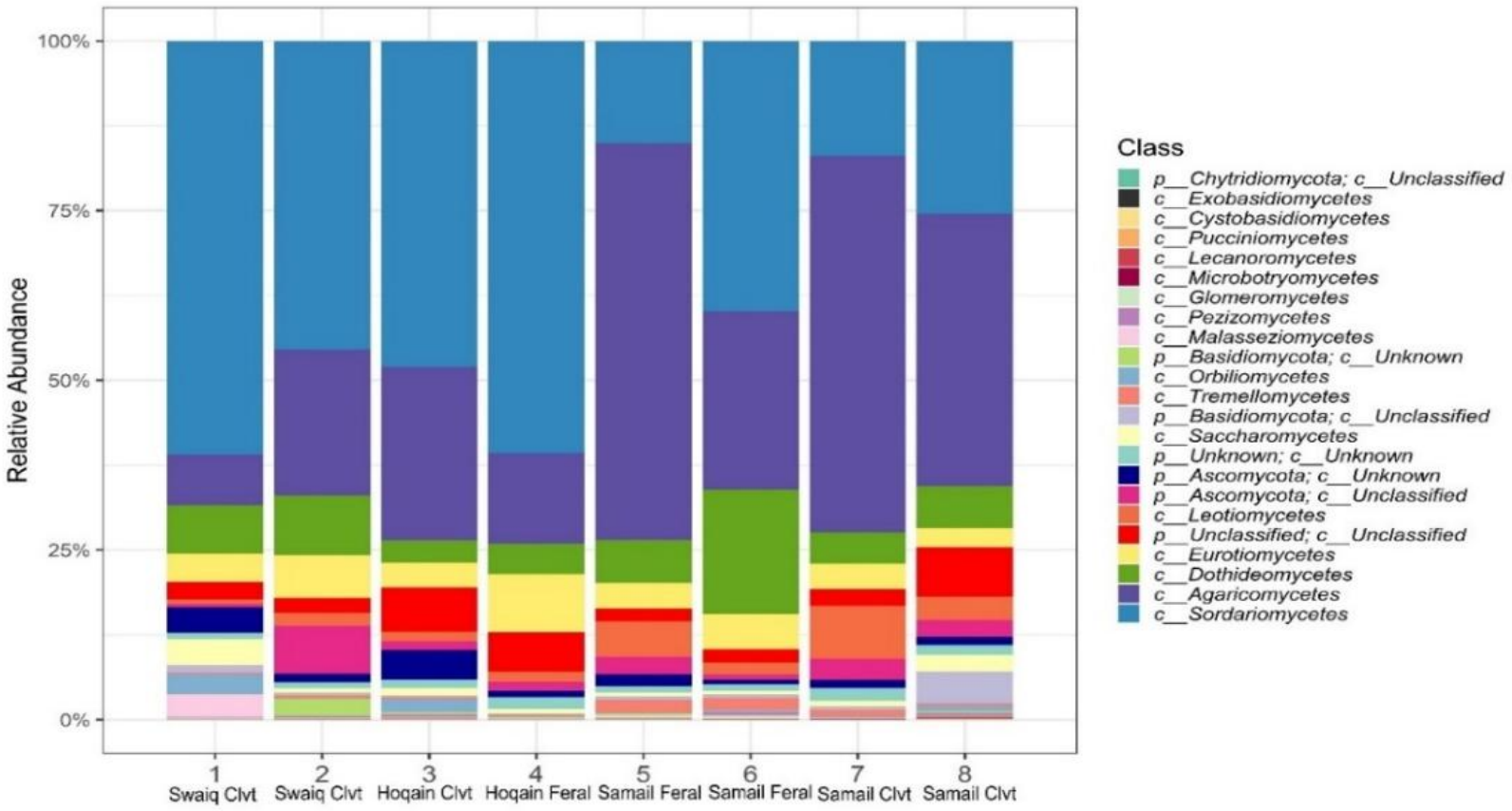


Fig 14: Relative abundance of fungal communities by Class level between all locations and cultivation types. The common classes were: Sordariomycetes, Agaricomycetes and Dothideomycetes respectively, with no significant differences between all groups regardless of location or cultivation type. The highest Sordariomycetes detected in Group 1 and the lowest was recorded for Group 5.

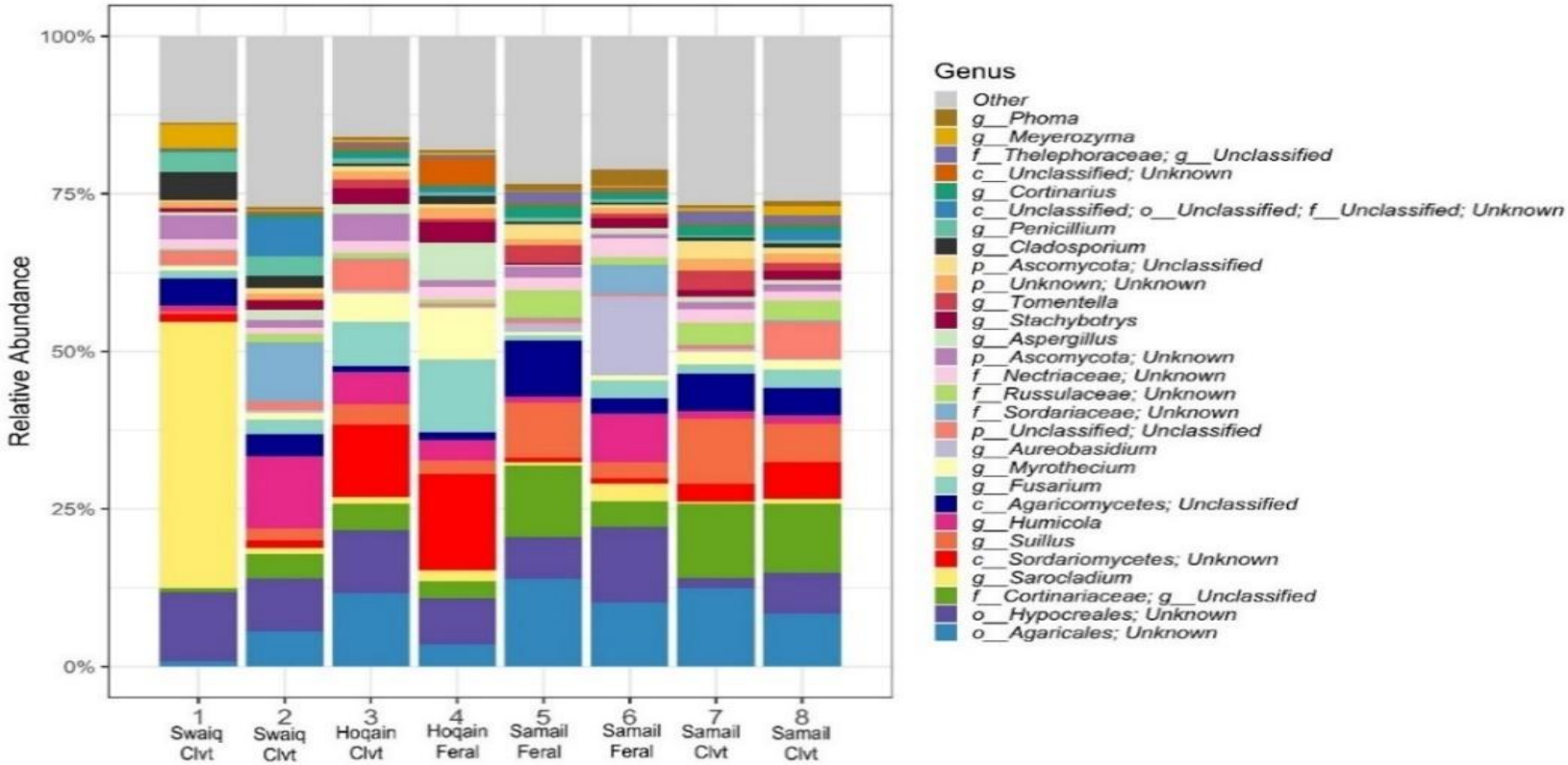


Fig 15: Relative abundance of fungal communities by Genus level between all locations and cultivation types. The common Genera were: *Sarocladium, Suillus, Humicola* and *Fusarium* respectively, with no significant differences between cultivation types. As for locations shows no difference between them. However, Swaiq (Group 1) shows a significant difference from all the other locations with common Genera being *Sarocladium, Cladosporium, Penicillium* and *Meyerozyma* respectively.

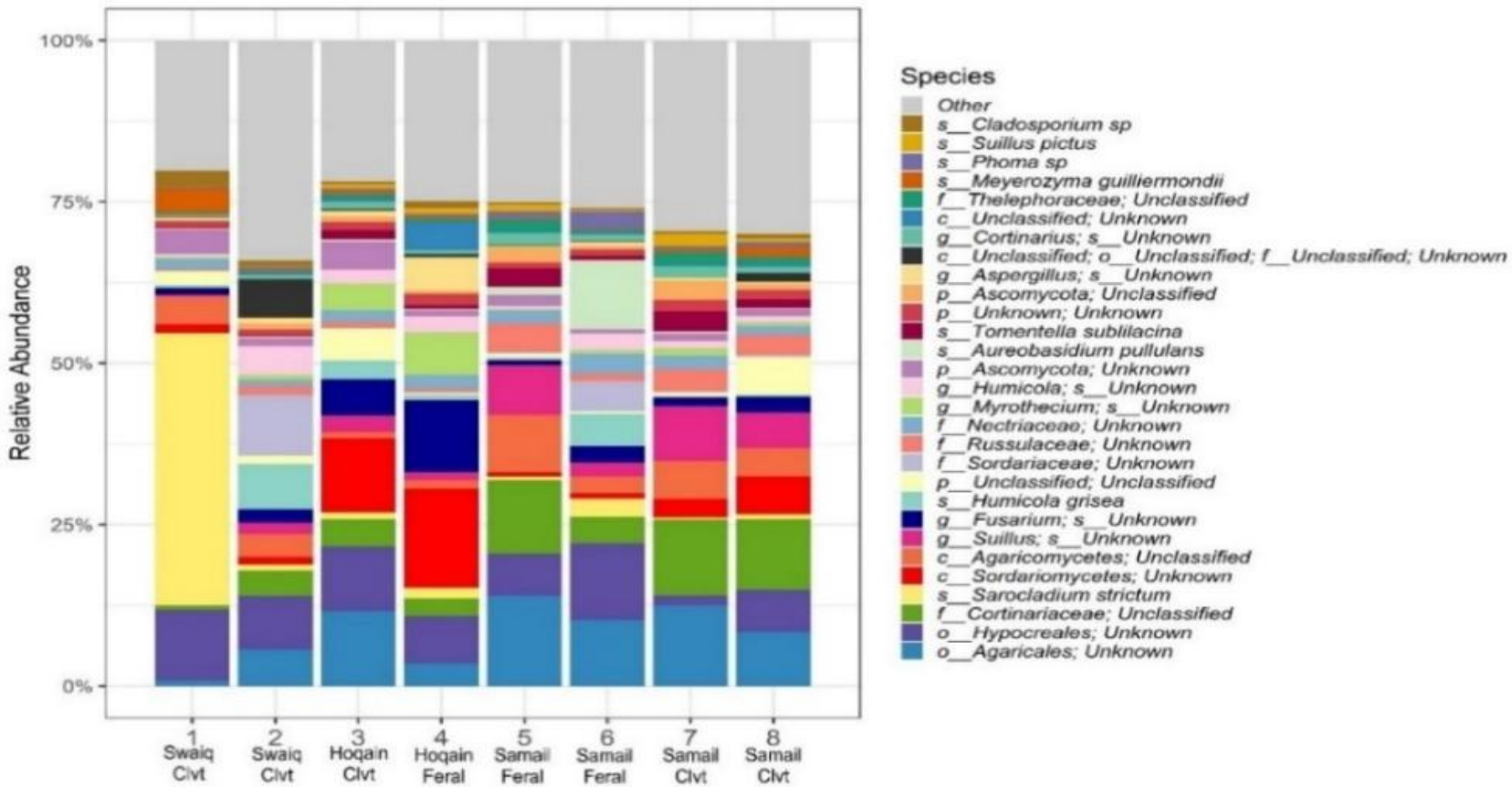


Fig 16: Relative abundance of fungal communities by Species level between all locations and cultivation types. The common species are: *Sarocladium strictum, Humicola grisea* and *Aureobasidium pullulans*. No significant differences between cultivation types. As for locations no significant difference between them. However, Swaiq (Group 1) shows a significant difference from all the other locations having the most common species: *Sarocladium strictum, Meyerozyma guilliemondi* and *Cladosporium* sp. respectively.

Fungal diversity

The fungal diversity analysis through Bray Curtis by PERMANOVA (Fig. 17) shows that the fungal diversity is affected by location. All samples from Group 3 and 4 from Hoqain had their own cluster around point 0.2 at Axis 2. However, Group 1 from Swaiq first location, was clustered with three samples from a total of 4, between point 0.1 to 0.2 at Axis 1. Group 5-8 (Samail) Group 2 (Swaiq) and one sample from Group 1 (Swaiq) were clustered together. The sample from Group 1 (Swaiq) was taken from a younger date palm that was planted in line adjacent to a plot of vegetables and not from the older orchard. Here, fungal diversity was not affected by cultivation types. Group 5-8 included feral and cultivated date palms.

In addition, the analysis of Un Weighted UniFrac (Fig. 18) clearly shows clustering between all groups indicating that the fungal diversity is not affected by cultivation type or location. Except for 2 samples from Group 4 of Hoqain feral is linked at a fair distance away from all the clusters. Also, one sample from Group 1 Swaiq cultivated is also linked away from the rest of the group clusters. This indicates that these are affected by location and cultivation.

The Weighted UniFrac analysis (Fig. 19) shows that the fungal diversity is affected by location, simple separation in clustering is evident, where Hoqain (Group 3 and 4) and Samail (Group 5, 7 and 8) are clustered separately, whereas Swaiq (Group1 and 2) is clustered with one location in Samail (Group 6). Again, cultivation types show no effect on fungal diversity.

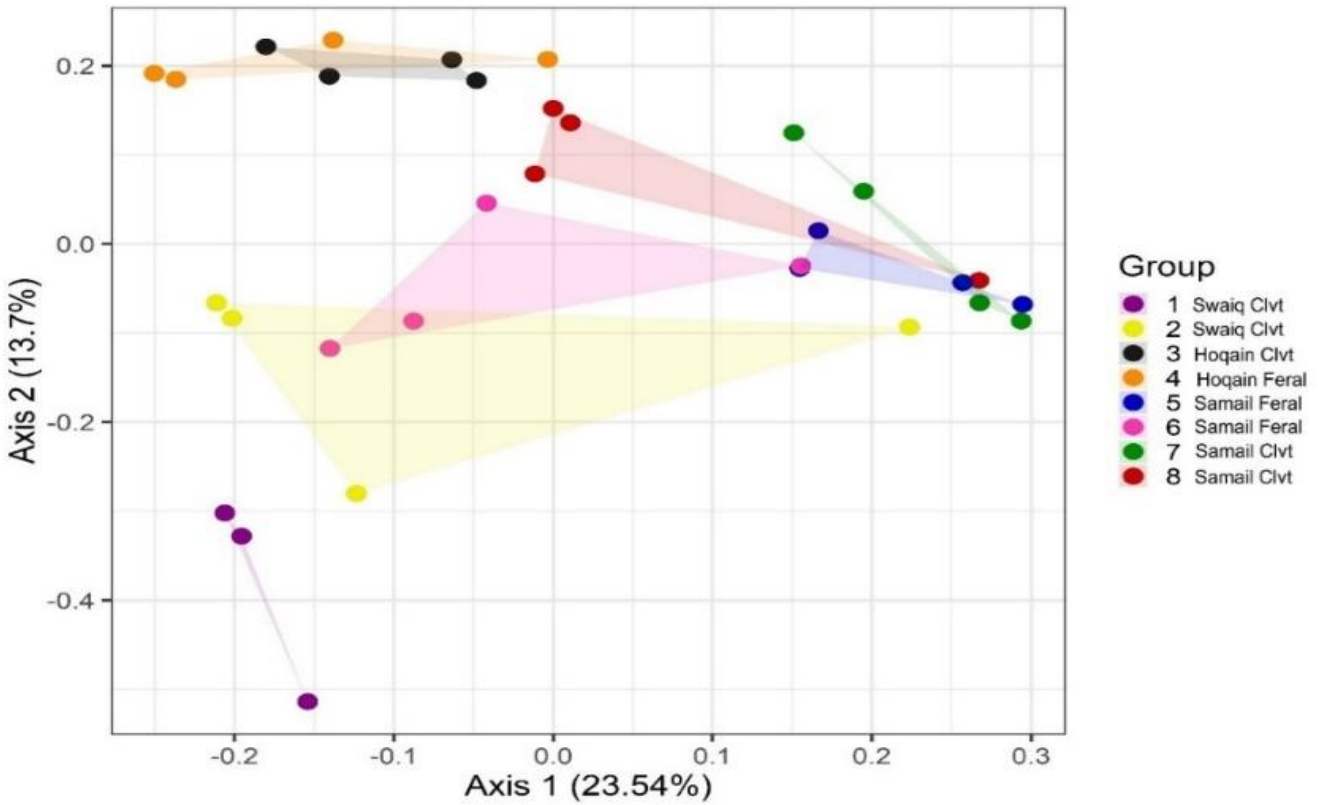


Fig 17: Bray Curtis of fungal communities between all groups (locations and cultivation type). The fungal diversity is affected by location shown by the clustering of Hoqian locations (Group 3 and 4) and Samail (Group 5-8) with one location from Swaiq (Group 2). Whereas the second location from Swaiq (Group 1) is clustered alone and away from all the other locations. However, fungal diversity is not affected by cultivation types.

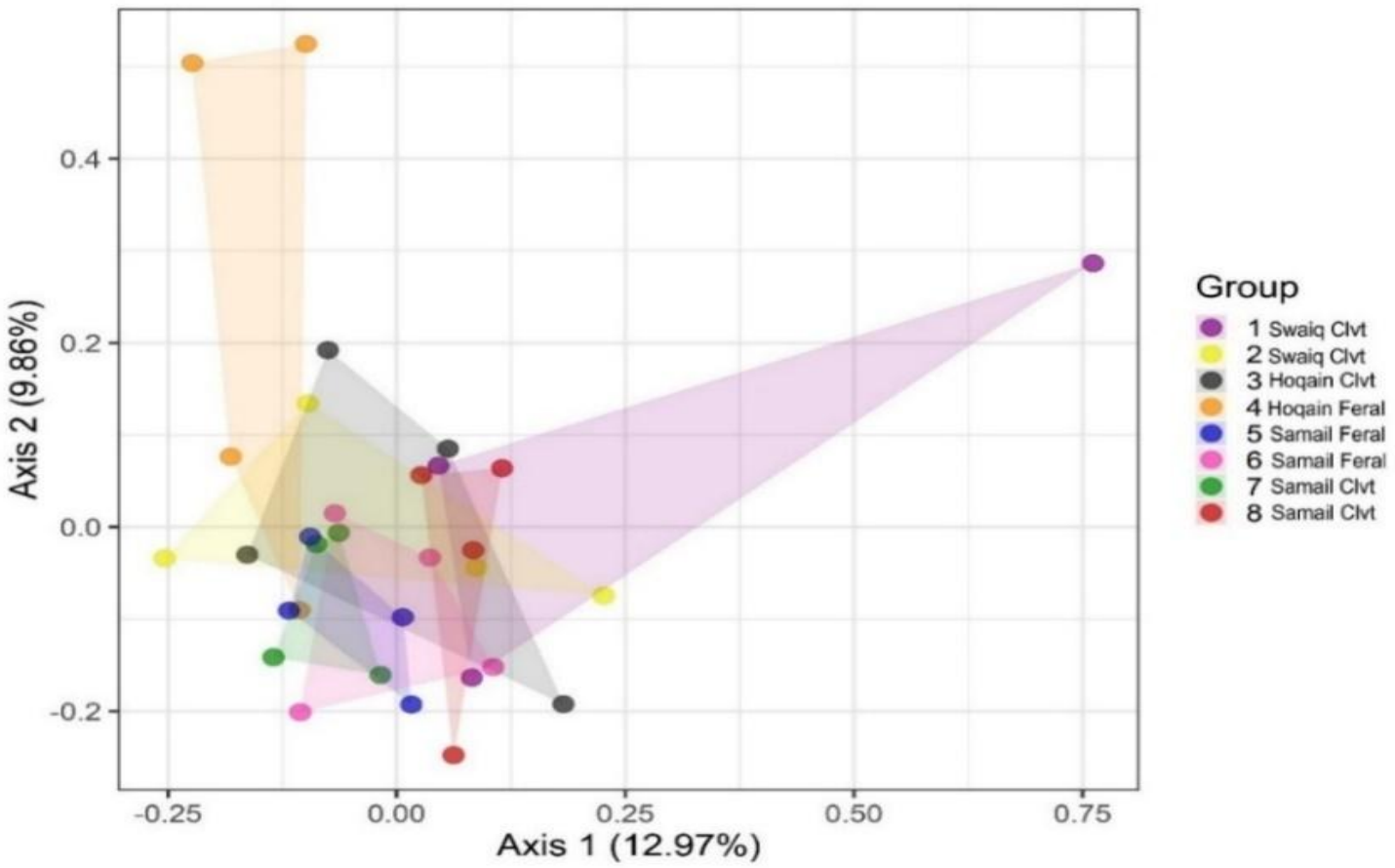


Fig 18: Principal Coordinate Analysis Un Weighted UniFrac of fungal communities between all groups (locations and cultivation type) shows clustering between all groups indicating that the fungal diversity is not affected by cultivation type or location. Except for first location from Group 1Swaiq cultivated and two locations from Group 4 Hoqain feral where fungal diversity is affected by cultivation type and location.

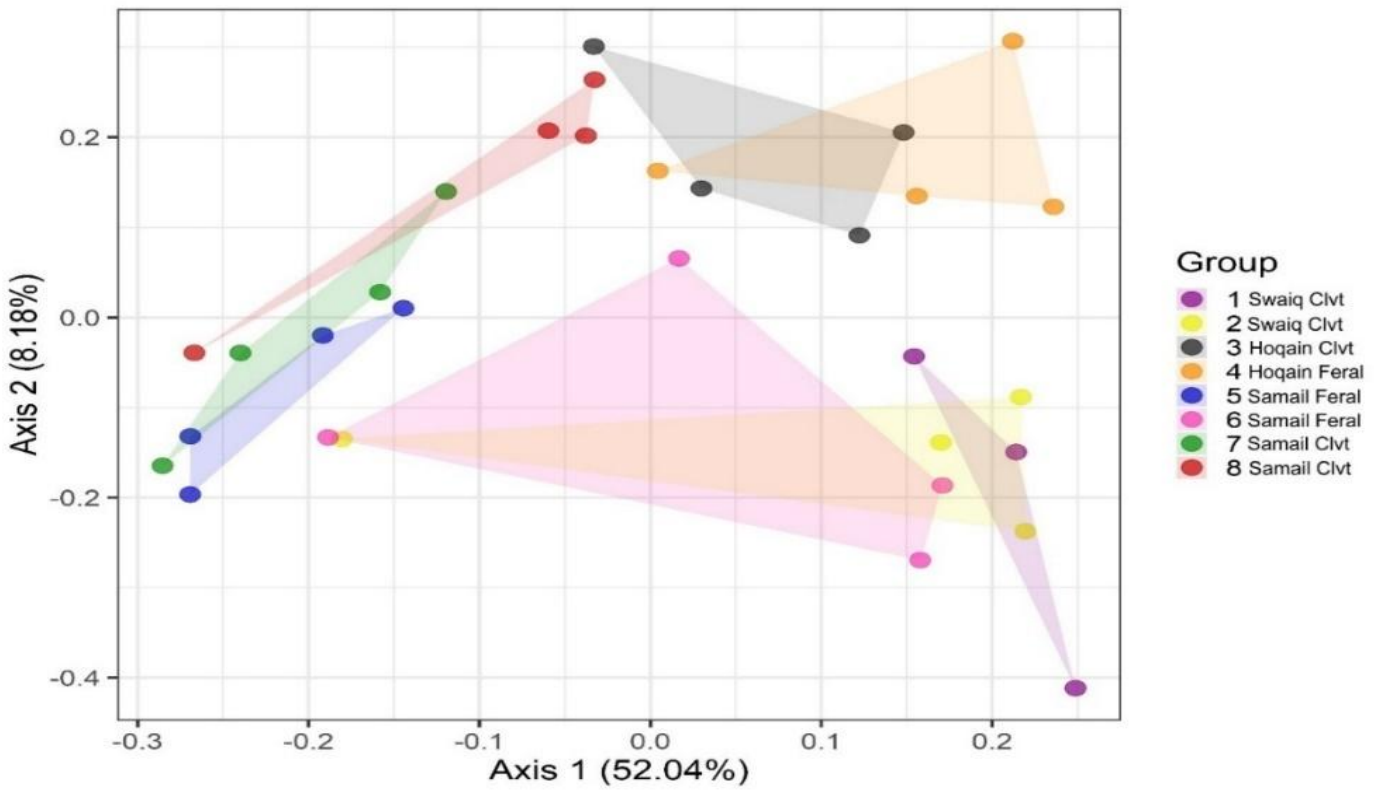


Fig 19: Principal Coordinate Analysis Weighted UniFrac of fungal communities between all groups (locations and cultivation type). Here the fungal diversity is affected by location with evidence of simple separation in clustering. Hoqain (Group 3 and 4) and Samail (Group 5, 7 and 8) are clustered separately, whereas Swaiq (Group1 and 2) is clustered with one location in Samail (Group 6). Also, fungal diversity is not affected by cultivation types.

Correlation between Operational Taxonomic Units (OTUs), soil minerals, cultivation practices and location.

The data generated of extracted DNA from soil as fungal species of Operational Taxonomic Units (OTUs) was used to construct a correlation network analysis using Graphia software with Pearson Correlation Coeffecient ($r \leq 0.8$). The graph generated defined clusters using Markov Cluster Alogrithem (MCL) with 1.1 granularity (Fig. 20). The correlation between OTUs and location and cultivation type was investigated. Total OTUs reached 1348 taxa.

As Fig. 20 shows, cluster 5, 7 and 9 were the furthest from all the clusters, suggesting much lower correlation with the other clusters. Cluster 12 and 13 were not even linked with the rest of the clusters.

Two clusters (4 and 5) were plotted in Fig. 21 and Fig. 22 and showed that the feral locations had the highest OTUs compared to the cultivated locations. For cluster 4, the OTU was in group 6 feral at 31724 taxa, whereas cluster 5 had the highest OTU is group 5 feral at 2814 taxa.

The interaction between generated OTUs and the total mineral content from soil from all locations and cultivation type was carried out using the Multivariate Principle component (PCA) using JMP14 (Fig. 23). Component 1 (x-axis) registered 28.9% of the variation while component 2 (y-axis) registered 12.2%. Positive correlation is represented by the cultivation parameter regardless of cultivation system (type 1 farming system, type 2 feral) along with the minerals: sodium, potassium, phosphorus, protein, nitrogen, TOC, calcium, zinc, aluminum, copper and iron. Clusters 1, 4, 5, 9 and 10 of OTUs from the correlation network analysis

were correlated together in the left quadrant while cluster 7 was separated on the right.

Heavy metals nickel, chromium and mercury with TIC showed a negative correlation along with the OTUs cluster 2, 3, 6, 8, 11, 12 and 13.

Cluster 4 with a positive correlation has the closest response to component 1, as seen from the graph, where the feral location registered the highest OTUs compared to the cultivated locations.

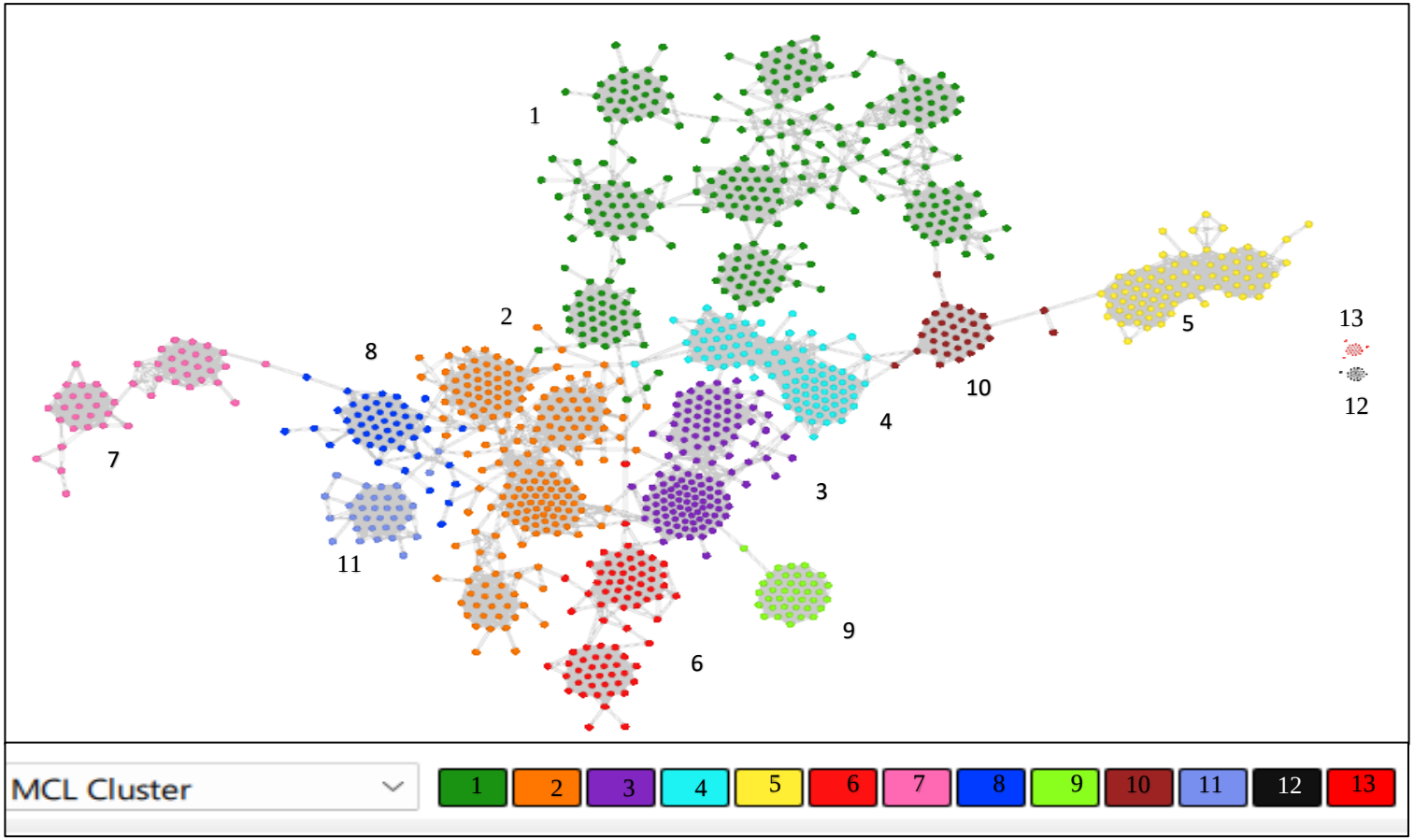


Fig 20: Correlation Network Clustering of Operation Taxonomic Units (OTUs) at Species between all groups (location and cultivation type). Markov Clustering (MCL) =1.01. Figure generated using Graphia software ($r \leq 0.8$).

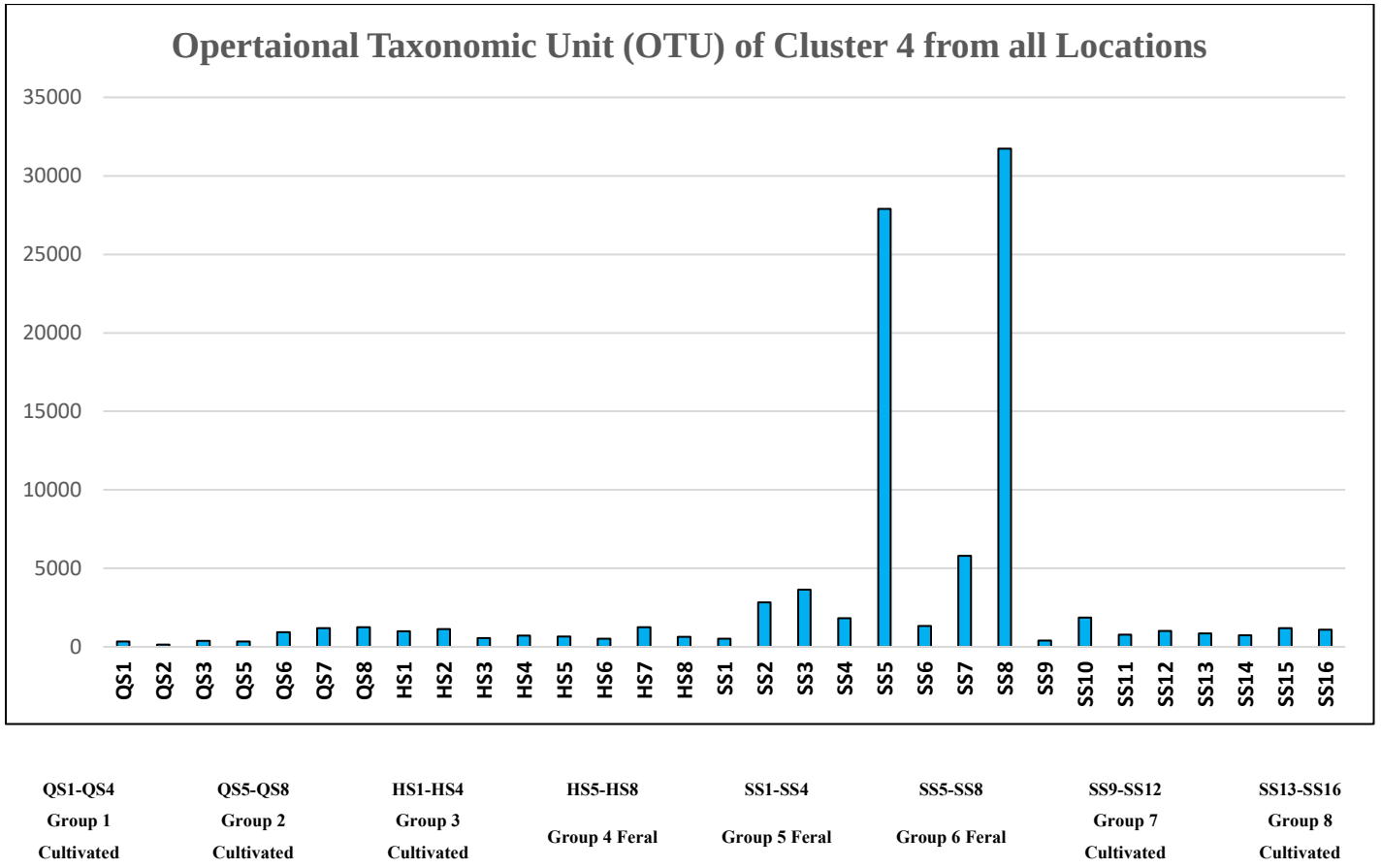


Fig 21 Operation Taxonomic Units (OTUs) from Cluster 4 of the Correlation Network Clustering at Species level between all groups (location and cultivation type), where highest OTU of cluster 5 are the samples from feral location of Group 4-5 compared to Groups 1-3 and Groups 7 and 8.

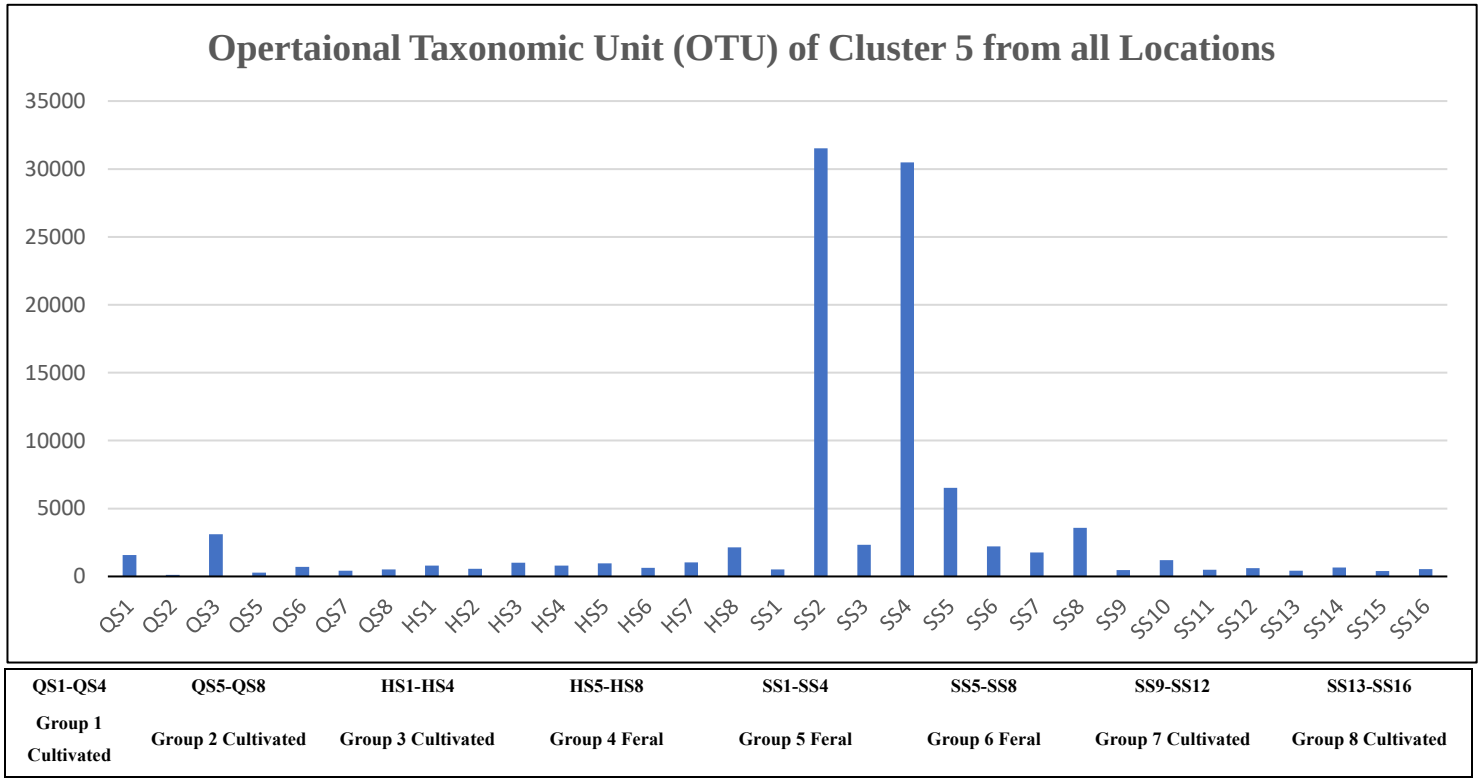


Fig 22: Operation Taxonomic Units (OTU) from Cluster 5 of the Correlation Network Clustering at Species level between all groups (location and cultivation type), where highest OTU of cluster 5 are the samples from feral location of Groups 5 and 6 compared to the other Groups.

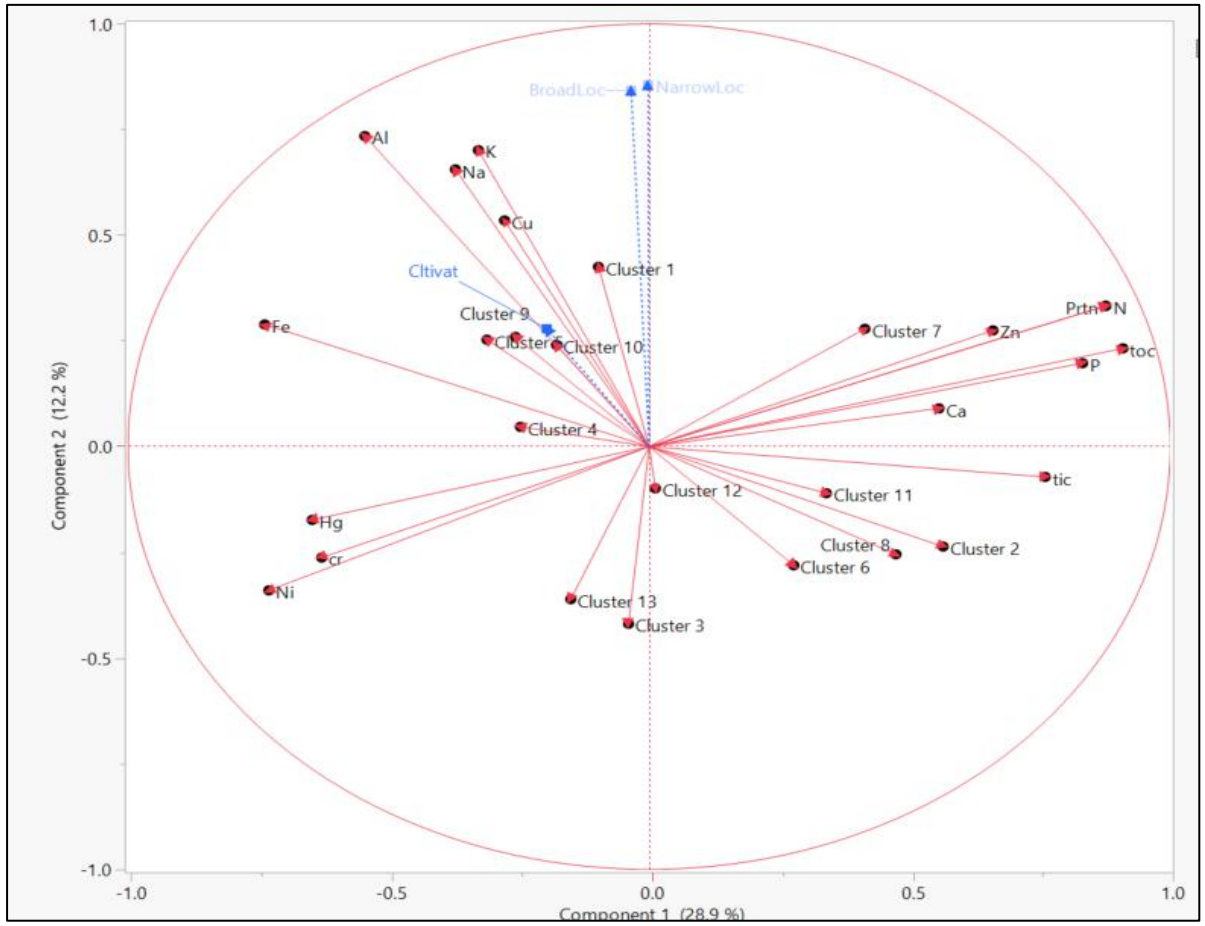


Fig 23: Multivariate Principal Analysis (PCA) between Operational Taxonomic Units (OTUs) MCL for all groups and total soil minerals. Markov Clustering (MCL) =1.01 Key Cluster 13 is not indicated. Figure generated using Graphia software.

2.4 Discussion

The soil chemical analysis from three different locations (Swaiq, Samail and Hoqain) collected from cultivated and feral date palms revealed that the TOC readings for feral ranged between 0.99 - 4.33% which is in accordance with the range of ≤1.5 % and 4% for temperate soil and semi-arid/rain fed areas that fall under the reading for the coarse texture soil (ICARDA 2013). The significant difference in TOC between feral and cultivated and between S1 feral location and all locations indicates that it is in agreement with findings from a physical and chemical analysis of rhizosphere soil of date palms in Jaipur, India by Sharma *et al.* (2014). The TOC positive correlation and TIC negative correlation is in line with the high percentage of TOC and lower percentage of TIC. This indicates a high inorganic carbon (TIC) reserves /stock in the soil owing to build up of CO_2 saturation at the soil surface via root respiration resulting in an acidic environment with organic carbon. This difference is determined by climate conditions i.e. precipitation and temperature, soil properties, land management, organic amendments and fertilization. High calcium leads to higher TIC content (Gao *et al.*, 2016). Heavy metal readings complied with readings from the assessment of soil properties in Swaiq plateau by Malik *et al.* (2018).

Nitrogen readings for all samples ranged between 0.01-0.3% regardless of cultivation type. The significant difference within Swaiq locations (Q1 and 2) with a high standard deviation, could be due to an error during the nitrogen analysis especially with the used standard during the test. The nitrogen content for the coarse

grains in arid regions ranges between 0.028 - 0.050% (Praveen *et al*., 2020). Soil analysis indicated the presence of differences in the levels of organic matter and nutrients between the soil samples. However, there was no relationship or effect of locations or cultivation systems on soil fertility. This may be related to the fact that most date palm growers in Oman use organic manures as fertilizers twice a year; manure application is a practice adapted by growers around the world (Chao *et al*., 2007; Al-Yahyai *et al.,* 2015). This could have resulted in soils having similar levels of fertility. Date palms in Oman are mostly intercropped with legumes since it serves as fodder. This could contribute to the fact that it provides sufficient nitrogen available to the date palm. An investigation on the effects of mineral and organic fertilizers and the supplementation of micronutrients on the chemical characteristics and quality of date fruits from two cultivars of date palm (Khalas and Khasab) concluded that maximum value of dry matter content was when mineral fertilizers (NPK) and organic peat and micronutrients were applied (El Mardi *et al.,* 2007). In addition, the tannin content increases after organic peat application (3 yrs) while mineral fertilizers reduced it (Yahyai *et al*., 2015).

Analysis of fungal diversity in soil samples obtained from different locations and from different cultivation systems indicated the lack of effect of locations and cultivation practices on fungal diversity, except in two locations, Swaiq 1 and Hoqain feral. For Swaiq 1 (Group 1), the samples were collected from date palms that were older than 40 years. They were initially fertilized by traditional fertilizers such as manure and ash in addition to inter cropping with lime trees and other citrus and fruit trees. They were uprooted after the lime witches' broom disease in the late

1990s as shown by Al-Yahyai *et al*. (2012). There are still a few fruit trees between the date palms but not as extensive as there used to be. The whole plot was included in a 3-year study by El Mardi *et al.* (2007) on the effect of pollination, fertilizer and mulch on physical and chemical characteristics of the fruit. The farm then adapted the fertilization and mulch programme. At this farm, the water quality is good and soil is fertile. As for Hoqian feral (group 3 and 4), the fungal diversity analysis Bray Curtis by PERMANOVA in Fig. 17, showed that the fungal diversity was affected by location and cultivation type. All samples from groups 3 and 4 from Hoqain had their own cluster around point 0.2 at Axis 2. This could be because Hoqain is an area with higher rainfall throughout the year, and the date palms sampled were younger than at the other locations. Dominant fungal groups in the rhizosphere of date palm roots showed less than 5% of unclassified group reads. These unclassified groups are bacterial and fungal taxa that do not match the latest data within taxonomic databases even at the highest taxonomic ranks (e.g. phylum phyla level). These taxa are classified as fungi or bacteria using taxonomic databases, but do not match any known phyla. As such, they are expected to be potential new phyla of fungi or bacteria (Delgado-Baquerizo, 2019).

These findings may be related to the fact that fungal diversity in the rhizosphere of date palms is affected by date palm roots which usually promote the growth of certain fungal species. A study by Al-Sadi *et al*. (2012) on fungi associated with roots of 111 date palm trees indicated that many of the fungi are common in different regions in the country. Additionally, most of the detected fungal classes in this study were similar to the classes reported by Kazerooni *et al*. (2017).

PCA analyses indicated the lack of clustering of fungal species based on cultivation systems or locations, which implies a lack of effect of cultivation systems and locations on fungal species distribution. This further supports that there is no effect of these factors on fungal diversity as well.

The study shows for the first time that fungal diversity in date palms is not affected by locations or cultivation systems except in two locations. This could be due to the fact that fungal diversity is mainly associated with date palm roots and there is less influence of locations or cultivation systems on them. Another reason for this is that even under managed farms, growers usually avoid adding any amendments to the soil or date palms, which makes them semi-organic and closely resembling the feral date palms. Future studies should investigate the potential of some of these fungi in suppressing date palm pathogens

Chapter 3

Evaluation of the antagonistic role of endophytic fungi against the date palm pathogens *Ceratocystis radicicola* and *Fusarium solani* via dual culture screening and identification of the eminent antagonistic fungi by morphology and molecular methods.

3.1 Introduction:

Date palm production in Oman is affected by wilt disease caused by the dominant and aggressive fungal pathogen Ceratocystis radicicola (Al Sadi et al., 2012b). Fusarium solani was reported by Al Yasiri et al. (2016) to cause yellowing and wilt in date palm. Date growers rely on pesticide applications as a quick way to manage the disease, however, restrictions of pesticide import have impacted the type and range of pesticides available to the farmers. A first record of pesticide resistance by Al Sadi et al. (2015) showed that 19% of Fusarium solani isolates from date palms, citrus and cucumber were resistant to hymexazol with an EC50 level that surpassed 1000µg/ml. Reducing use of pesticides and using biological control agents (BCAs) is the way forward for a more sustainable agriculture.

Endophytes and rhizosphere BCAs derived from the host plant and environment will provide an effective and durable since they are exposed to the same environmental stresses and fluctuations (Karunasinghe et al., 2020). The aim of this study was to isolate rhizosphere fungi from the rhizosphere soil and roots of cultivated and feral date palms and few fungal isolates were selected for screening as potential antagonist and identified morphologically and by DNA sequencing Theses isolates

were screened against two date palm wilt pathogens Ceratocystis radicicola and Fusarium solani.

Application of plant protection products (PPPs) is one of the management approaches used to control plant diseases. Historically, these have been synthetic chemicals that are designed to disrupt the target pest organism life cycle or its cellular composition. For example, acarids or insects are killed on contact by suffocation and outer membrane (exoskeleton) abrasion leading to desiccation (Rabiey *et al*., 2019). Recently, use of these products has become more limited due to ecological concerns. For trees, the methods of application are either above ground as in aqueous sprays to the foliage or bark, in which the chemicals break down or disintegrates over time. The other method is internal i.e. through direct injection into the tree base to reach the vascular system where additives can be included to facilitate penetration through the bark. Alternatively, in the case of root and soil borne diseases, the tactic for soil application is by injection into soil or adding a sterilizing agent such as phenols or methyl bromide. However, these chemicals will persist for longer periods due to binding to the soil particles.

Another management method is the application of biocontrol agents (BCAs), which involves the use of microorganisms (fungi, bacteria, viruses, nematodes) that already co-exist within the host environment. BCAs from the host environment are generally used because they provide a narrower range of target specificity which reduces their harm to non-target organisms (Rabiey *et al*., 2019). The BCAs reach a certain threshold that will have an ecological and economic impact to reduce the pest population, which enables the host to gain health and strength. They act

specifically on the target pest organism, so minimal harm occurs to non-target organisms. That is why they are considered to be substantially safe. Another positive aspect is that the BCAs do not move or travel away from the application site. Application mode is similar to that used for PPPs, aiming to maximize contact with the target pest (Rabiey *et al.*, 2019). Challenges encountered for use of BCAs or PPP's for trees is generally the restricted access to the canopy and the growing area, and the main constraints with developing BCA are identification, characterization, formulation and application mode and frequency (Rabiey *et al.*, 2019).

According to Rabiey *et al.* (2019), the mode of action of BCA's can be through several mechanisms. The first is direct, through antibiosis by secretion of allelochemicals that are either diffusible metabolite (lipopeptides, bacteriocins, antibiotics, biosurfactants and cell wall degrading enzymes) and/or volatile compounds that interfere with the phytopathogen metabolism leading to inhibition of pathogen development. The second mode of direct action is parasitism, which is either necrotrophic by killing the host cell or biotrophic that is living with the host. Another mode of action is reducing pathogen virulence and infection pressure by competition, whilst an indirect mode of action is through induced plant resistance and priming. One such mode of action is where an endophyte induces delocalized plant defence reactions known as induced systemic resistance when used as an antagonist against a pathogen (Rabiey *et al*., 2019). During the initial stages of endophyte colonization, the interactions between the plants and the beneficial microorganisms trigger the plants immune response similar to the response against plant pathogens. At later stages of plant growth and/or interaction, mutualists are

able to escape their hosts defence response and colonise the plants (Rabiey *et al*., 2019). For example, tomato wilt caused by *Fusarium oxysporum* has been suppressed with the combined treatment of salicylic acid and *Trichoderma harzianum* (Houssien *et al.,* 2010). Salicylic acid is involved in inducing enzymes in the plant that catalyze biosynthetic reactions to produce defence compounds such as polyphenols and pathogenesis related (PR) proteins. It was shown that the combined treatment amplified the activity of polyphenol oxidase (POP) and polyphenol peroxidase (POD) levels and that this correlated with pathogen resistance (Houssien *et al*., 2010).

Endophytic fungi are symbiotic fungi that grow in different plant parts externally and/or internally. As with all microbiota of the soil, fungi have a two-way influence on the plant. They are either destructive by operating as a pathogen to the plant (as a single pathogen or in complexes), or they have a constructive and beneficial effect on the plant by decomposing plant residues and supplying nutrients, determining the rhizosphere microbiome, stimulating growth and providing a stimulus to increase plant resistance to pathogens or acting as an antagonist to the pathogens (Miao *et al.,* 2016).

Endophytes and rhizosphere fungi have been the subject of a lot of studies that focus on finding alternative biocontrol agents against plant diseases. For example, Miao *et al.* (2016) reported the isolation of 113 fungi from the soil adhering around the roots (rhizosphere) of Chinese ginseng (*Panax notoginseng*) plantations in which 13 isolates showed antagonistic effects against four pathogens of Chinese ginseng root rot. The isolates were from the genera of *Pestalotiopsis, Cladosporium,*

Trichoderma and *Chaetomium*. In an extensive review by Lahlahi *et al.* (2022) it was stated that the "Rhizosphere is a Potential Reservoir of Biopesticides". The authors discussed research that covered the use of bacteria, fungi and yeasts as biocontrol agents (BCAs) and the impact, biology, mode of action and other data are still being researched on plant diseases on different crops. Also, Lahlahi *et al.* (2022) provided a list of available commercial BCA products and presented the obstacles encountered in screening for new BCAs from the research laboratories up until registering and marketing the product.

The *Trichoderma* spp. are amongst the most studied antagonistic fungi. In Oman, along with *Trichoderma* spp., other antagonistic fungal species from *Aspergillus* and *Talaromyces* have also been investigated (Al Sadi *et al.*, 2015; Halo *et al.*, 2019; Al Shibli *et al.*, 2019; Kazerooni *et al.*, 2019; Karunasinghe *et al.,* 2020). The antagonism effects of *Aspergillus* and *Talaromyces* species against cucumber damping off caused by *Pythium aphanidermatum* were shown by Karunasinghe *et al.* (2020) and Halo *et al.* (2019) respectively. The antagonism was shown by detecting and extracting glucanases, siderophores and cellulase metabolites.

A number of *Trichoderma. harzianum* strains have been established as commercial BCAs (Lahlahi *et al.,* 2022). For example, Omara *et al*. (2023) reported that a bioformulation mix of *cowpea* waste, cassava scraps and *T. lixii* applied to soil infected with *Fusarium oxysporum* increased the length and vigour of cowpea seedling. The mixture also reduced infection by inducing systemic resistance and activating the plant to produce defense related enzymes. Furthermore, *T. lixii*

colonizing the root system served as a physical barrier and released antimicrobial exudates into the rhizosphere.

There are several methods used for screening the rhizosphere biome that are determined by the microorganism used and type of disease. One method is the diffusion method where the tested antagonist is grown in liquid media to obtain the lytic enzymes or other metabolites and the suspension is then used to treat the cultured pathogen and record the inhibition zone (Miao *et al.,* 2016). Another method is the dual-method, where direct culture of mycelial plugs from the tested isolate and the pathogen are inoculated in one Petri dish at equal distances, incubated and the inhibition zone is recorded (Redda *et al.,* 2018; Karunasinghe *et al.,* 2020). In this study the dual culture method was used.

Only a few studies have been reported on the date palm rhizosphere, especially that from feral date palms. Therefore, its potential for providing BCAs for date palm diseases has not yet been tapped.

The first objective of this study was to screen fungal isolates from soil and roots isolated from cultivated and feral date palm as potential antagonists against two date palm wilt pathogens; *Ceratocystis radicicola* and *Fusarium solani*. The second objective was identification of the selected antagonistic fungi morphologically and by DNA sequencing .

3.2 Materials and Method:

3.2.1 Isolation and selection of endophytes

The soil and root samples used were from the collection mentioned previously in Chapter 2. The soil was spread directly on PDA in Petri dishes and no dilution was done. The roots were washed and cut 1-5 cm in length, surface sterilized in 5% sodium hypochlorite (household bleach) for 3 min, followed by 3 rinses in sterile distilled water and blotted on sterile filter paper. Root samples were cultured directly onto the PDA in Petri dishes. The PDA in Petri dishes were prepared by adding agar to the PDA in a ratio of 3:1 (PDA: agar). This was done to ensure that any fungi will develop and to prevent over growth of fast developing fungi. All cultures were incubated at 23-24℃ for 3- 7 days and observed daily for fungal growth. Pure isolates were prepared by using a cooled sterile inoculating needle to lightly touch the colony picking up spores and avoiding any PDA medium. It was then inoculated into a new PDA in Petri dish, labeled and sealed with parafilm. The inoculating needle was sterilized by dipping in 95% ethanol and flaming. The isolates were incubated at 23-24℃ for 3-7 days and observed daily for colony growth. Isolates were selected for the test based on formation of exudates apparent by discoloration of the PDA around the colony. Other isolates of *Trichoderma* and *Aspergillus* were also selected. In addition, *Trichoderma asperellum* from the fungal collection of the Plant Pathology lab, University of Nottingham, UK was also used.

The isolates were evaluated for their antagonism by investigating their ability to suppress growth of date palm wilt pathogens *Fusarium solani* and *Ceratocystis*

radicicola, from the fungal collection at the Plant Pathology lab, College of Agriculture and Marine Science, SQU, Al Khodh, Oman and Plant Pathology Research Lab Ministry of Agriculture and Fisheries, Sohar, Oman. The evaluation was carried out as dual culturing following a modified protocol of Redda *et al.* (2018), Anees *et al.* (2010), Goes *et al.* (2002) and Sreeshama *et al.* (2016).

The dual cultures were carried out using diluted PDA of 3:1 ratio (PDA: agar) due to rapid growth. A 5 mm borer disc acquired from the rim of the fungal growth from 5–7-day old isolates were cultured on opposing sides of 90 mm PDA in Petri dishes. They were incubated at 24°C and observed the following day for mycelial growth and measured (T) daily until the growth stopped or the two fungi met. This generally occurred from 3-10 days. The inhibition zone was also measured. For the controls, all the isolates used were cultured using 5 mm discs and placed at the center of the PDA in Petri dish. The growth of the mycelia was measured daily and considered as the negative control (C). Each isolate combination and control had 3 replicates. The inhibition percentage (I%) was calculated using the equation as per Redda (2018):

$$I\%=(C-T)/C \times 10$$

Where C is the measurement of the mycelial growth in the control, T is the measurement of the mycelial growth in the dual culture and I% is the inhibition percentage.

3.2.2 Molecular identification of the antagonist endophytic fungi

The endophytic isolates that showed antagonism against *Fusarium solani* and *Ceratocystis radicicola*, and the *Fusarium solani* isolates as cross checks were identified molecularly. Isolates aged between 6-10 days were used. Two plates of each isolate were used as replicates. The cultures were scraped under a laminar hood and added to a lysing tube G. The tubes were immersed in liquid nitrogen for 3 minutes, then they were lysed and ground using an MP BIOMEDICALS FastPrep®24 instrument. After grinding, the DNA was extracted using Qiagen DNA DNeasy Plant Mini Kit. The quality was checked by a nanometer.

For PCR, the procedures of Al Sadi *et al.* (2011b) were used as follows; reaction mix of 25 µl was: 0.4mM each of primer ITS1 and ITS4, 25ng of DNA template, with PuReTaq Ready-To-Go PCR beads (GE Healthcare) and Milli-Q water up to a final volume. The PCR conditions were 95ºC (10 min), 95ºC (30 s) for 35 cycles, 55ºC (30s), 72ºC (90s) and final extension 72ºC (10 min). The modified conditions included the change in ITS primer and reaction volumes and conditions. The PCR conditions was modified twice till the resulting ITS amplification was clear. The DNA template of 1µl was added to the PCR beads (PuRETaq TM Ready- to- go ™ PCR beads, GE Healthcare) with 1µl each primer: Forward Primer ITS 5, Backward Primer ITS 4 and Milli-Q water 22 µl. The primers sequences were ITS 5 Forward (5'GGAAGTAAAAGTCGTAACAAGG-3') ITS 4 Reverse (5'-TCCTCCGCTTATTGATATGC-3') (White *et al.,* 1990). The PCR tubes were mixed and were placed in a Applied Biosystem Veriti 96 well Thermal cycler (Model 9902) with reaction conditions herewith for denaturation at 94ºC for 3

minutes, annealing at 94ºC for 1 minute then 50ºC for 1 minute then 72ºC for 3 minutes repeated for 35 cycles. Finally, extension at 72ºC for 7 minutes for 1 cycle. The PCR products were loaded for electrophoresis in 1% agarose gel in 1x TBE buffer and were dispatched to Macrogen Korea to be purified and sequenced. Maximum Likelihood for Maximum Parsimony and Bayesian Inference phylogeny tree was constructed as per the protocol shown in Annex 6.

3.2.3 Morphological and molecular analysis of three potential new *Talaromyces* species.

The endophyte labeled C that was cultured from cultivated date palm roots from Samail location 1 (referred to as S15 /group 8 from Chapter 2) was considered as a previously unknown species and was identified as *Talaromyces* species by DNA sequencing. The *Talaromyces* species was examined for further identification. The DNA was labelled as C11 and C12 each with 2 replicates a and b. Sample C11a and C11b were extracted from the same culture which was characterized by a single colony with prominent red pigmentation on PDA media. Sample C12a and C12b were extracted from the same culture which was characterized by multiple dispersed colonies with or without prominent red pigmentation on PDA media. Only C11a, C11b and C12b were used for morphological and molecular identification since C12a proved difficult to maintain uniform growth.

Morphological identification was carried out following procedures by Frisvad *et al*. (2013) and Wei *et al*. (2021). However, whilst Frisvad *et al*. (2013) used 8 types of media, Wei *et al*. (2021) only used only 4 media, described in Table 7. Both methods

inoculated the strains at three points in each Petri dish and incubated at 25°C in darkness for 7 days. The colony diameter, colour and morphology and presence of media pigmentation was recorded.

Due to availability of the media and also the rate of growth of the isolates, the procedure we used was modified as follows. Each strain was cultured on 7 different media as shown in Table 8. The isolate was inoculated at the center of the 90 mm Petri dish in 3 points. Every isolate was replicated with 3 Petri dishes from each media. They were incubated at 25°C in darkness between 7-14 days, according to rate of growth. After the incubation period, the diameter of each colony was measured for each plate. The Petri dishes were photographed obverse and reverse. Colony diameter was statistically analyzed by R software (version 4.0.3). Comparison of data was performed via one-way analysis of variance (ANOVA) followed by Tukey's test ($p < 0.05$). All the values are expressed as the mean ± standard deviation (SD) for three measurements.

Table 7: Media used for morphological identification of 3 *Talaromyces* spp.

Media for morphological identification	Abbreviation	Frisvad *et al.* (2013)	Wei *et al.* (2021)
Czapek-Dox Yeast Autolysate Agar	CYA	✓	✓
Czapek-Dox Yeast Autolysate Agar with 5%NaCl	CYAS	✓	-
Yeast Extract Sucrose Agar	YES	✓	✓
Creatine Sucrose Agar	CREA	✓	-
Dichloran 18% Glycerol Agar	DG18	✓	-
Malt Extract Agar	MEA	✓	✓
Blakeslee Malt Extract Agar	MEA2	✓	-
Oatmeal Agar	OA	✓	✓

Table 8: Media and incubation conditions used for identification of 3 *Talaromyces* spp.

	Media	Incubation conditions
1	CYA (Czapek-Dox Yeast Autolysate Agar)	25˚C dark 14 days
2	YESA (Yeast Extract Sucrose Agar)	25˚C dark 7 days
3	CDA (Czapek-Dox Agar)	
4	MEA (Malt Extract Agar)	
5	OA (Oatmeal Agar)	
6	CMA (Corn Meal Agar)	
7	CYA (Czapek-Dox Yeast Autolysate Agar)	37˚C dark 7 days followed by 30˚C dark 7 days
8	MEA (Malt Extract Agar)	37˚C dark 7 days

The DNA of C11a, C11b, and C12b was amplified using PuRETaq TM Ready- to-go ™ PCR beads from GE Healthcare for the PCR reactions. The PCR reactions were done separately with three primers with different conditions as detailed in Table 9. Each PCR tube contained 1µl DNA template, 1µl of each primer (forward and reverse) and finally SDW at 22 µl. The SDW used was checked prior to use by Nano drop to ensure purity. The PCR tubes were vortexed to ensure homogenized mixture and placed in an Applied Biosystem Veriti 96 well Thermal cycler (Model 9902) with reaction conditions as per requirement mentioned in Table 7.

PCR products were loaded for electrophoresis in 1% agarose gel in 1x TBE buffer with 2-log dye ladder (0.1-10 kb) and viewed for strong bands. The PCR products were dispatched to Macrogen Korea to be purified and sequenced. Maximum Likelihood for Maximum Parsimony and Bayesian Inference phylogeny tree was constructed as per the protocol shown in Annex 6.

Table 9: PCR reaction used for each primer and its sequence.

Primer name	Code	Sequence	PCR conditions
Large subunit of nuclear ribosomal DNA (28S)	LROR	ACC CGC TGA ACT TAA GC	Denaturation at 94ºC for 3 minutes, Annealing at 52 ºC for 1 minute then 72 ºC for 3 minutes repeated for 35 cycles. Extension at 72 ºC for 7 minutes for 1 cycle.
	LR5	TCC TGA GGG AAA CTT CG	
Translation elongation factor 1-alpha (TEF-1a)	EF1-983F	GCY CCY GGH CAY CGT GAY TTY AT	Denaturation at 94ºC for 3 minutes, Annealing at 60 ºC for 1 minute then 72 ºC for 3 minutes repeated for 35 cycles. Extension at 72 ºC for 7 minutes for 1 cycle
	EF1-1567R	ACH GTR CCR ATA CCA CCR ATC TT	
DNA-dependent RNA polymerase II subunit 2 (RPB2)	bRPB2-6F	TGG GGY ATG GTN TGY CCY GC	
	bRPB2-7R	GAY TGR TTR TGR TCR GGG AAV GG	

3.3 Results

3.3.1 Endophyte antagonism

Three unidentified *Trichoderma* species were isolated from location 1 (Samail Feral). Fungi labeled B and D were isolated from the soil of Feral date palms, while fungus C was isolated from cultivated date palm roots.

Antagonism was demonstrated by the endophytic fungi with varying degrees. Fungus A, identified as a mix of *T. harzanium* and *T. lixii*, had unclear antagonistic effect due to its rapid growth rate that had covered the pathogens as seen in Figs 24 and 25.

Fungus D, identified as *Penicillium griseofulvum*, had the least antagonistic effect. The growth pattern was scattered and very difficult to take measurements even on a daily basis (see Figs 26 and 27).

Fungus B, identified as *Aspergillus terreus* showed antagonism with a clear inhibition area (Figs 28 and 29) even after a month from culturing. In addition, a discoloration of the PDA media and a more yellow pigmentation was apparent.

Finally with Fungus C, identified as two *Talaromyces* species (Fig. 30), both species had a strong antagonism although with different growth patterns. *Talaromyces* species a, had a uniform growth, while Talaromyces species b, had a more dispersed growth (Figs 31 and 32). Therefore, taking a measurement was challenging since initially the two species were mixed and were only later distinguished after multiple re-isolations. Producing pure isolates also proved difficult. Antagonism of both isolates was apparent with clear inhibition zones that remained even after a month of culturing. Both isolates produced a deep red pigment in the PDA as shown in Figs 33 and 34.

Ceratocystis radicicola and *Fusarium solani* average growth measurement for 4 days with *Talaromyces* sp. and *Aspergillus terreus* with the controls are shown in Table 10, along with the inhibition zone measurements. The smallest inhibition zone recorded was with dual culture of *Talaromyces* x *Fusarium solani and Talaromyces* x *Ceratocystis radicicola* at 3.6% and 13.3% respectively, whilst *Aspergillus terreus* resulted in a higher percentage of inhibition at 38.9% with *Ceratocystis radicicola* and 13.8% with *Fusarium solani*.

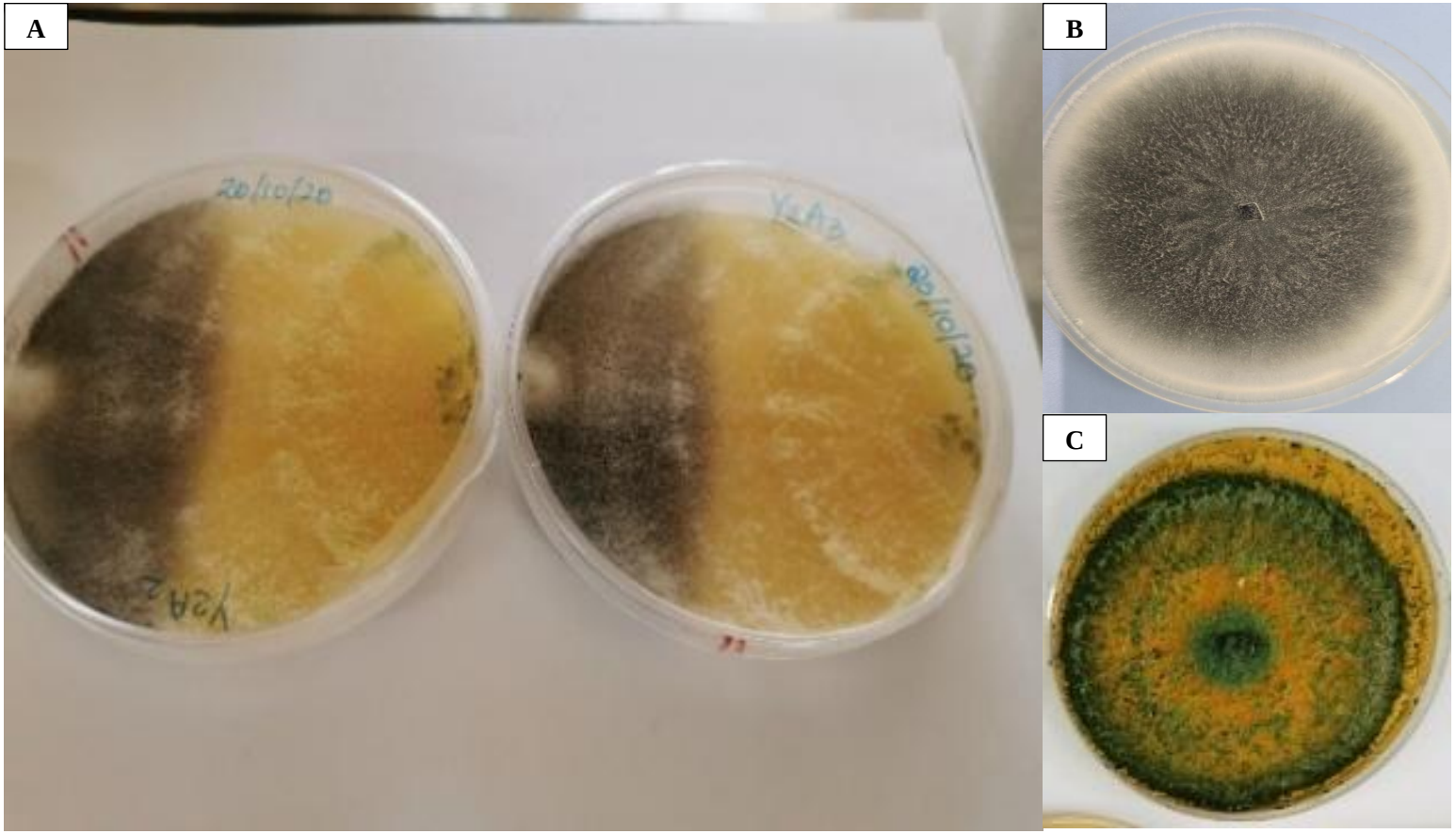


Figure 24: Dual Culture. **A:** *Ceratocystis radicicola* (left) with a mix of *Trichoderma. harzanium* and *T. lixii* (right) antagonism effect is not clear, *T. harzanium* and *T. lixii* are growing over *C. radicicola* which seem restricted. **B:** *C. radicicola* pure culture **C:** Mixed culture of *T. harzanium* and *T. lixii.*



Figure 25: Dual culture. **A:** *Trichderma harzanium* and *T.lixii* **B:** *Fusarium solani* pure culture. **C,D and E:** Dual culture of mix of *T. harzanium* and *T. lixii* (left) with *F. solani* (right) showing clear over growth of *Trichoderma* on *F.solani*, where its growth remains without disruption with clear red pigmentation on the perimeters of *F.solani*.

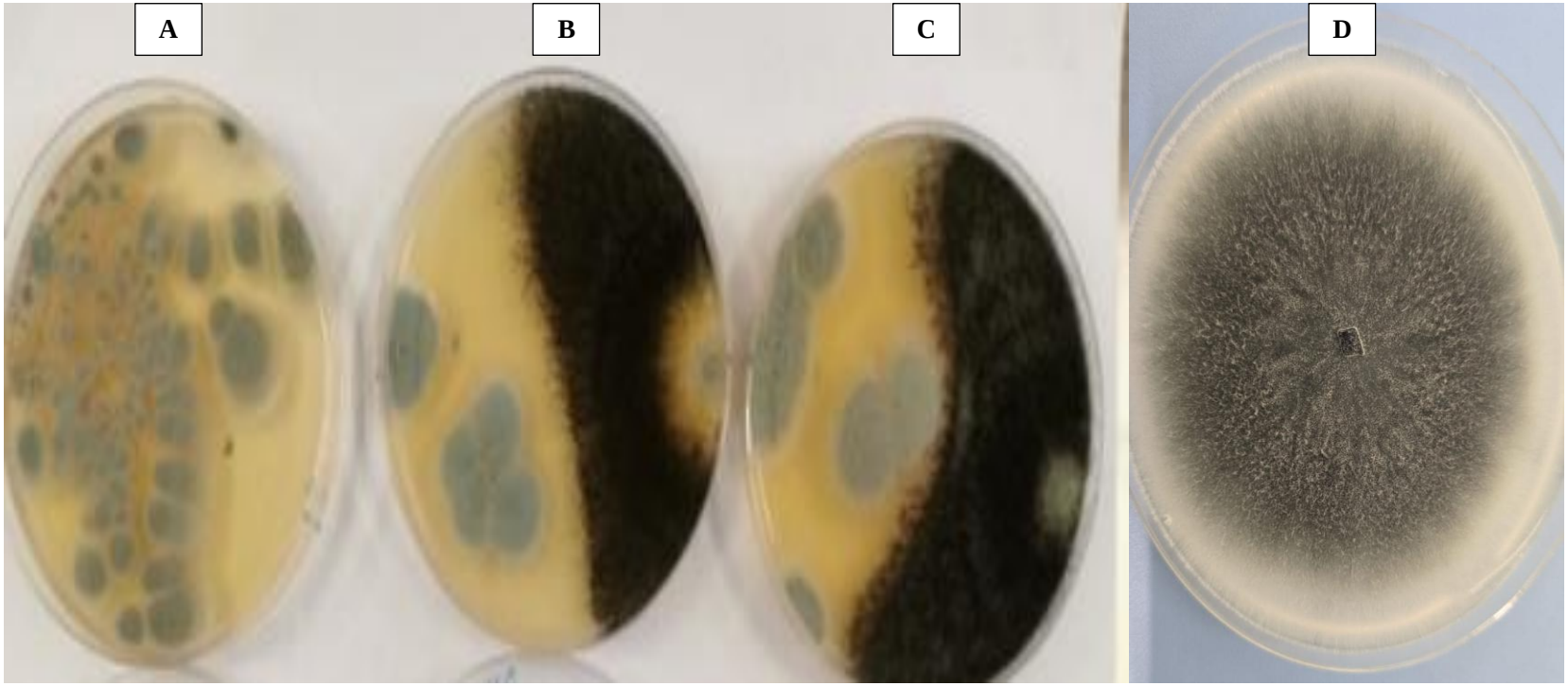


Figure 26: Dual Culture. **A:** *Penicillium griseofulvum* pure culture with clear dispersal of the colonies **B**:Dual culture of *P. griseofulvum* (on the left) with *Ceratocystis radicicola* (on the right) showing good antagonism effect and inhibition zone **C:** Dual culture of *P. griseofulvum* (on the left) with *C. radicicola* (on the right) showing restricted growth of *C.radicicola* without a clear inhibition zone **D:** *C. radicicola* pure culture.

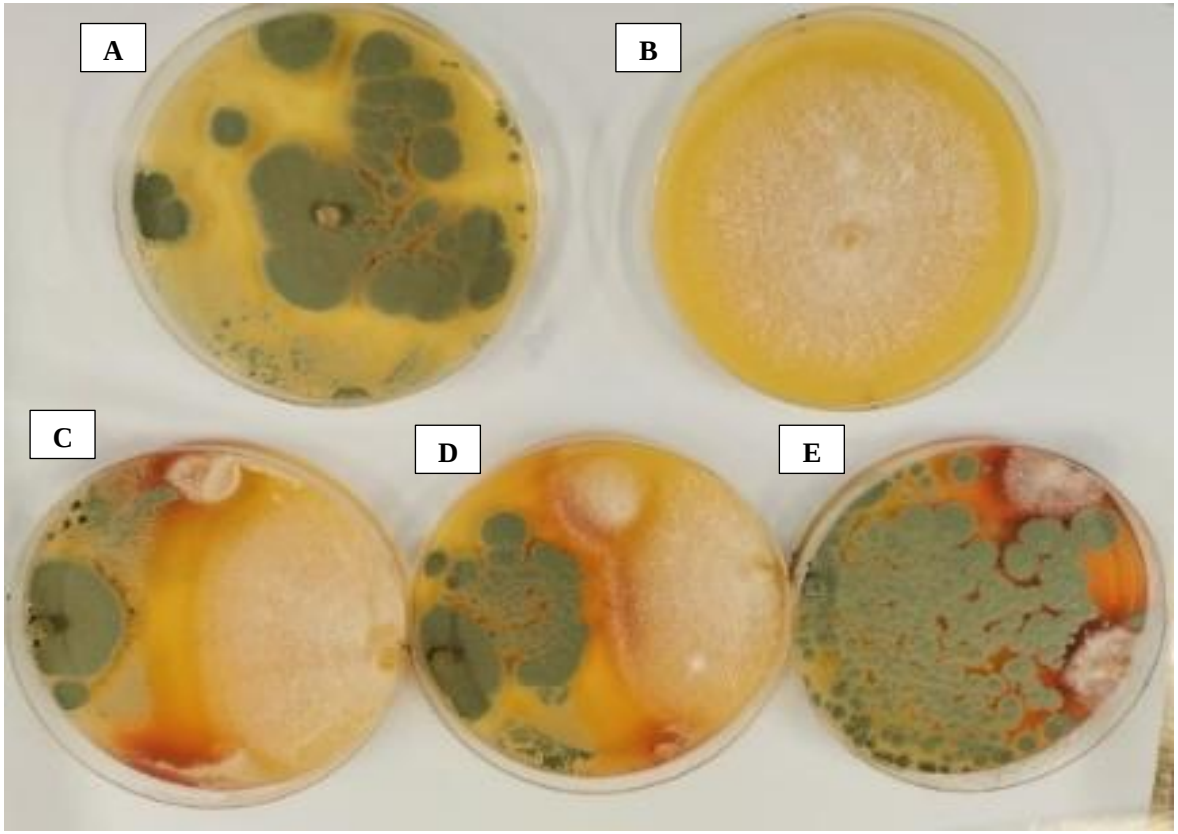


Figure 27: Dual Culture. **A:** *Penicillium griseofulvum* pure culture **B:** *Fusarium solani* pure culture **C:** Dual culture of *P. griseofulvum* (left) with *F. solani* (right) showing antagonism effect and clear and wide inhibition zone and red\ orange pigmentation only on the far edges of the inhibition zone. **D:** Dual culture of *P. griseofulvum* (left) with *F. solani* (right) showing antagonism effect and smaller inhibition zone and red\ orange pigmentation spread in most of the inhibition zone **E:** Dual culture of *P. griseofulvum* (left) with *F. solani* (right) showing restricted growth with no clear or minimal inhibition zone, but higher red/ orange pigmentation.

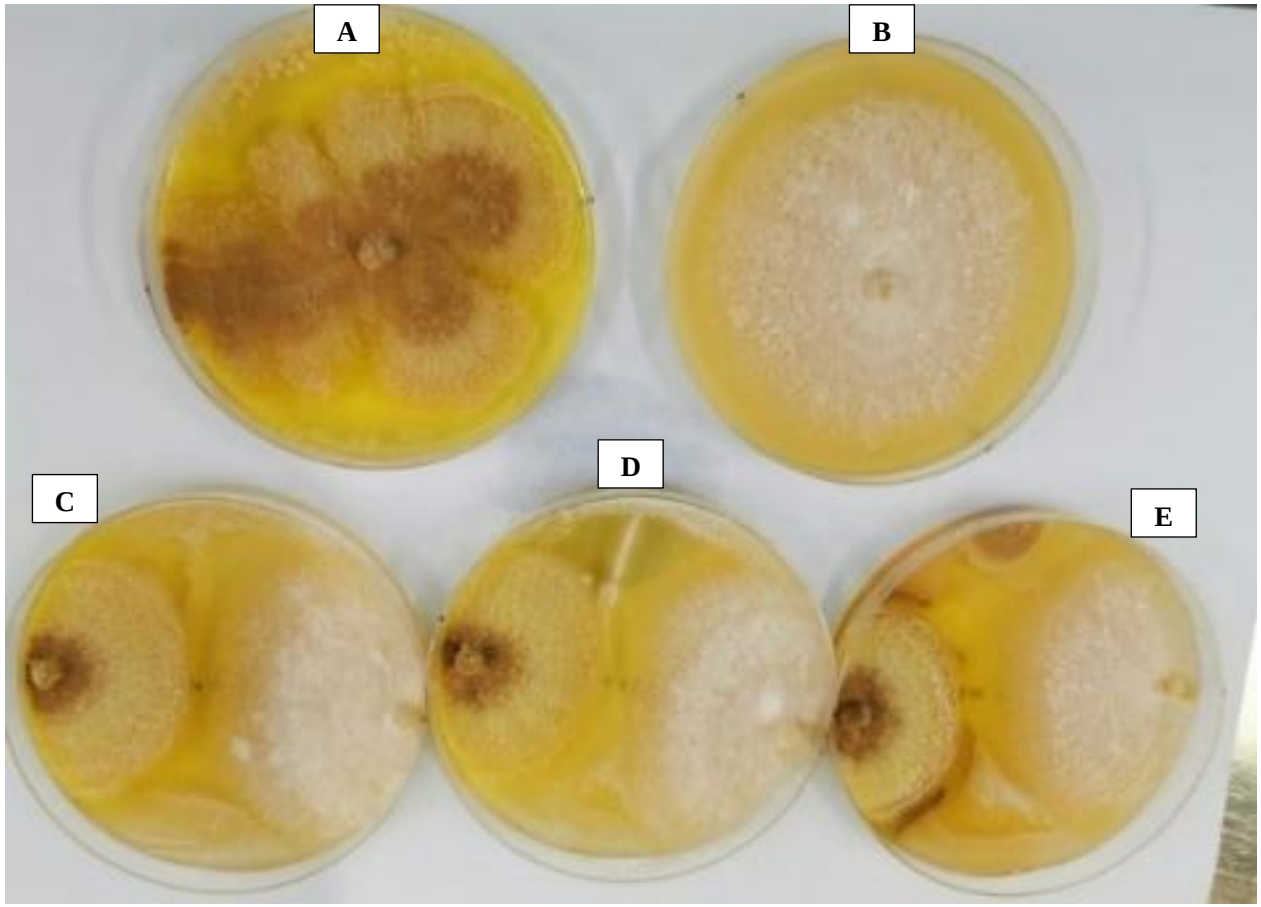


Figure 28: Dual Culture. **A:** *Aspergillus terreus* pure culture **B:** *Fusarium solani* . **C, D and E**: Dual culture of *A. terreus* (left) with *F. solani* (right) showing good antagonism effect and inhibition zone with a deep yellow pigmentation.

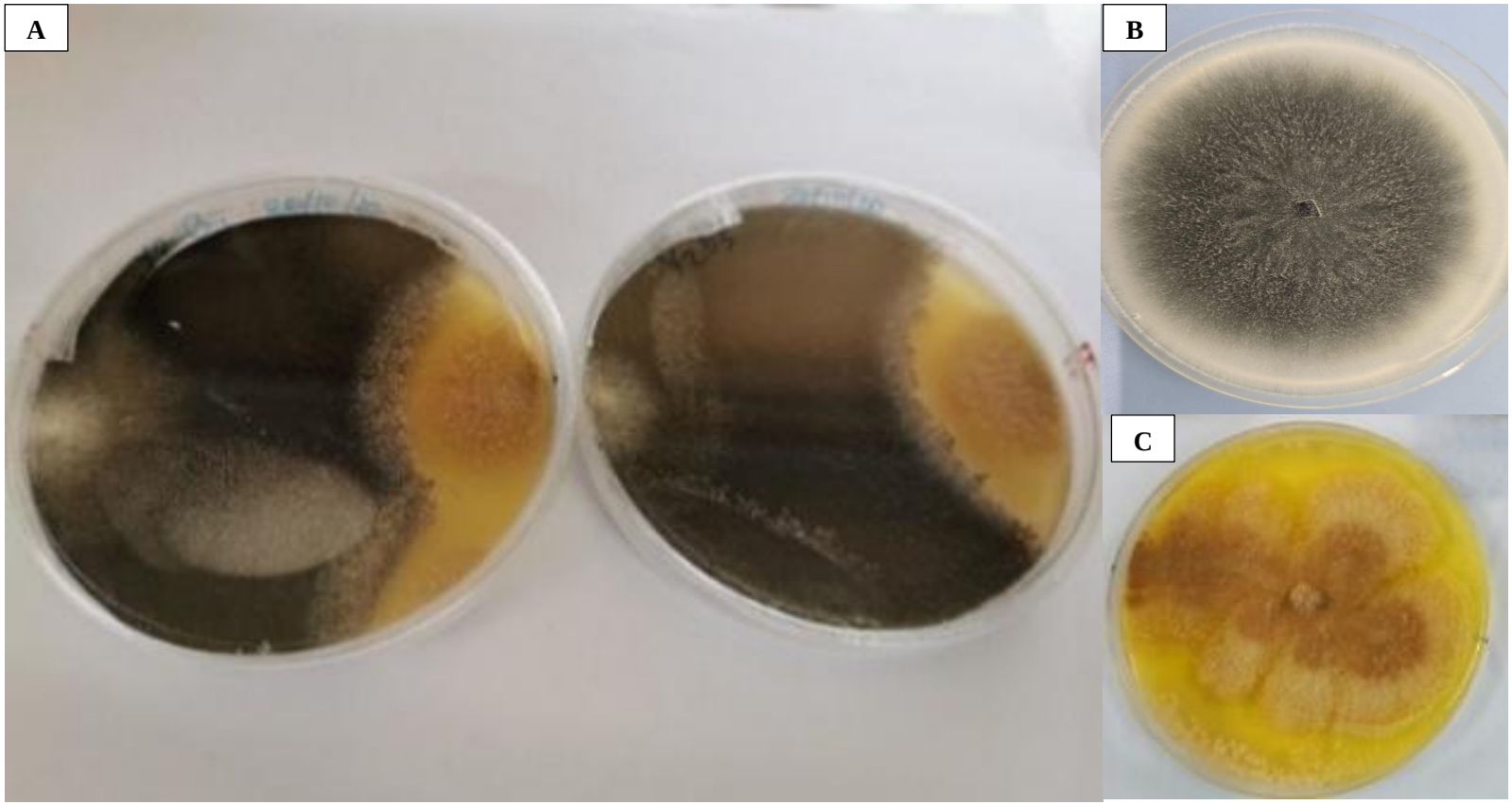


Figure 29: Dual culture **A:** *Ceratocystis radicicola* (left) with *Aspergillus terreus* (right) showing good antagonism effect and inhibition zone Due to the fast growth of the *C. radicicola* the growth of *A.terreus* looks restricted and the inhibition zone was narrow 30 days after inoculation. **B:** *C. radicicola* pure culture **C:** *A. terreus* pure culture.

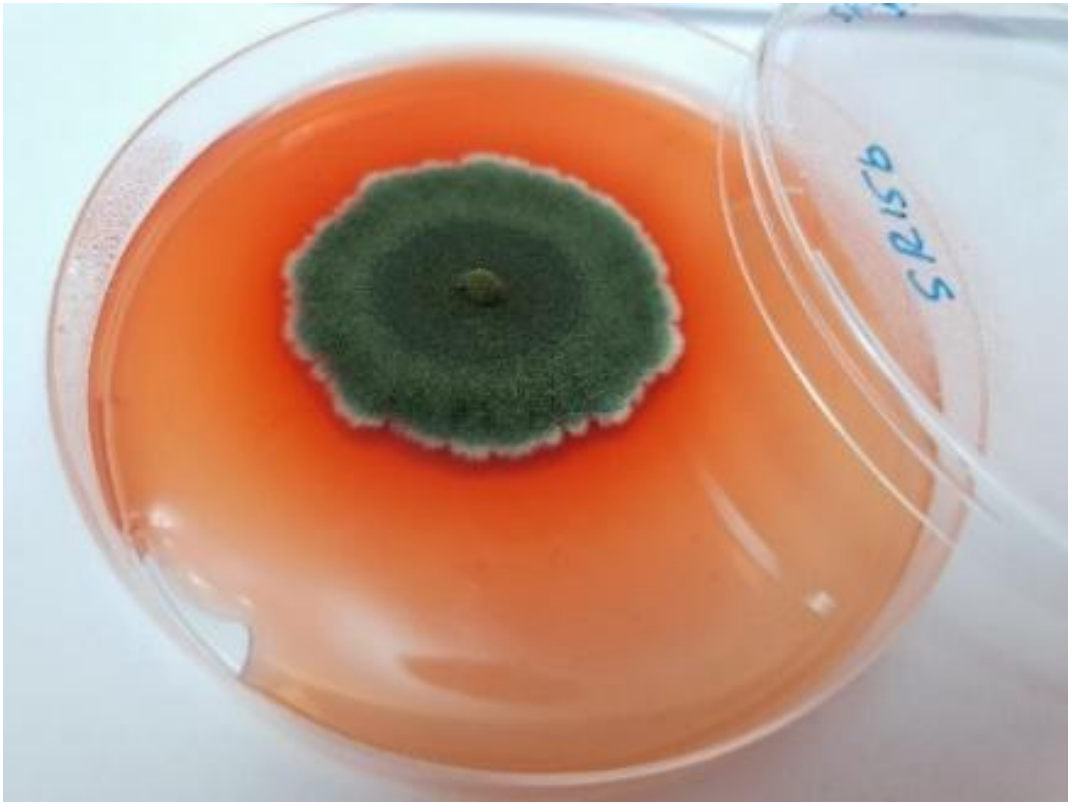


Figure 30: A pure isolate of *Talaromyces* species from the initial direct culture from date palm roots. It was isolated from Samil location 1 of cultivated date palm (sample S15). Evident uniform growth and production of red pigment (azaphilone polyketide).

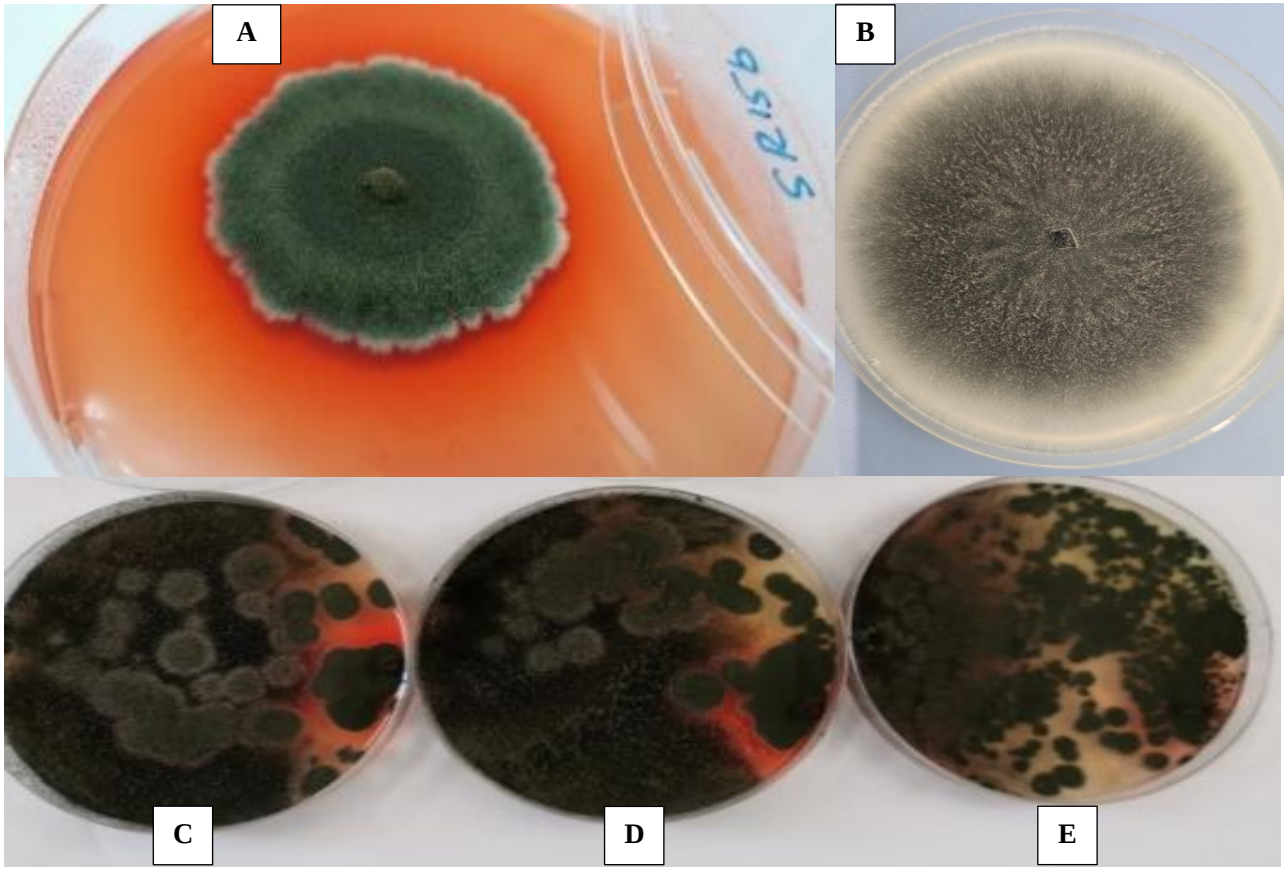


Figure 31: Dual Culture. **A:** *Talaromyces* species pure culture **B:** *Ceratocystis radicicola* pure culture. **C and D:** *C. radicicola* (left) with mixed *Talaromyces* species a and b (right) showing antagonism effect and clear inhibition zone with red pigmentation from *Talaromyces* Due to the fast growth of the *C. radicicola* the growth of *Talaromyces* was dispersed but the inhibition zone was clear 30 days after inoculation. **E:***C. radicicola* (left) with mixed *Talaromyces* species (right) shows the *Talaromyces* species b with very dispersed and quick growth, inhibition zone not clear and patches of mild red pigmentation.

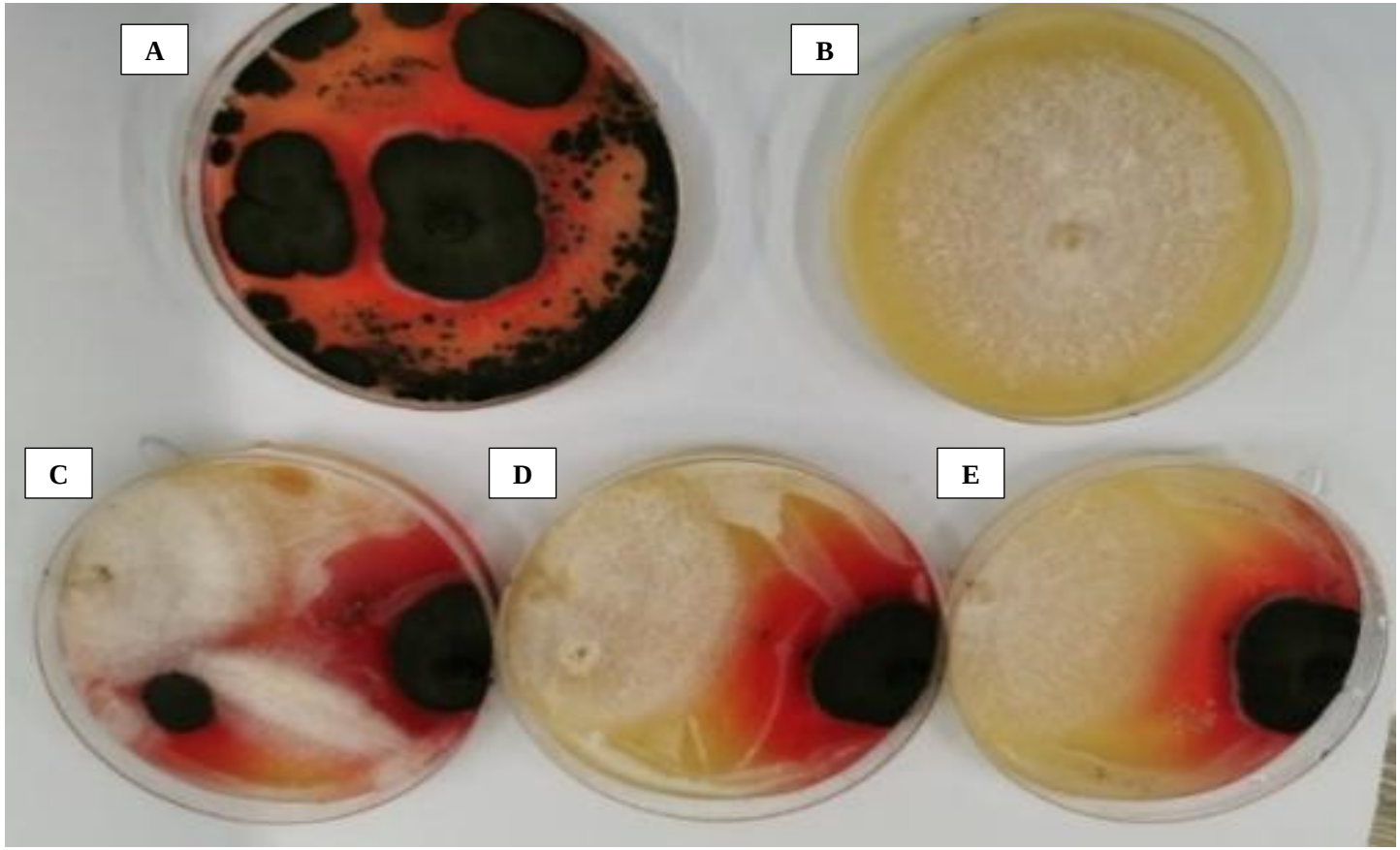


Figure 32: Dual culture. **A:** Pure culture of mixed *Talaromyces* species with 3 colonies in the center and dispersed smaller colonies of *Talaromyces* b on the edges of the petri dish **B:** *Fusarium solani* pure culture**. C,D,and E:** *F. solani* (left) with mixed *Talaromyces* species (right) showing good antagonism effect and inhibition zone with strong red pigmentation.

Table 10: Average growth measurement (cm) from day 1-4 and Inhibition percentage of dual culture of *Ceratocystis radicicola* and *Fusarium solani* with *Talaromyces* species and *Aspergillus terreus.* Average growth measurement (cm) of each control.

	Average Growth (cm)				**Inhibition %**
Isolate	**Day 1**	**Day 2**	**Day 3**	**Day 4**	
Ceratocystis	0.7	2.05	3.45	4.75	13.3%
Talaromyces	0.4	1.1	1.85	2.65	
Ceratocystis	1.2	1.55	2.275	3.35	38.9%
Aspergillus	0.4	0.7	1.175	1.375	
Fusarium	0.4	0.8	1.05	1.73	3.6%
Talaromyces	0.3	0.6	0.9	1.8	
Fusarium	0.6	1	1.55	1.9	13.8%
Aspergillus	0.3	0.6	0.8	1.1	
Control	**Day**				
	1	**2**	**3**	**4**	
Ceratocystis	0.933	2.50	3.98	5.48	
Fusarium	0.533	0.93	1.30	1.67	
Talaromyces	0.6	1.17	1.63	1.83	
Aspergillus	0.7	2.9	1.36	2.06	

3.3.2 Molecular identification of the antagonist endophytic fungi

The sequence results and identification of the endophyte fungi are shown in Table 11. The *Fusarium solani* used for the experiments was identified as strain KHK2, whereas the *Ceratocystis radicicola* (*Thielaviopsis radicicola*) was identified earlier as accession 1322. As for the endophytes, A was labelled as *Trichoderma asperellum* from the collection of the Plant Pathology Laboratory, School of Biosciences, University of Nottingham, UK. The sequence showed it was a mixture of *T. harzanium* and *T. lixii*. Fungi B and D were isolated from the soil of feral date palms in location 1 and were identified as *Aspergillus terreus* and *Penicillium griseofulvum* respetively. Fungus C from cultivated from date palm roots in location 1, and was initially suspected to be phylogenetically similar to *T. atroroseus*. The Maximum Likelihood for Maximum Parsimony and Bayesian Inference phylogeny tree from ITS sequence showed that it is potentially 3 new species of *Talaromyces* (Fig. 29). The tree was constructed following the protocol in Annex 5.

Table 11: Sequence results, best GenBank matches, strain, identity percentage, accession, variation /BP for isolates.

Isolate No.	Closest match in GenBank	Strain	% Identity	Accession	Variation/ BP	Remarks
1	Fusarium solani Species Complex	JUF0030	98.42%	MH368148	6/566	FSSC strain
2	Fusarium solani Species Complex	KHK2	100%	MH559637	0/566	FSSC strain KHK2
3	Fusarium solani Species Complex	KHK2	100%	MH559637	0/572	FSSC strain KHK2
Aa	Trichoderma harzianum	TH7	98.48%	KC403944	5/591	Trichoderma harzianum
Ab	Trichoderma lixii	SHMH1102	99.82%	JQ617299	0/570	Trichoderma lixii
Ba replicate 1	Aspergillus terreus	HA1N	99.82%	KR364880	0/560	Aspergillus terreus
Ba replicate 2	Aspergillus terreus	LGO13	99.82%	MH470250	0/556	Aspergillus terreus
Bb replicate 1	Aspergillus terreus	MXH-23	99.64%	KC287086	0/557	Aspergillus terreus
Bb replicate 2	Aspergillus terreus	LGO13	99.64%	MH470250	0/561	Aspergillus terreus
C11 a	Talaromyces purpurogenus	A3S3_40	99.45%	KC344978	1/549	Not included in the final analysis
C 11 b replicate	Talaromyces purpurogenus	NRC415	99.45%	MT232241	1/551	Potential new species
C12 a	Talaromyces purpurogenus	A3S3_40	99.45%	KC344978	2/550	Potential new species

Isolate No.	Closest match in GenBank	Strain	% Identity	Accession	Variation/ BP	Remarks
C 12 b replicate	Talaromyces purpurogenus	NRC415	99.45%	MT232241	2/544	Potential new recognized species
Da replicate 1	Penicillium griseofulvum	PG3	99.62%	KJ467353	1/532	Penicillium griseofulvum
Da replicate 2	Penicillium sp.	DS34	99.81%	OP647349	0/530	Penicillium griseofulvum
Db replicate 1	Penicillium griseofulvum	PG3	100%	KJ467353	0/531	Penicillium griseofulvum
Db replicate 2	Penicillium griseofulvum	PG3	99.81%	KJ467353	0/533	Penicillium griseofulvum

3.3.3 Morphological and molecular analysis of three potential new recognised *Talaromyces* species

Morphological analysis

The diameters of the colonies per culture Petri dish for each media were recorded in centimetres as shown in Annex 6, where readings show the total average colony diameter for three replicates per medium. A comparison of colony growth between YESA, MEA, CDA and CMA media, in terms of colour, shape and exudate colour and intensity in media was presented for both the obverse and reverse side of each plate (Figs 33 - 37). The OA medium was only photographed on the obverse side since the media was too dense to show the colony from the reverse side (Fig. 36). The MEA plates incubated at 37˚C presented for both obverse and reverse side of each plate (Fig. 37).

For the cultures growing on CYA and CYAS after 7 days at incubation of 25˚C and 37°C, they had shown very slow growth. Therefore, the cultures were left for another 7 days for the 25°C incubation, whereas the 37°C incubation was reduced to 30°C and left for another 7 days. The CYAS media was discarded since the growth was very slow and colonies were very small and widely dispersed, which was difficult to measure. All other isolate colony diameters were measured, and the averages are shown in Table 12.

There was no significant difference in growth between all media for Isolate C11a. Isolate C11b showed no significant difference in growth between YESA, CDA and MEA. However, there was a significant difference individually for growth between the YESA, CDA and CMA media each with growth in OA and CMA media. For isolate C12b, there was no significant difference in growth between YESA, CDA and MEA media and between OA and CDA media. However, there

was a significant difference in growth singly between YESA, CDA and MEA media each with OA and YESA, CDA and MEA media each with CMA media. Colony morphology description for each isolate in each media is explained under corresponding figure.

Table 12: Average colony diameter per media at 25°C dark 7 days for identification of 3 *Talaromyces* isolates. Means and Standard Deviation(n=3) followed by same letter in a column are not significantly different (Tukey's test P< 0.05).

Isolate C11 a		Isolate C11 b		Isolate C12 b	
Media	Average colony diameter (cm)	Media	Average colony diameter (cm)	Media	Average colony diameter (cm)
CYA	Slow growth	CYA	Slow growth	CYA	Slow growth
YESA	1.80 ± 1.04^{a}	YESA	2.13 ± 1.23^{a}	YESA	1.93 ± 1.11^{a}
CDA	1.48 ± 0.86^{a}	CDA	0.99 ± 0.57^{a}	CDA	0.91 ± 0.53^{a}
MEA	1.78 ± 1.03^{a}	MEA	1.88 ± 1.09^{a}	MEA	1.89 ± 1.10^{a}
OA	1.70 ± 0.99^{a}	OA	1.92 ± 1.11^{b}	OA	1.93 ± 1.11^{b}
CMA	1.24 ± 0.72^{a}	CMA	1.33 ± 0.77^{c}	CMA	1.20 ± 0.70^{b}

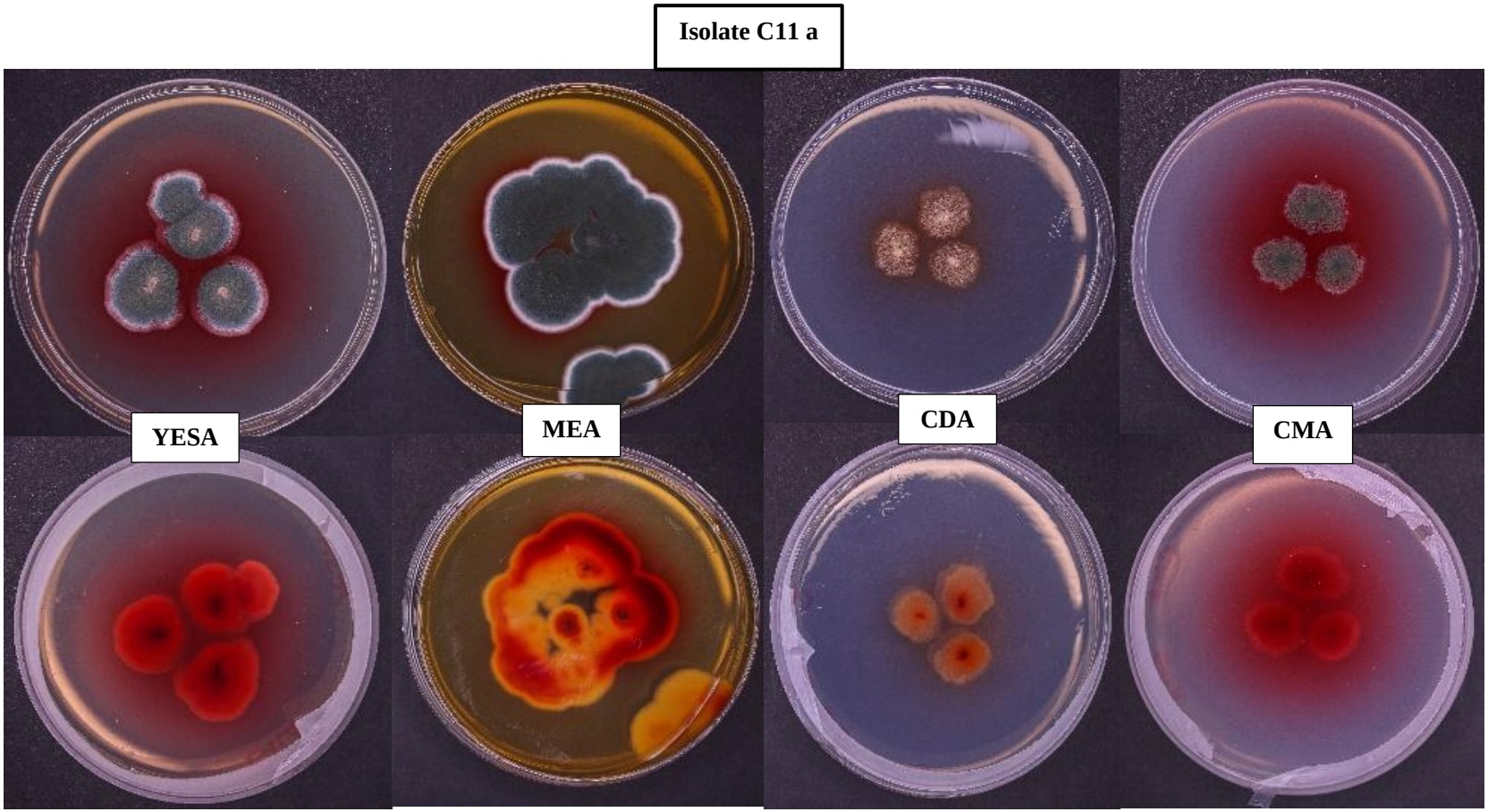


Figure 33: Cultures of C11a isolates (top plate anterior, lower plate reverse) from left to right respectively are YESA, MEA, CDA, CMA medium incubated at 25˚C for 7 days**. YESA:** Colony average diameter 180 mm, white mycelia, velvety texture, dense spores, conidia *en masse* dark and dull green slightly blueish grey on the edges, red soluble pigment, color on reverse dark red. **MEA:** Colony average diameter 178 mm, white mycelia, velvety texture, dense spores, conidia *en masse* dark and dull green, yellowish exudate, red soluble pigment, moderate color on reverse dark red. **CDA:** Colony average diameter 148 mm, white to beige mycelia, sparse spores, yellowish red soluble pigment, color on reverse orange red at the center of colony. **CMA:** Colony average diameter 180 mm, white mycelia, velvety texture, dense spores, conidia *en masse* dark and dull green, red soluble pigment, color on reverse dark red.

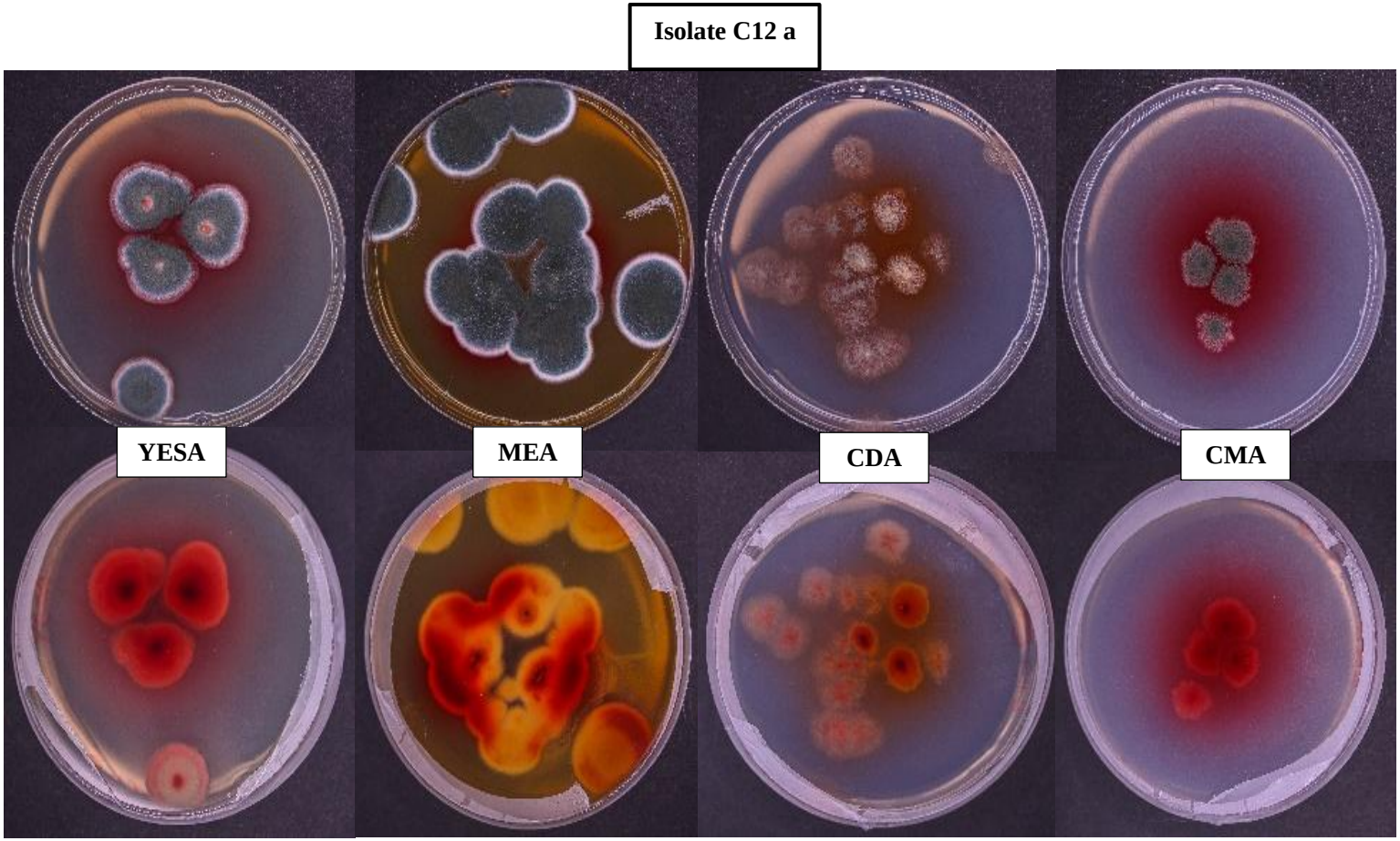


Figure 34: Cultures of C11b isolates (top plate anterior, lower plate reverse) from left to right respectively are YESA, MEA, CDA, CMA medium incubated at 25˚C for 7 days. **YESA:** Colony average diameter 193 mm, white mycelia, velvety texture, dense spores, conidia *en masse* dark and dull green slightly blueish grey on the edges, red soluble pigment, color on reverse dark red. **MEA:** Colony average diameter 189 mm, white mycelia, velvety texture, dense spores, conidia *en masse* dark and dull green, yellowish exudate, red soluble pigment, moderate color on reverse dark red. **CDA :** Colony average diameter 91 mm, white to beige mycelia, sparse dark and dull green spores, yellowish orange soluble pigment, color on reverse orange red and red at the center of colony.**CMA :** Colony average diameter 120 mm, few white mycelia, velvety texture, moderate dense spores, conidia *en masse* dark and dull green, red soluble pigment, color on reverse dark red.

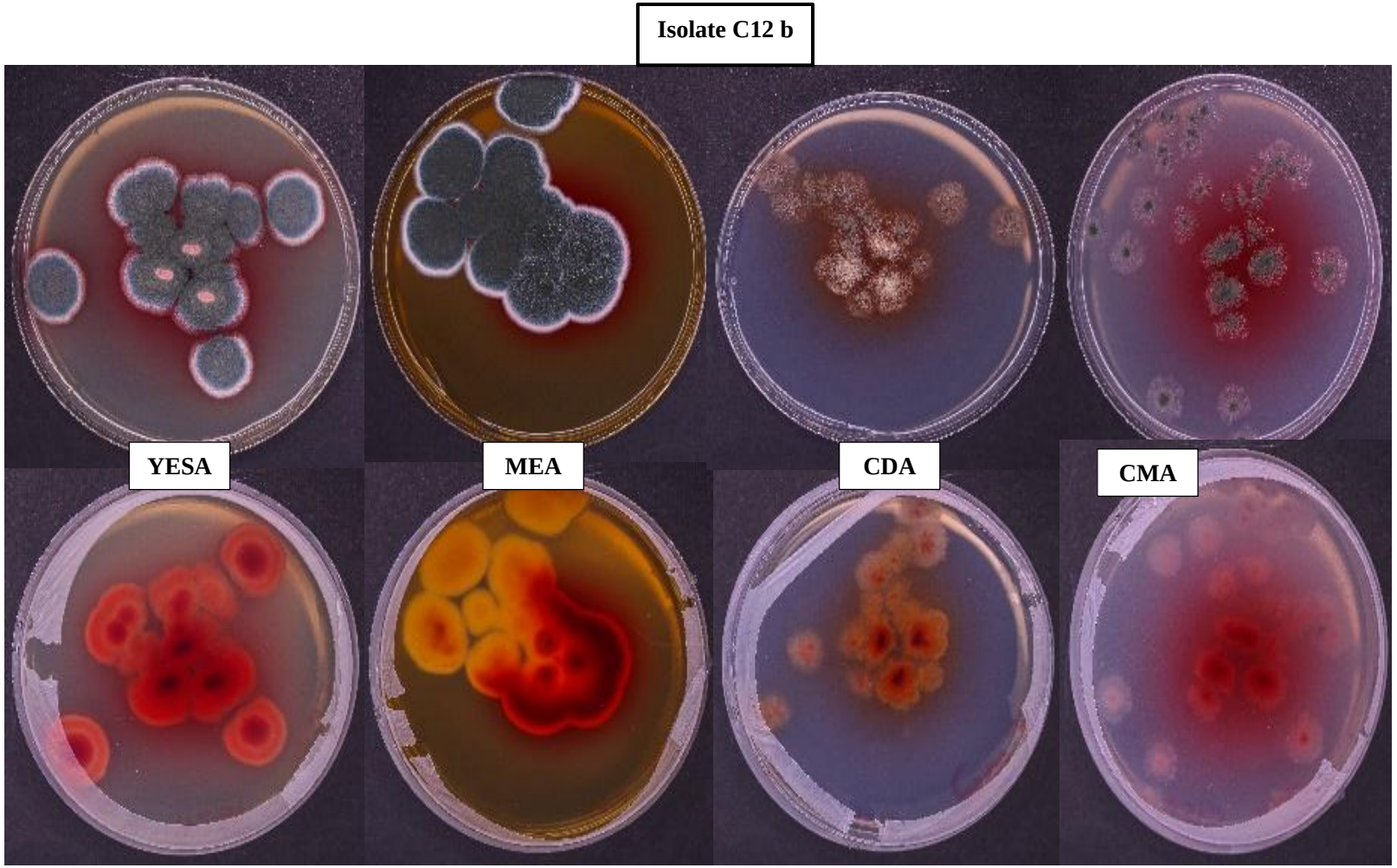


Figure 35: Cultures of C12b isolates (top plate anterior, lower plate reverse) from left to right respectively are YESA, MEA, CDA, CMA medium incubated at 25°C for 7 days **YESA:** Colony average diameter 213 mm, white mycelia, velvety texture, dense spores, conidia *en masse* dark and dull green, red soluble pigment, color on reverse dark red colony has white interior edges. **MEA:** Colony average diameter 188 mm, white mycelia, velvety texture, dense spores, conidia *en masse* dark and dull green, yellow and reddish exudate, red soluble pigment, color on reverse dark red, some colonies with no pigment. **CDA 25°C dark 7 days:** Colony average diameter 99 mm, white to beige mycelia, sparse spores, yellowish red soluble pigment, color on reverse orange red at the center of the colony. **CMA:** Colony average diameter 133 mm, white mycelia, velvety texture, dense spores, conidia *en masse* dark and dull green at center only, red soluble pigment, color on reverse dark red, some colonies without pigment.

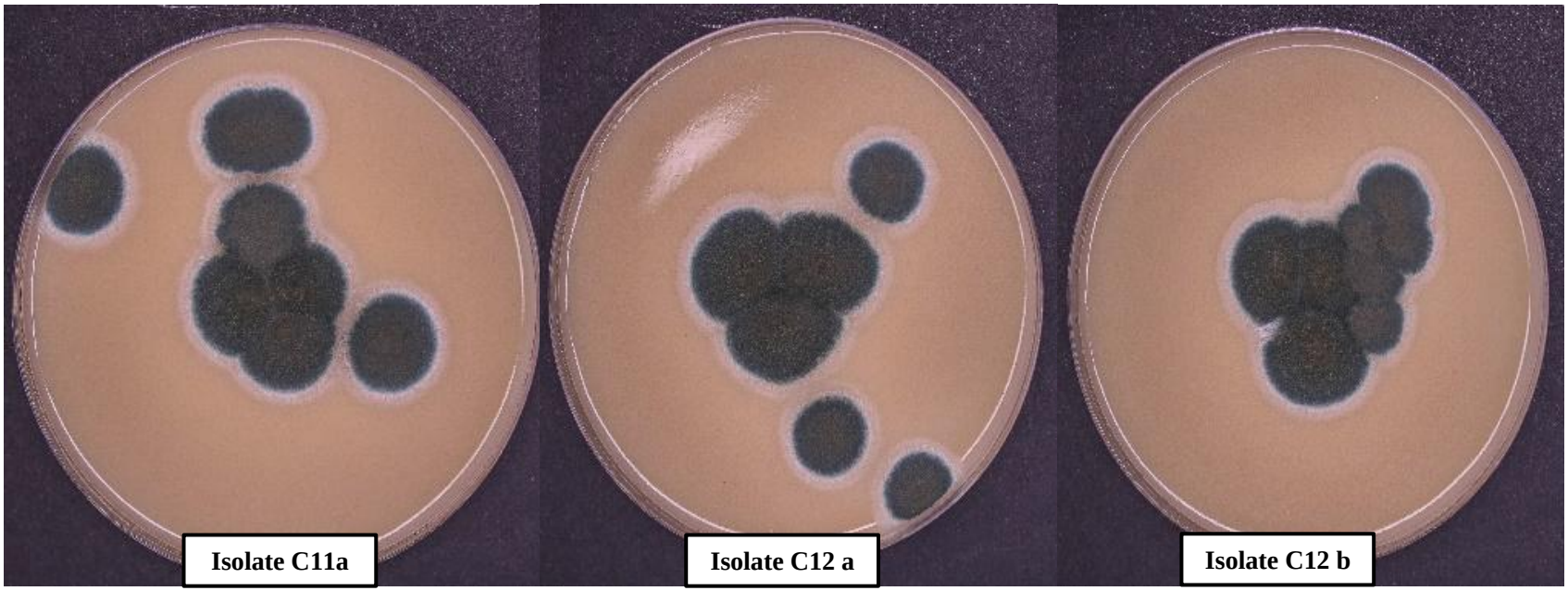


Figure 36: Cultures of C11a isolates anterior (No reverse) from left to right respectively are C11a , C12a and C12b in OA medium incubated at 25˚C for 7 days. **Isolate C11a:** Colony average diameter 170 mm, white mycelia, velvety texture, dense spores, conidia *en masse* dark and dull green, soluble pigment absent, no observation on reverse due to dense media. **Isolate C11b:** Colony average diameter 193 mm, white mycelia, velvety texture, dense spores, conidia *en masse* dark and dull green, soluble pigment absent, no observation on reverse due to dense media. **Isolate C12b:** Colony average diameter 192 mm, white mycelia, velvety texture, dense spores, conidia en masse dark and dull green, soluble pigment absent, no observation on reverse due to dense media.

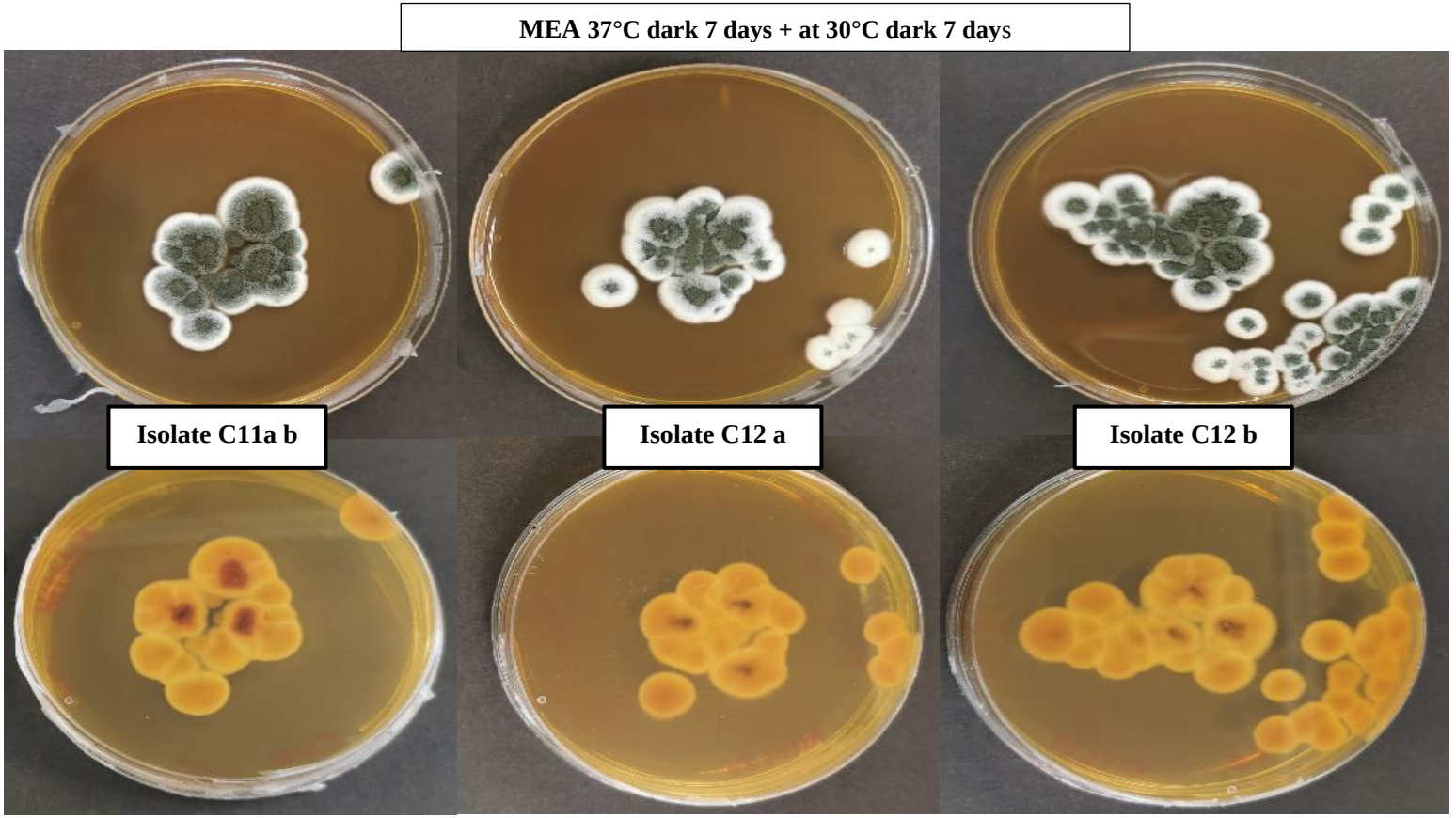


Figure 37: Cultures of isolates (top plate anterior, lower plate reverse) from left to right respectively are C11a, C11b and C12b in MEA medium incubated at 37 °C for 7 days. **Isolate C11ab**: Colony average diameter 153 mm, beige mycelia with light and dark red at the center of colony, sparse spores, no soluble pigment, color on reverse similar to top. **Isolate C11b**: Colony average diameter 178 mm, Colony average diameter 153 mm, beige mycelia with light and dark red at the center of colony, sparse spores, no soluble pigment, color on reverse similar to top. **Isolate C12b:** Colony average diameter 230 mm, Colony average diameter 153 mm, beige mycelia with light and dark red at the center of colony, sparse spores, no soluble pigment, color on reverse similar to top.

Molecular analysis

The DNA of the potentially three new *Talaromyces* species (C11a, C11b and C12b) was amplified using 3 primers: translation elongation factor 1-alpha TEF-1a, EF1-983F/ EF1-1567R and DNA-dependent RNA polymerase II subunit 2 RPB2 primer bRPB2-6F/ bRPB2-7R. Two replicates for each isolate PCR product. The amplified bands are shown in Fig. 38 with negative in between each sample. Imaging revealed strong positive bands. For *Talaromyces* species (C12a), it was amplified alone with the same 3 primers and 3 negatives. The imaging also revealed strong bands for all PCR products as shown in Fig. 39.

The Maximum Likelihood for Maximum Parsimony and Bayesian Inference phylogeny tree from the ITS sequence showed that the potential three new recognized species of *Talaromyces* belonged to *Talaromyces* section *Trachyspermi* (Fig. 40). Therefore, a combined dataset of ITS-RPB2 sequences was constructed, including the species of sect. *Trachyspermi* and some representative species of other sections of *Talaromyces* (accessions shown beside each representative in phylogentic tree in Fig. 45) in which C11a was recovered with a long branch, so it was excluded as illustrated in Fig. 45.

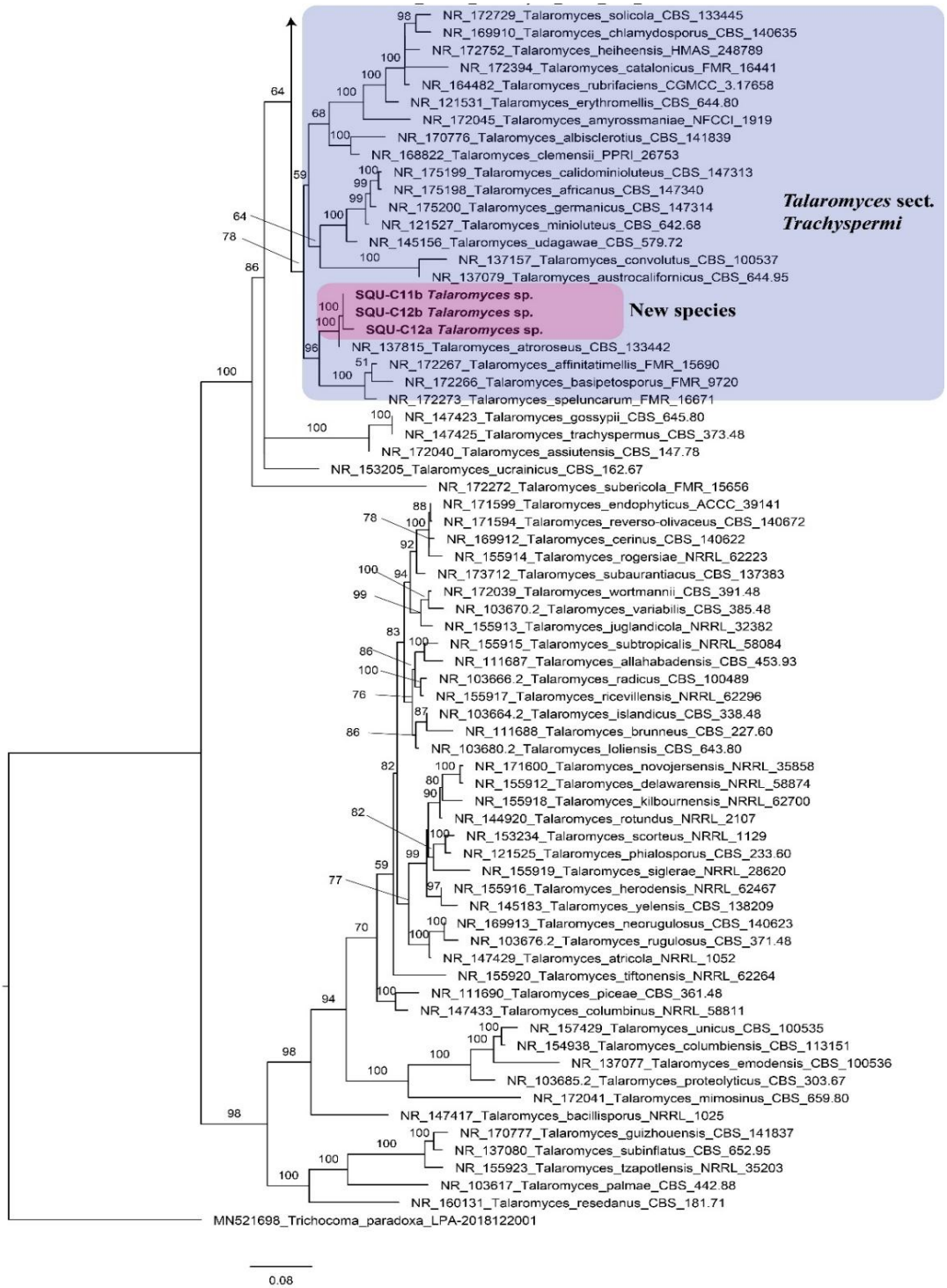


Figure 38: Maximum Likelihood tree from ITS5 sequence of *Talaromyces* isolate C11b, C12a and C12b reconstructed using RaxML. *Talaromyces* isolate C11b, C12a and C12b where potential new recognized species are shown in pink box in *Talaromyces* sect *Trachyspermi* with bootstrap value 100% in the nodes. Bar =0.08 substitutions per nucleotide position.



Figure 39 : Imaging of positive PCR product of potential new species of *Talaromyces* species Samples**1-6** amplified with large subunit of nuclear ribosomal DNA (28S) primer LROR/ LR5. **1**.C11a **2.**C11a* replicate **3.**C11b **4**. C11b* replicate **5.** C12b **6.**C12b* replicate **7.** Negative. Sample **8-6** amplified with translation elongation factor 1-alpha (TEF-1a) primer EF1-983F/ EF1-1567R.**8**.C11a **9.**C11a* replicate **10.**C11b **11**. C11b* replicate **12**. C12b **13**.C12b* replicate (absence of band may be due to pipetting error) **14.** Negative. Sample **15-20** amplified with DNA-dependent RNA polymerase II subunit 2 (RPB2) primer bRPB2-6F/ bRPB2-7R. **15**.C11a **16.**C11a* replicate **17.**C11b **18**. C11b* replicate **19**. C12b **20**.C12b* replicate. **21.** Negative **L.**0.1-10 kb 2 log ladder.

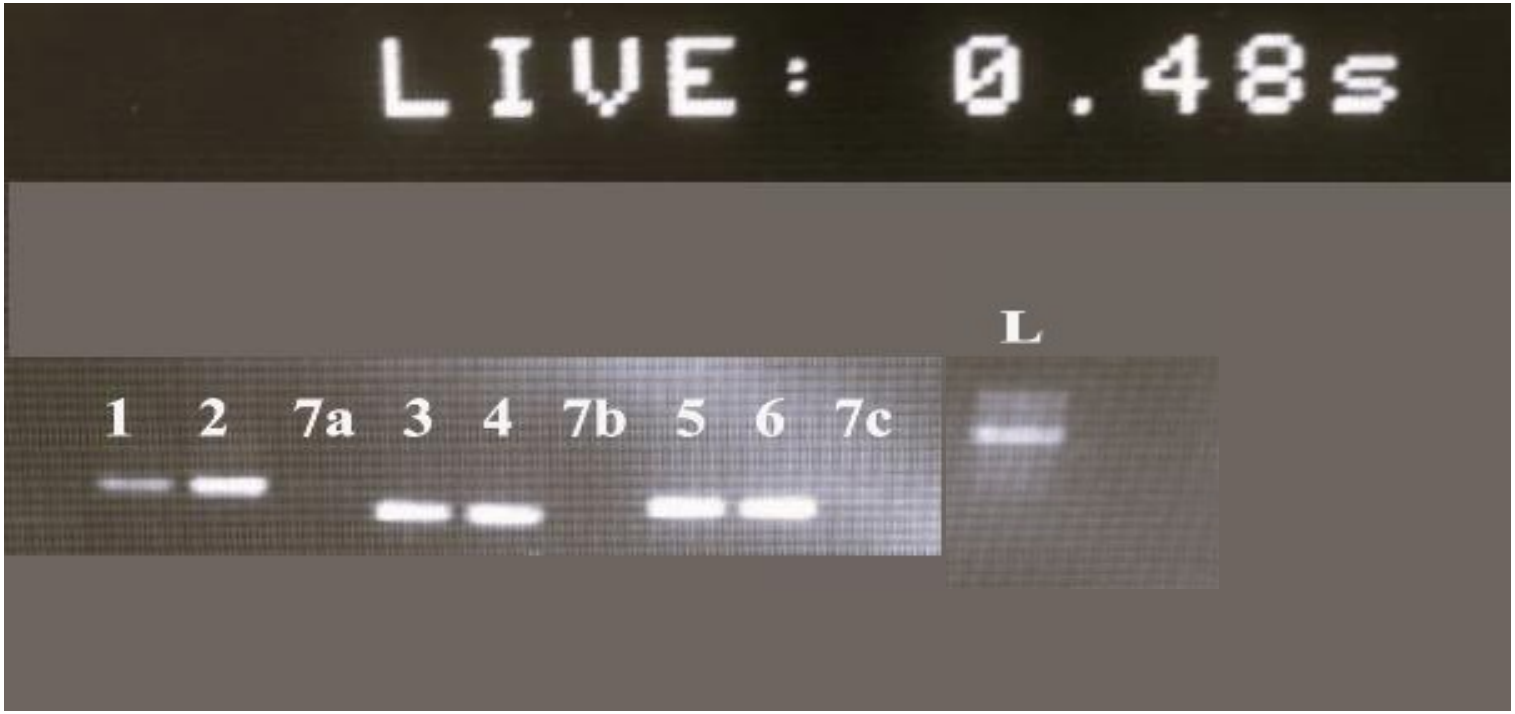


Figure 40: Imaging of positive PCR product of potential new species of *Talaromyces* species C12a. Samples**1**and**2** amplified with large subunit of nuclear ribosomal DNA (28S) primer LROR/ LR5. **1**.C12a **2.**C12a* replicate **7a** Negative. Sample **3**and**4** amplified with translation elongation factor 1-alpha (TEF-1a) primer EF1-983F/ EF1-1567R. **3.**C12a **4**. C112a* replicate **7b.** Negative. Sample **5and6** amplified with DNA-dependent RNA polymerase II subunit 2 (RPB2) primer bRPB2-6F/ bRPB2-7R.**5**. C12a **6**.C12a* replicate. **8**.C11a **9.**C11a* replicate **7c** Negative **L.** 0.1-10 kb 2 log ladder.

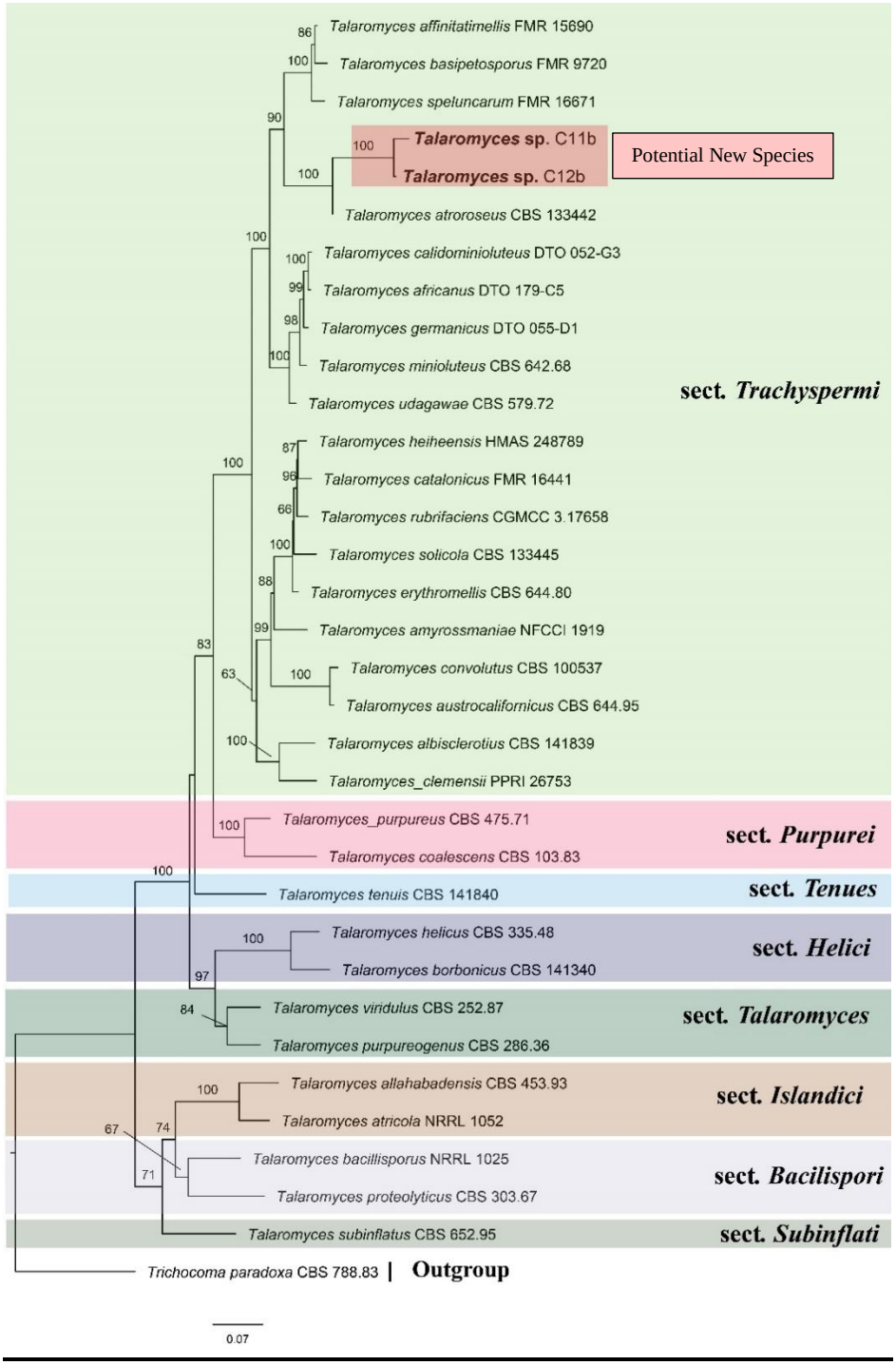


Figure 41: Maximum Likelihood tree Comparing ITS-RPB2_36 all sections of *Talaromyces* isolate C11b, C12b reconstructed using RaxML. *Talaromyces* isolate C11b and C12b where potential newly recognized species depicted in the tan box with bootstrap value 100% in the nodes in *Talaromyces* sect *Trachyspermi.* Isolate C11a was recovered with a long branch, thus was excluded in the final analysis. Bar =0.07 substitutions per nucleotide position

3.4 Discussion

The results of testing the antagonistic activity of different fungal isolates on *Ceratocystis* and *Fusarium* species indicated that *Aspergillus* and *Talaromyces* species had achieved an apparent and consistent antagonistic effect on the pathogenic fungi compared to the other fungi. One of several modes of action that BCAs have is antibiosis. Antibiosis is the secretion of diffusible metabolites of allelochemicals: bacteriocins, lipopeptides, antibiotics, bio-surfactants, cell wall degrading enzymes or microbial volatile compounds (Lahlali *et al.*, 2022). These results are in line with Luo *et al*. (2021), which stated that *Talaromyces* mode of action is through antibiosis by producing anti-fungal compounds that create an inhibition zone in dual culture tests. Further evidence was shown by Halo *et al*. (2019) that *Talaromyces variabilis*, an endophyte from desert Bean capers (*Zygophyllum coccineum*) and Harmal (*Rhazya stricta*), affected growth of *Pythium aphanidermatum,* the causal agent for damping-off disease of cucumber. The cell wall degrading enzymes cellulase, glucanase and siderophore compounds were extracted from *Talaromyces variabilis* (Halo *et al*., 2019). Unlike true fungi, cell walls of Oomycetes contain cellulase along with several other carbohydrate polymers (McGowen *et al*., 2020). Of the top ten Oomycetes plant pathogens, *Phytophthora* species was at the top of the list and *Pythium* species as the eighth with other pathogens in between (Kamoun *et al.,* 2015). This could explain why *Talaromyces variabilis* (Halo *et al*., 2019) and *T. pinophilis* isolated from the rhizosphere of tomato and cucumber (Kazerooni *et al*., 2019) were both antagonistic to *Pythium aphanidermatum* by degrading the cell walls. The results of the

antagonistic action of *Aspergillus terreus* indicates a similar mode of action to *Talaromyces*. According to Gao *et al*. (2008), *A. terreus* also produces cellulases. This is in line with the results of Halo *et al*. (2018) that indicated that *Aspergillus terreus,* obtained from native plants of Harmal (*Rhazya stricta*) and Wild indigo (*Tephrosia apollinea*), resulted in morphological abnormalities in the mycelium of *P. aphanidermatum* through glucanase enzymes and production of siderophore compounds leading to suppression of cucumber damping-off. Similar findings were reported for *A. terreus* isolated from Mangrove (*Avicennia marina*) and Purslane (Sesuvium *portulacastrum*) from Al Shibli *et al*. (2019) and Karunasinghe *et al*. (2020) respectively.

Talaromyces has been shown as a biocontrol agent against other plant pathogens that do not belong to the oomycetes. According to Stosz *et al*. (1996) and Madi *et al*. (1997) *Talaromyces flavus* was reported to control soil borne pathogens such as *Rhizoctonia solani*, *Sclerotinia sclerotiorum* and *Verticillium dahliae*. The mechanism postulated was mycoparasitism, nutrient competition and antibiosis. It was proven that antibiosis was by production of hydrogen peroxide that is catalyzed by glucose oxidase a (glycoprotein) in the presence of glucose (Stosz *et al*., 1996). Stosz *et al*. (1996) also showed that filtrates of *T. flavus* inhibited the germination of *V. dahliae* microsclerotia only when glucose oxidase was added. Different mechanisms of *T. flavus* were shown by Madi *et al*. (1997) with two pathogens, *V. dahlia* and *Sclerotium rolfsii*. Their study showed that enzymatic activity of chitinase, gluconase, cellulase and glucose oxidase varied between 12 isolates of *T. flavus*. Mycoparasitism was the mechanism to control *S. rolfsii* by colonizing the

sclerotia and hyphae and high positive correlation occurred between mycoparasitism and disease suppression. Glucose oxidase killed microsclerotia of *V. dahlia* and antibiotic metabolites inhibited melanization (i.e. infiltrate with melanin) of newly developed *V. dahliae* microsclerotia, whereas newly developed *S. rolfsii* microsclerotia were not affected (Madi *et al*., 1997).

In another study, Luo *et al*. (2021) investigated the effect of *Talaromyces* species isolated from sea water of the Yap Trench at the western Pacific Ocean on *Fusarium equiseti*, causal agent of cucumber wilt. The results showed that *Talaromyces* sp. DYM25 had an antagonistic effect on *F. equiseti* by antibiosis. *Talaromyces* sp. DYM25 produced bioactive substances that were stable regardless of exposure to UV light, high temperatures and metal ions. The bioactive substance remained active under neutral and alkaline conditions. Antimicrobial extracts were proven to be a type of alkaloid salt. The cucumber seedlings which were treated with fermented broth of strain DYM25 and then inoculated with culture solution of *F. equiseti* suppressed cucumber wilt significantly compared to the seedlings only inoculated with the pathogen (Luo *et al*., 2021).

The new potential species of *Talaromyces* identified in our study produced red pigmentation. The pigment is probably an extrolite known as azaphilone polyketide red pigment (Frisvad *et al*., 2013). Also the study proved a new species of *Talaromyces astroseus* that was initially believed to be *Penicillium purpurogenum* and *P. rubrum* (Frisvad *et al*., 2013) and *T. flavus* as anamorph of *Penicillium dangeardii* and *P. vermiculatum* (Stosz *et al*., 1996 and Madi *et al*., 1997). *T. astroseus* is the producer of the red pigment of mitorubrin, monascorubrin,

glauconic acid, PP-R and ZG-1494α and the compounds are recommended for use as food coloring since its free of mycotoxins (Frisvad *et al*., 2013).

The molecular and morphological analysis were in agreement with the findings from Frisvad *et al.* (2013), Jiang *et al.* (2018), Han *et al.* (2021) and Wei *et al.* (2021). The DNA of the potentially three new *Talaromyces* species were amplified using ITS and 3 specific gene sequence (1-α TEF-1a, RPB2 and LROR). The constructed phylogenetic trees, the first with the ITS that revealed *Talaromyces* in section *Trachyspermi* with bootstrap value 100%, were verified further by the second tree with ITS-RPB2 sequences. In this section most of the species have only ITS and RPB2. According to Xiao *et al.* (2022), the most reliable identification genes for *Talaromyces* species are ITS, BenA, CaM, PBP1 and RBP2.

Findings from this study showed that some fungal species isolated from date palm roots may help protect dates against some pathogenic fungi, including *Ceratocystis* and *Fusarium* species that are known to result in wilt diseases (Al-Sadi *et al.*, 2012). This appears to be achieved by antibiosis, mycoparasitism of the pathogen, and inhibiting pathogen development as described earlier. Future studies should investigate 1) the mechanisms by which the antagonistic fungi affect date palm pathogens; 2) the effect of the isolated and identified antagonistic fungi on date palm seedlings to test their effect under field conditions and to determine the best concentration and application methods that will achieve results similar to the *in vitro* experiments; 3) further identification of the new potential species of *Talaromyces* through extensive morphological measurements and molecular work; 4) extraction

and investigation of the metabolites of *Aspergillus terreus* and *Talaromyces* new potential species and determine their antagonistic effect on date palm pathogens.

Chapter 4

Scanning Electron Microscopy imaging of the antagonistic effect of endophytic fungi *Aspergillus terrus* and *Talaromyces* sp. on *Ceratocystis radicicola* and *Fusarium solani* and the effect of culture filtrate of the antagonistic fungi on electrolyte leakage of *Ceratocystis radicicola* and *Fusarium solani*.

4.1 Introduction:

Traditionally, imaging of fungi through microscopy has been important for identifying morphological features and differentiating between different genera and species and also to guide in proper diagnosis of fungal diseases (Ijaz *et al*., 2022). In addition, microscopy facilitates observations and understanding of the distinctive colonization patterns of plant pathogens to cell types and tissues within a plant, different interactions, resistance and susceptibility mechanisms (Cladwell *et al*., 2019). Light microscopy has allowed the recording and documentation of various morphological characteristics that provided a better and a more accurate species identification, including for unculturable species (Ijaz *et al*., 2022). However, its limits are low resolution and limited specimen compatibility (Cladwell *et al*., 2019; Watts *et al*., 2021).

More powerful forms of imaging have subsequently been developed, including Transmission Electron Microscopy (TEM) and Scanning Electron Microscopy (SEM), to allow documentation of the changes in microorganism isolates, the antagonistic mechanisms and new morphological features of fungi and other microorganisms (Sampere *et al.*, 2011). According to Golding *et al*. (2016), negative staining TEM has been used traditionally but its setback is its requirement for a higher concentration or titer of the sample, which usually needs to be achieved though

centrifugation, for adequate concentration of microbial samples such as bacteria or viruses to adsorb to a thin support film. This can prove to be difficult if the sample obtained is initially low in titre or it is non-culturable. Therefore, SEM is a better option. In addition, SEM allows higher magnification to detect certain characteristics that are not imaged or detected in normal microscopy, such as any variations between isolates in the same stratum, new morphological features or mechanisms of antagonism (Sampere *et al*., 2011). Also, Sampere *et al.* (2011) stated that SEM does have a setback with chemical fixation to preserve and stabilize specimen structures, post fixation, dehydration and sputter coating which require long processes and time.

There are several types of SEM technologies, including ambient temperature and low temperature /cryo SEM (CSEM). In ambient SEM, the samples are dehydrated either with Critical Point Drying (CPD) or freeze drying or chemicals are used (Cladwell *et al*., 2019). In this study ambient SEM with Hexamethyldisiazane (HMDS) has been used. This is a chemical with low surface tension that allows fixed and dehydrated samples to air dry which also prevents shrinkage or collapse of soft tissues during the dehydration process (Bhattacharya *et al*., 2020).

Any biological stress on a plant or a fungus imposed by another microorganism (bacteria of fungi) releases enzymes, bioactive metabolites and other compounds. Cell membranes lose their integrity and leakage of nutrients, sugars, amino acids and charged ions i.e. electrolytes, occurs (Chavan *et al*., 2020). This is known as electrolyte leakage. Electrolyte leakage is a quick, simple quantitative bioassay technique. It is used to measure the effects of temperature, competitive inhibitors and metabolic inhibitors on a host (Kwon *et al.,* 1996). For example, Manhas *et al.* (2016) used it to study the effect of bioactive metabolites from *Streptomyces hydrogenans* strains on *Alternaria brassicicola* causing damping off and leaf spot on radish. Similarly, Chavan *et al*. (2020) investigated the effect of epiphyte extracts from various plants on *Fusarium oxysporum*, *Fusarium*

solani, *Colletotricum dematium* and *Drechslera oryzae*, whilst Al Shibli *et al*. (2019) tested *Aspergillus terrus* isolated from mangroves on the cucumber damping off pathogen *Pythium aphanidermatum*. This technique has been adapted according to the type of host investigated and the compound tested in various biocontrol research projects.

Several endophytic fungi that produce extracellular enzymes have been reported. For example, Halo *et al*. (2018) showed that *Aspergillus terreus* produced glucanases enzymes and Mevastatin that suppressed growth of *Pythium aphanidermatum*. Karunasinghe *et al*. (2020) showed the effect of the metabolites β-gluconase and cellulase from several *Aspergillus* strains isolated from the rhizosphere of Sea Puslane on *P. aphanidermatum*. The evident effect of these metabolites on degrading the cellulose in the cell walls of *P. aphanidermatum* were shown by SEM.

Talaromyces spp. have been reported to have an antagonistic effect on plant pathogens. Inhibition of the damping off pathogens *P. aphanidermatum* and *Rhizoctonia solani* of cucumber by *Talaromyces pinophilus* isolated from the rhizosphere soil of several tomato and cucumber fields was reported by Kazerooni *et al.* (2019). Halo *et al*. (2018) first reported on the efficacy of *Talaromyces variablis* as a biocontrol agent isolated from the desert shrubs, Bean capers (*Zygophyllum coccineum*) and Harmal (*Rhazya stricta*). The bioactive compounds glucanases, cellulases and siderophores were extracted via growth media and their antagonism was tested by dual culture, electrolyte leakage on *P. aphanidermatum* and their effect on hyphal tip morphology at the inhibition zone.

The first objective of this study was to use SEM imaging to visualize the effect of *Talaromyces* species and *Aspergillus terreus* isolated and identified as described in previous chapters on the date palm pathogens *Ceratocystis radicicola* and *Fusarium solani.* The second objective was to

test the effect of *Talaromyces* species and *Aspergillus terreus* metabolites on *Ceratocystis radicicola* and *Fusarium solani* by using the electrolyte leakage technique.

4.2 Materials and Method:

4.2.1 Scanning electron microscopy imaging

In collaboration with the EM Unit, College of Medicine, SQU, Oman, the effect of the antagonistic fungi on the date palm pathogens was screened. The dual cultures and control of *Aspergillus terreus* and *Talaromyces* sp. with *Ceratocystis radicicola* and *Fusarium solani* along with the pure cultures of *C. radicicola, F. solani*, *A. terreus* and *Talaromyces* sp. were prepared for Scanning Electron Microscopy imaging as follows.

The standard protocol follows Goldstein *et al*. (2003). Mycelial discs (6 mm) were acquired from the inhibition zones and from pure isolates. The discs were placed in vials containing EM primary fixative (Karnovsk's fixative: 2.5% glutaraldehyde EM grade with paraformaldehyde) overnight.

The discs were then dissected into fragments each about 1 mm^3 size and put in cacodylate buffer (pH 7.2-7.4) twice, each for 5 minutes. The samples were post fixed in osmium tetroxide for one hour and washed twice with distilled water each for 10 minutes followed by washing with ethanol at different strengths (25%, 50%. 75%) for 10 minutes, followed by two rinses with absolute ethanol for 10 minutes and twice for 20 minutes. The samples were then dried using HMDS, two washes each for 10 minutes. Next the samples were mounted on the Al stub and coated with a conductive material (gold) and screened under SEM (JEOL JSM 4500LV SEM).

4.2.2 Culture filtrate effect of the antagonistic *Aspergillus terrus* and *Talaromyces* sp. fungi on electrolyte leakage of *Ceratocystis radicicola* and *Fusarium solani*

Electrolyte leakage was investigated following the methods of Karunasinghe *et al.* (2020), Halo *et al.* (2018) and Chavan *et al.* (2020). The fungal inoculum consisted of 6 mm plugs from actively growing isolates, which were used to inoculate broth media. Either Czapek Dox broth or Potato Dextrose broth were used. *Ceratocystis radicicola* only grew in Potato Dextrose broth while *Aspergillus terreus* only grew in Czapek Dox broth. All other isolates had good growth in both broths. Each isolate was grown in 150 ml broth in a 250 ml conical flask. They were incubated in a shaking incubator at 28°C, between 95-100 rpm for 10 days.

After complete growth of the pathogens *Ceratocystis radicicola* and *Fusarium solani*, the cultures were centrifuged at 4000 x g for 40 minutes. All the processes described herewith were carried out under a Laminar flow hood except use of the centrifuge. The cultures were filtered through sterile filter paper in a funnel and the supernatants were discarded. The mycelium was washed with sterile distilled water, blotted dry on sterile filter paper then further dried in the oven at 36°C for 60 minutes. After drying, 0.5 g was weighed out and placed in a sterile 15 ml centrifuge tube. At this stage the mycelium was soft, viable and active and stored at 10-15°C until use.

For the antagonistic endophytic fungi *Aspergillus terreus* and *Talaromyces* spp. the broth was filtered through sterile filter paper in a funnel, the mycelium was discarded and the supernatant was collected in 50 ml sterile centrifuge tubes. This was to ensure that the supernatant only contained the metabolites extracted from the endophyte without any contaminants. The supernatant was centrifuged at 4000 x g for 15 minutes, filtered again through a sterile micro filter

(0.2 µm pore) to obtain CF (Cell Free Culture Filtrate). Ten milliliters was collected in 15 ml sterile centrifuge tubes.

Each 0.5 g of pathogen mycelium was placed into 10 ml of antagonist CF. Electrical conductivity (EC) and pH was measured immediately as initial reading at time zero. The reading was taken for 3 replicates of each pathogen and 3 replicates as controls (antagonists CF only). The treatments were left at room temperature at 24°C. The EC was measured after 2 hours and after 24 hours. Between readings, the electrode was washed with sterile distilled water, dried and re-calibrated by using the provided pH buffers.

The experiment was repeated twice, since in the first experiment, *Aspergillus terreus* did not grow in Potato Dextrose broth but grew in Czapek Dox broth. The measured parameters (mV and pH) were examined with R (version 4.0.3). Comparison of data was performed via one-way analysis of variance (ANOVA) followed by Tukey's test ($p < 0.05$). All the values are expressed as the mean ± standard deviation (SD) for three measurements.

4.3 Results

4.3.1 Scanning electron microscopy imaging

The results of the SEM imaging clearly show the effect of the endophytic fungi *Talaromyces* species and *Aspergillus terreus* on *Ceratocystis radicicola* and *Fusarium solani*. The SEM images of the *C. radicicola* and *F. solani* controls were not very clear. Therefore, SEM images from Al Naemi *et al.* (2016) and Hashem *et al.* (2016) (Figs 42 and 43) were added for comparison to the images of the effects of antagonism. Fig. 44 shows the effects of *Talaromyces* spp. on *C. radicicola* spores by forming chains or a net-like structure around them and shrinkage of the spores just below it. The effect of *Aspergillus terreus* on *Ceratocystis radicicola* in Fig. 45shows the shriveled *C.*

radicicola hyphae and how the *A.terreus hyphae* are smooth, and its spores cover the hyphae and form clumps around *C. radicicola* spores.

In Fig. 46, the effects of *Talaromyces* spp. on *F. solani* are evident through the shriveling of the hyphae and some spores are attached to the hyphae. The effect of *Aspergillus terreus* on *F. solani* is shown in Fig. 47 as wrinkled spores and distorted hyphae, while tissue degradation of the hyphae is apparent in Fig. 48.

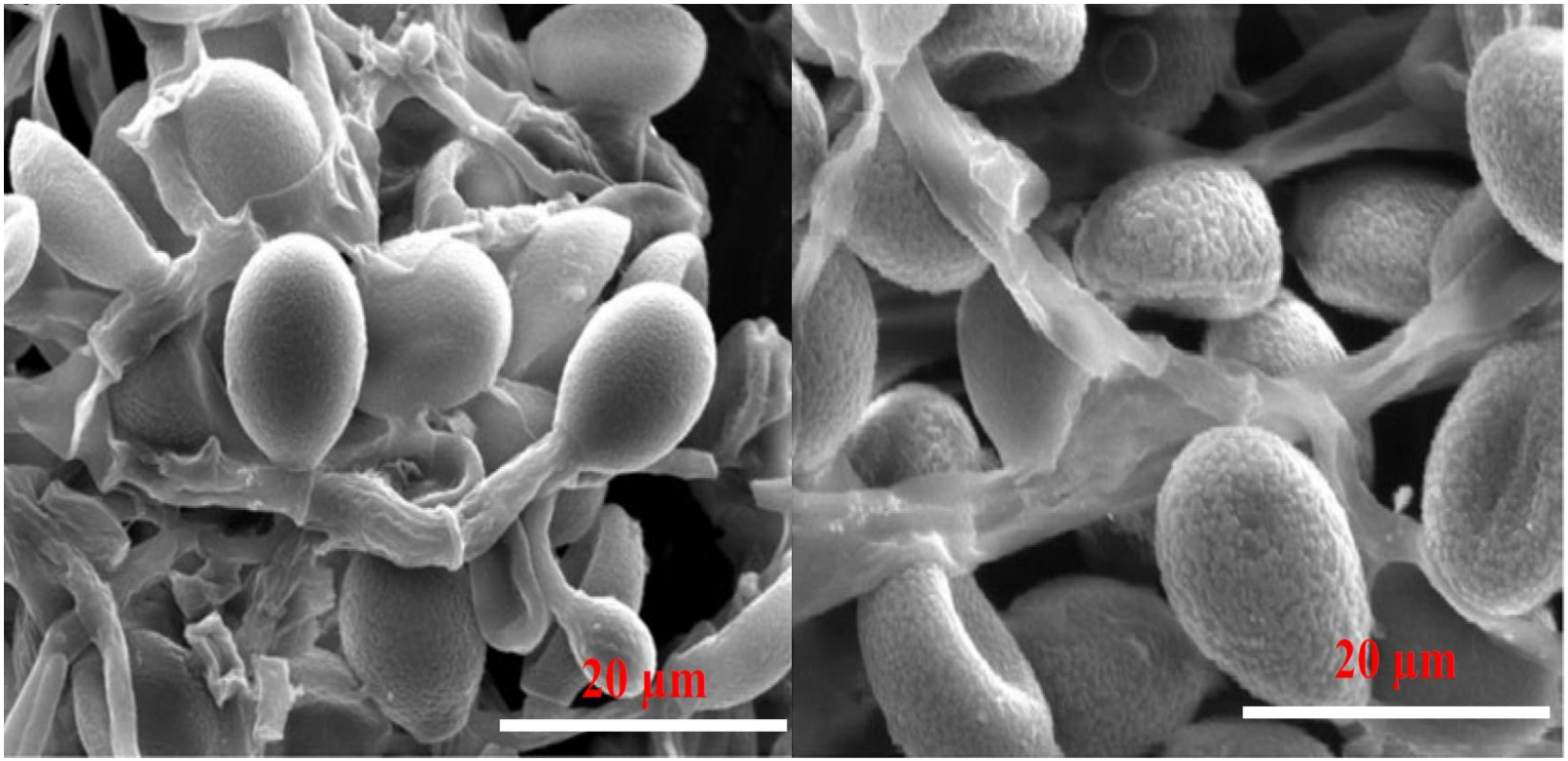


Figure 42: SEM images showing conidia and hyphae of *Ceratocystis radicicola* isolated from date palm. Al Naemi *et al.* (2016).

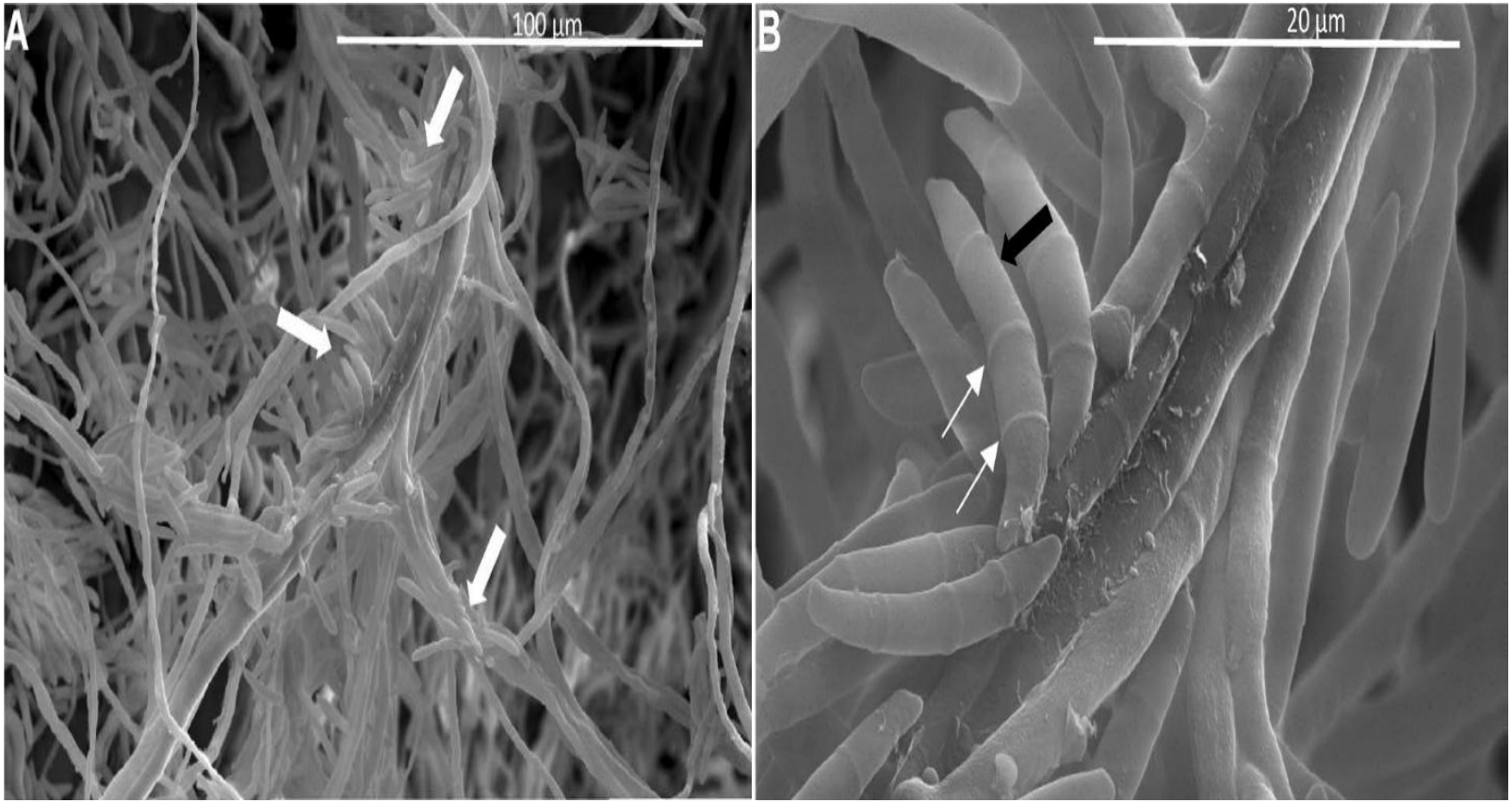


Figure 43: *Fusarium solani* **A.** Smooth hyphae and conidophores. The white arrows indicate conidiophores. **B.** Conidiophores; the black arrow indicates multiseptated macroconidia and the thin white arrows indicate septum. SEM image from Gutierrez-Santa Ana *et al*

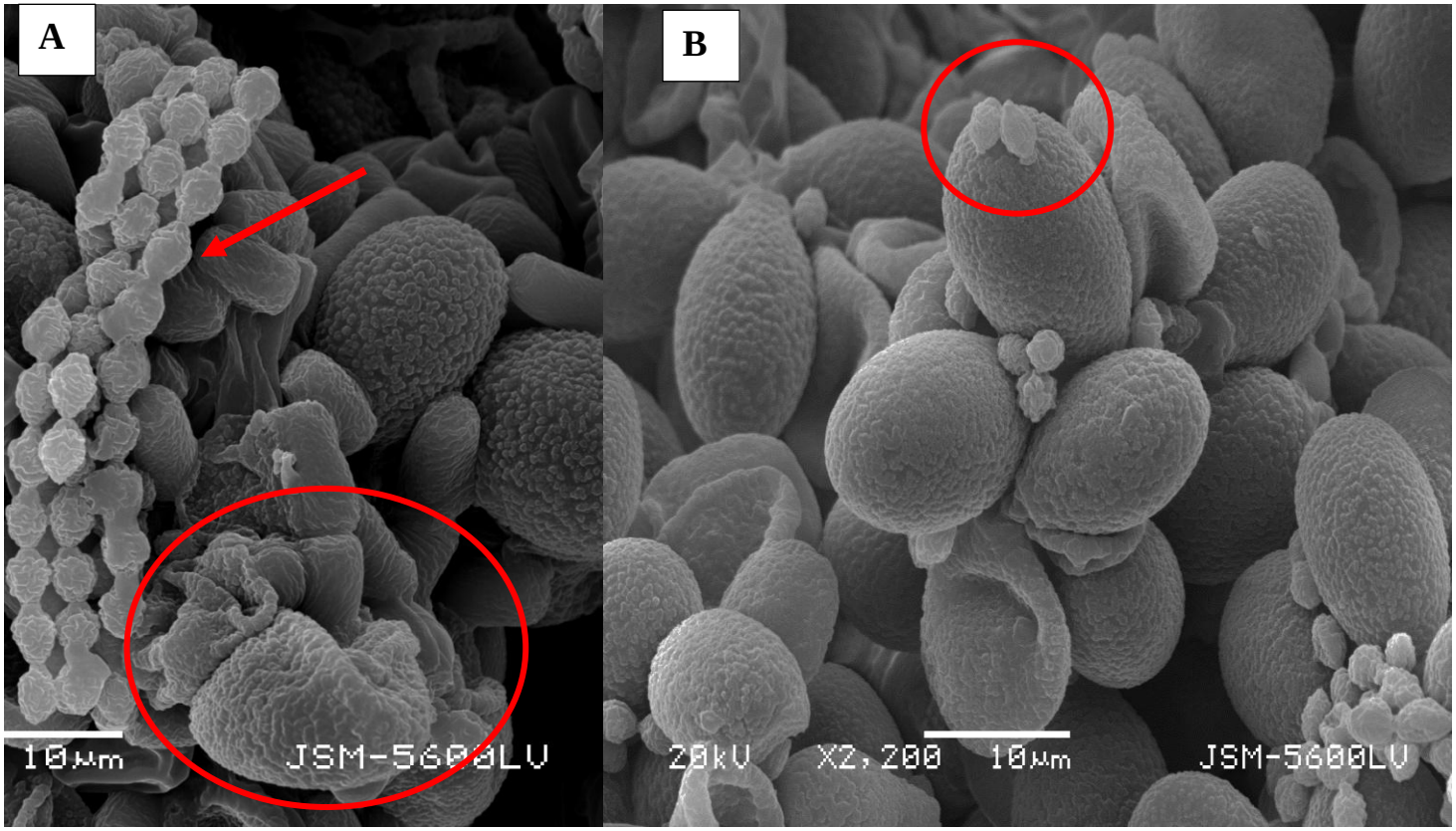


Figure 44: Scanning Electron Microscopy image of the effect of the antagonistic endophyte *Talaromyces* spp. on *Ceratocystis radicicola*. A: *Talaromyces* spp. chain of spores shown by the arrow. Red circle shows the shrinkage/distortion of *C. radicicola* spores B: *Talaromyces* spp. spores on *C. radicicola* spores; the red circle shows two *Talaromyces* spp. spores hooked on the *C. radicicola* spore.

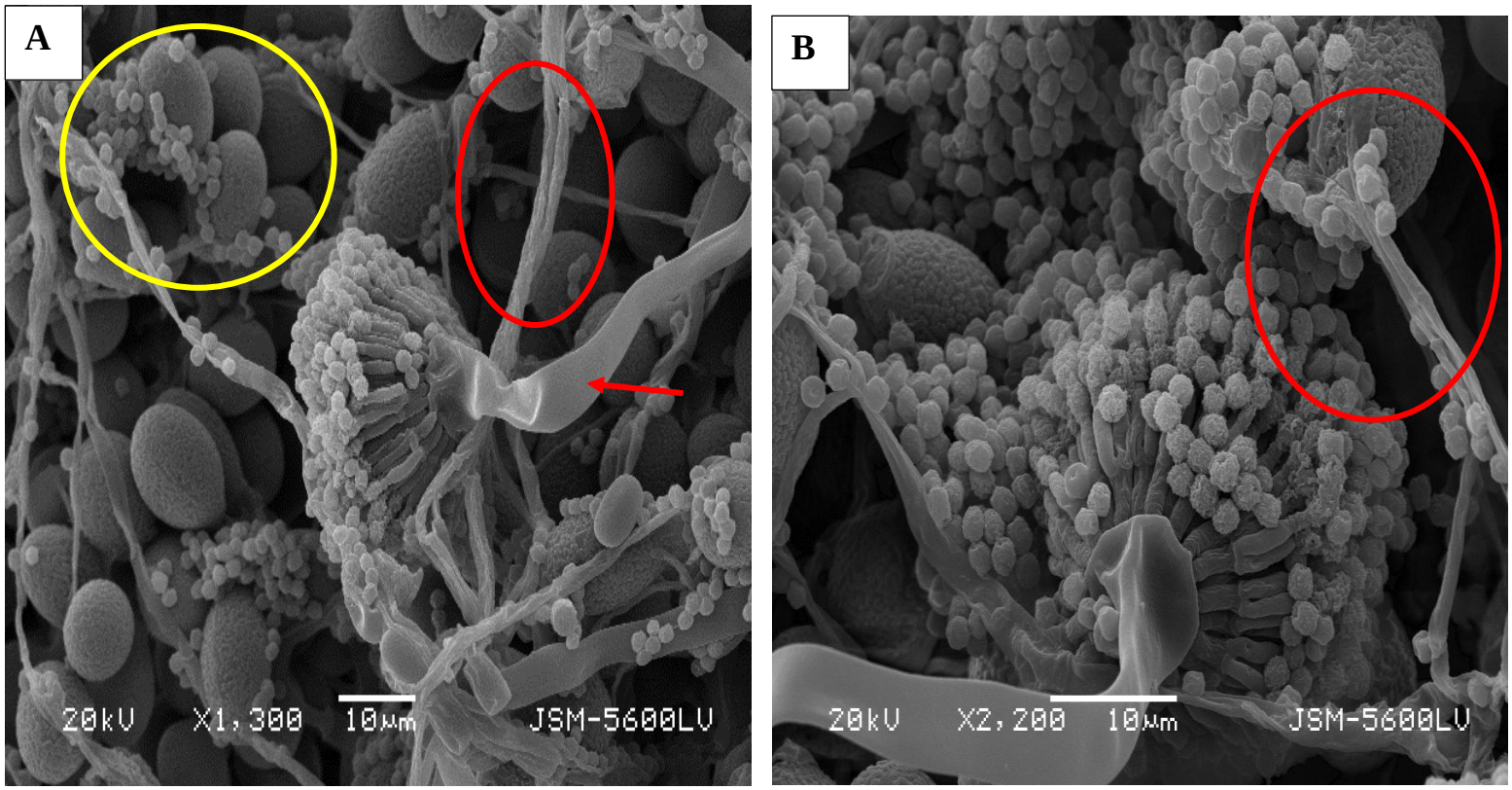


Figure 50 now 45: Scanning Electron Microscopy image of the effect of the antagonistic endophyte of *Aspergillus terreus* on *Ceratocystis radicicola* **A**: *Ceratocystis radicicola* hyphae shriveled as seen in the red circle compared to smoothness of hyphae of *Aspergillus terreus* indicated by the red arrow; the yellow circle shows *A. terreus* spores covering hyphae and spores of *C. radicicola*. **B**: Hyphae of *Ceratocystis radicicola* shriveled as seen inside the red circle and *Aspergillus terreus* spores are attached to it.

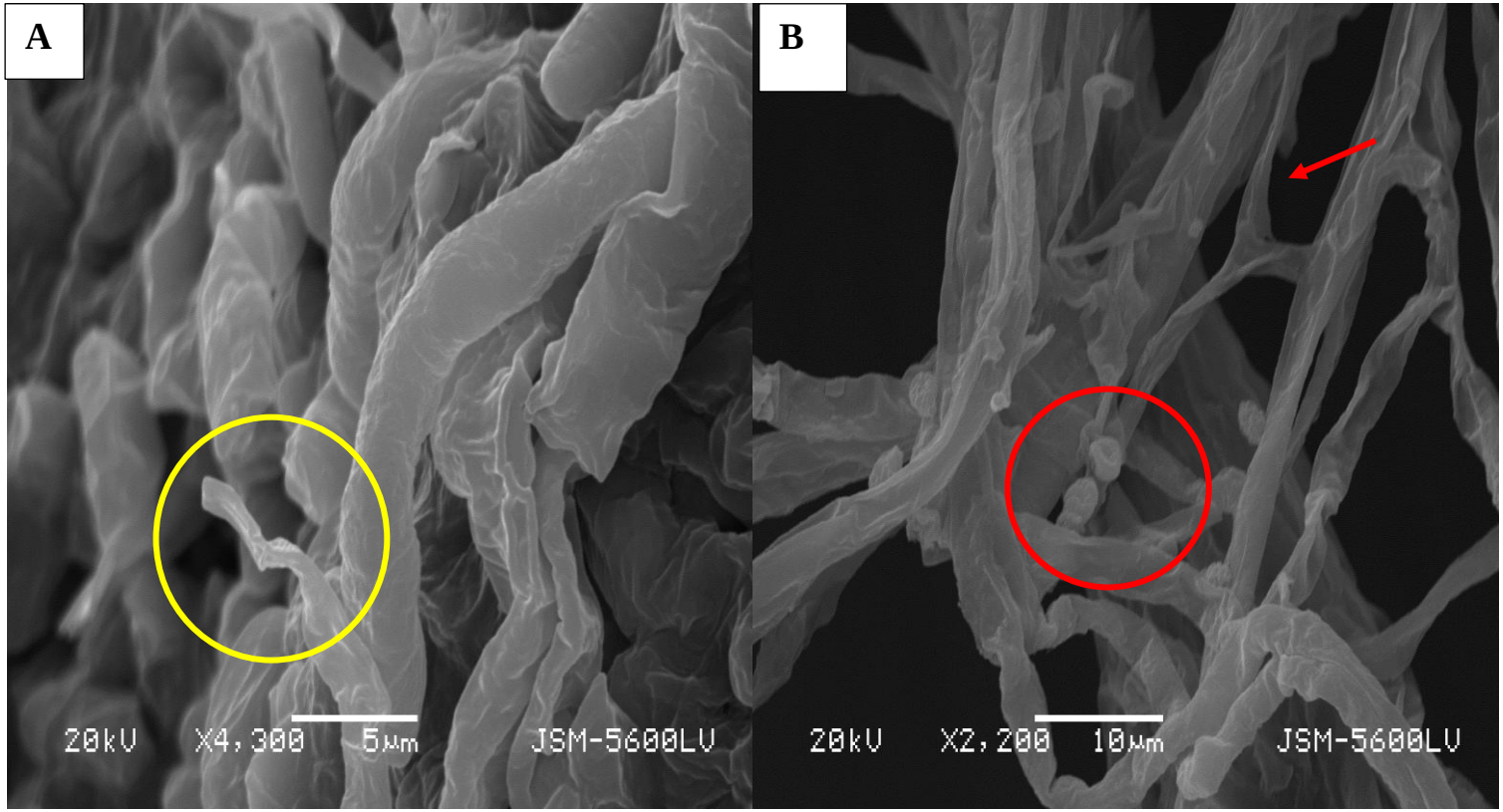


Figure 51 now 46: Scanning Electron Microscopy image of the antagonistic endophyte *Talaromyces* spp., effect on *Fusarium solani*. **A**: *Fusarium solani* hyphae shriveled **B**: *Talaromyces* spp spores attached on shriveled hyphae of *Fusarium solani* as shown inside the red circle.

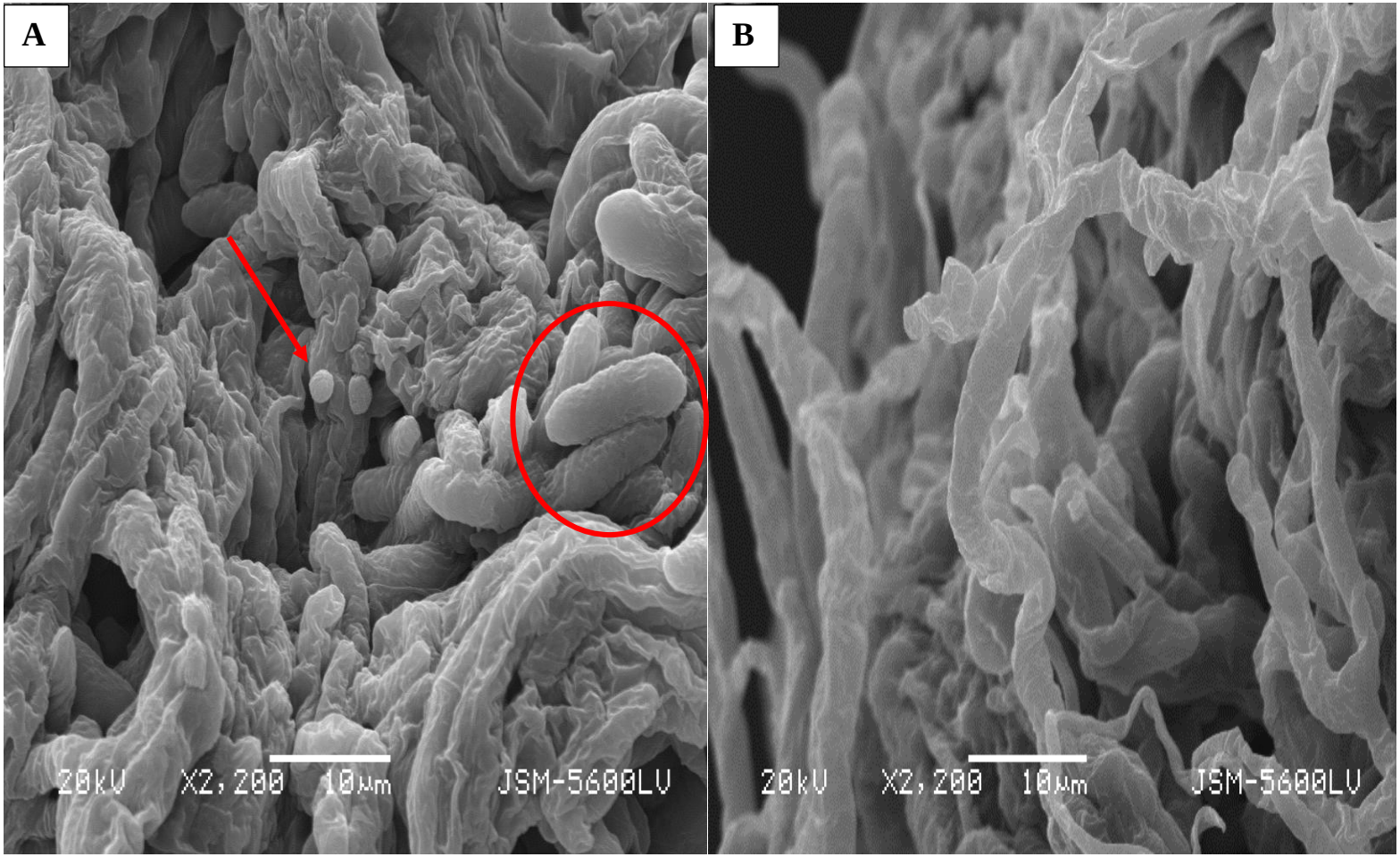


Figure 52 now 47: Scanning Electron Microscopy image of the effect of the antagonistic endophyte *Aspergillus terreus* on *Fusarium solani*. **A**: Red circle shows *Fusarium solani* wrinkled; the red arrow points to the spores of *Aspergillus terreus* **B**: *Fusarium solani* shriveled hyphae.

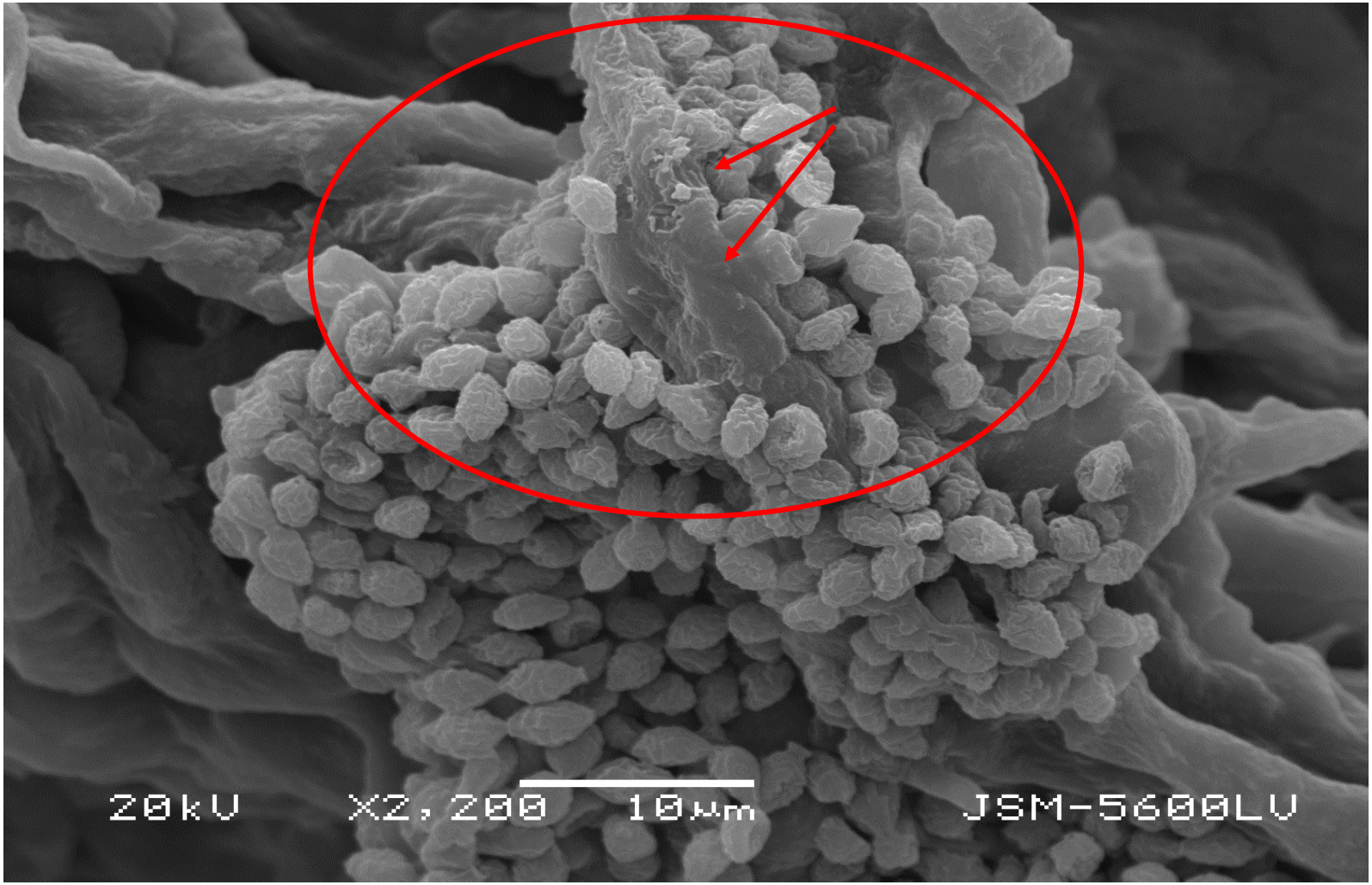


Figure 53 now 48: Close up image in the red circle showing the degeneration of the of *Fusarium solani* hyphae by the spores of *Aspergillus terreus*. The red arrows point at the degenerated section and at the smoother section right below it.

4.3.2 Culture filtrate effect of the antagonistic *Aspergillus terreus* and *Talaromyces* sp. fungi on electrolyte leakage of *Ceratocystis radicicola* and *Fusarium solani*

All the raw data for results of electrolyte leakage and pH are shown in Annex 7.

The results for *Ceratocystis radicicola* and *Fusarium solani* following addition of the CF of *Talaromyces* spp. resulted in a reduction in extracellular conductivity and rise in pH for both pathogens (Table 13).

For *Ceratocystis radicicola* with *Talaromyces* spp. the average values increased from pH 4.01 at initial administration (0 hours) to a reading of 5.08 at 24 housr, while the control was stable at pH 4 from 0 - 24 hours. As for extracellular conductivity, the average values decreased from 170.86 mV at initial administration (0 hours) to a reading of 109.33mV at 24 hours, while the control was stable at 170.8 mV from 0 - 24 hours. The results for the *Talaromyces* with *C. radicicola* showed that there was no significant difference in pH between all times (0, 2 and 24 hours). For electrolyte leakage, however, there was a significant difference between the times of 0 hours and 2 hours and between the times of 0 hours and 24 hours, while there was no significant difference between 2 hours and 24 hours. For the control, there was a significant difference in pH between the times of 0 hours and the 24 hours and also between 2 hours and 24 hours. However, there was no significant difference between 0, 2 and 24 hours.

For *Talaromyces* with *Fusarium solani* the average pH values increased from 4.01 at initial administration (0 hours) to a pH reading of 4.14 at 24 hours, while the control was stable at pH 4.01 from 0 - 24 hours. For extracellular conductivity, the

average values decreased from 170.8 mV at initial administration (0 hours) to a reading of 163.43 mV at 24 hours, while the control from 0 - 24 hours was stable at 170.8 mV. For *Talaromyces* with *F. solani* showed there was no significant difference in pH between all times (0, 2 and 24 hours). For the electrolyte leakage, however, there was a significant difference between the times of 0 hours and 24 hours and between the times of 2 hours and 24 hours, whereas between the times of 0 hours and 2 hours there was no significant difference. For the control, there was a significant difference in pH between the times of 0 hours and 24 hours and also between 2 hours and 24 hours, whereas no significant difference was shown between 0 hours and 2 hours. Finally, for the electrolyte leakage in the control, there was no significant difference between all times (0, 2 and 24 hours).

Table 13 : Electrolyte leakage (mV) and pH measurement for *Ceratocystis radicicola* and *Fusarium solani* after application of *Talaromyces* spp. culture filtrate CF at 0, 2 and 24 hours.

Talaromyces X *C. radicicola*						
	0 hr		2hr		24hr	
	pH	mV	pH	mV	pH	mV
Replicate avg	4.01[a]	170.8[a]	4.96[a]	116.38[b]	5.08[a]	109.33[b]
Control *Talaromyces* CF	4.01[a]	170.8[a]	4.01[b]	170.8[a]	4.01[b]	170.8[a]
Talaromyces X *F. solani*						
	0 hr		2hr		24hr	
	pH	mV	pH	mV	pH	mV
Replicate avg	4.01[a]	170.8[a]	4.01[a]	170.86[a]	4.14[a]	163.43[b]
Control *Talaromyces* CF	4.01[a]	170.8[a]	4.01[a]	170.8[a]	4.01[b]	170.8[a]

Means and Standard Deviation(n=3) followed by same letter in a column are not significantly different (Tukey's test $P< 0.05$)

For *C. radicicola* with the CF of *Aspergillus terreus* (Table 14) the average values increased from pH 4.27 at initial administration (0 hours) to 4.336 at 24 hours. For extracellular conductivity, the average value was 153.72 mV at initial

administration (0 hours) to a reading of 152.19 mV at 24 hours. The control averages ranged from 4.17 - 4.21 from 0 hours to 24 hours and electrolyte leakage averages ranged from 159.24 to 161.52 mV between 0 hours to 24 hours. For of *A. terreus* with *C. radicicola***,** there was no significant difference in pH between all times (0, 1 and 24 hours). For electrolyte leakage, there was a significant difference between the times of 0 hours and 1 hour and also between the times of 0 hours and 24 hours, but no significant difference between the times of 1 hour and 24 hours. For the control, there was no significant difference in pH between the times of 1 hour and 24 hours, and a significant difference between the times of 0 hours with 1 hour and 24 hours. For electrolyte leakage in the control, there was no significant difference between the times of 0, 1 and 24 hours.

For *F. solani* with the CF of *Aspergillus terreus*, the pH average values increased from a value of 4.35 at initial administration (0 hours) to a pH reading of 4.42 at 24 hours. For extracellular conductivity, the average values clearly increased from 151.05 mV at initial administration (0 hours) to 163.43 mV at 24 hours. The control averages ranged from pH 4.17 to 4.21 from 0 - 24 hours and electrolyte leakage ranged from 160.38 to 161.52 mV from 0 - 24 hours. The results for *F. solani* with CF of *Aspergillus terreus* showed there was no significant difference in pH between all times (0, 1 and 24 hours). For the electrolyte leakage, however, there was a significant difference between 0 hours and 24 hours and between the times of 1 hour and 24 hours, but no significant difference between 0 hours and 1 hour. For the control, there was no significant difference in pH between 0, 1 and 24 hours and no significant difference in electrolyte leakage between 0, 1 and 24 hours.

Table 14: Electrolyte leakage (mV) and pH measurement for *Ceratocystis radicicola* and *Fusarium solani* after application of *Aspergillus terreus* culture filtrate CF at 0, 1 and 24 hours.

A. terreus X *C. radicicola*						
	0 hr		1hr		24hr	
	pH	mV	pH	mV	pH	mV
Replicate avg	4.27[a]	153.72[a]	4.35[a]	150.66 [b]	4.336[a]	152.19[b]
Control CF *A.terrus*	4.19[a]	160.38[a]	4.21[b]	159.24[a]	4.17[b]	161.52[a]
A. terreus X *F. solani*						
	0 hr		1hr		24hr	
	pH	mV	pH	mV	pH	mV
Replicate avg	4.35[a]	151.05[b]	4.39[a]	149.14[b]	4.42[a]	163.43[a]
Control CF *A.terrus*	4.19 [b]	160.38[a]	4.21[b]	159.24[a]	4.17[b]	161.52[a]

Means and Standard Deviation(n=3) followed by same letter in a column are not significantly different (Tukey's test $P< 0.05$)

4.4 Discussion

The use of Scanning Electron Microscopy (SEM) imaging has increased understanding of biological changes, through magnification that detects certain characteristics that are not possible to attain through normal light microscopy. Importantly for this study, the technology allows visualization of interactions between microorganisms.

In this study, SEM images provided evidence that the *Aspergillus terreus* and *Talaromyces* species resulted in deformation and morphological abnormalities in the mycelium and conidia of *Ceratocystis radicicola* and *Fusarium solani* when they interacted with them. This was in line with several previous studies. Al Naemi *et al.* (2016) isolated 12 strains of *Trichoderma harzianium* from the rhizosphere of healthy date palms, and one strain had an inhibitory effect on *Ceratocystis radicicola,* the cause of Black Scorch disease of date palm. SEM images showed evidence of ultrastructural defects in the hyphae and spores of *Ceratocystis radicicola*. Ahmed *et al.* (2019) also showed the effect of *Trichoderma harzianium, Trichoderma viride* and the bacterium *Bacillus subtilis* on *Ceratocystis manginecans* causing Mango Quick Wilt. *Trichoderma* species have proved successful as biocontrol agents against diseases caused by *Ceratocystis* species *(Caberra et al.,* 2016). This study is the first to investigate the antagonism of *Aspergillus terreus* and *Talaromyces* species on *Ceratocystis radicicola.*

Previous studies on antagonism and mode of action of *Talaromyces* species and *Aspergillus terreus* showed that they are either through antibiosis (secretion of antimicrobial metabolites) or mycoparasitism (direct physical contact and coiling

around hyphae of the host to absorb nutrients and cause disintegration). The results of our study agrees with those of Luo *et al.* (2021) where SEM images showed *Fusarium equiseti*, the pathogen of cucumber wilt, was inhibited by species of *Talaromyces*, where the hyphae were loosely twisted and cohesive with node like protrusions at the center and tip. Halo *et al.* (2018) also showed that *T. varibalis* induced entanglement and antibiosis of hyphae. Furthermore, Luo *et al.* (2021) extracted three antimicrobial bioactive substances that had thermostability and insensitivity to UV and metal ions. *Talaromyces flavus* was shown to have different mechanisms with *Sclerotium rolfsii* and *Verticillium dahliae* (Madi *et al.,* 1997).

Aspergillus terreus also had the same effect through antibiosis and the results were consistent with those of Al Shibli *et al.* (2019) and Karunasinghe *et al.* (2020). The antagonistic fungi have previously been shown to release metabolites that interfere with the growth and morphology of the pathogenic fungi (Halo *et al.,* 2018). Melo *et al*. (2006) also showed that *Sclerotina sclerotiorum,* the wilt pathogen of tomato, dry beans, soybean, lettuce and sunflower, was antagonized by *A. terreus*. SEM images showed disintegration of *S. sclerotiorum* hyphae with an extensive mass of *A. terreus* conidia on it. This was similar to the findings of this study with SEM images of *A. terreus* on *C. radicicola.* Similarly, *Rhizoctonia solani* was suppressed on broad bean wilt by 58% percent and on bean wilt by 42% with application of *A. terreus* (Abdelaziz *et al.,* 2023), whilst tomato wilt caused by *Fusarium oxysporum* f.sp. *lycopersici* and potato soft rot caused by *Dickeya chrysanthemi* (formerly *Erwinia chrysanthemi*) were also inhibited by *A. terreus* (Choi *et al.,* 2023).

The electrolyte leakage experiments from *Aspergillus* and *Talaromyces* species were in line with the findings from Halo *et al.* (2018 and 2019), Kazerooni *et al.* (2019), Al Shibli *et al.* (2019) and Karunasinghe *et al.* (2020). The results for *Talaromyces* species with *Ceratocystis radicicola* showed significant differences in the EC readings between the initial timing at 0 hours with the 2 hour and 24 hour readings. This was similar to findings also shown with *Fusarium solani* and *Aspergillus terreus* with both pathogens. This may be due to the fact that the culture filtrate (CF) of *Talaromyces* and *A. terreus* required a relatively longer time to act on these pathogens. A quicker reaction may be possible through placing CF disks directly on pathogen isolates, where inhibition zones were evident and persistent in dual culture experiments. Luo *et al.* (2021) had shown that the bioactive substances extracted from *Talaromyces* were effective in neutral and alkaline conditions, but not under acidic conditions. In this study all the CFs were acidic and remained acidic with pH's ranging from 4 to 5.1 even after 24 hours. Halo *et al.* (2018 and2019), Kazerooni *et al.* (2019), Al Shibli *et al.* (2019) and Karunasinghe *et al.* (2020) all used *Pythium aphanidermatum* as the pathogen, which is an oomycete with a cell wall made up of cellulose amongst other compounds. *Talaromyces* and *A. terreus* both secrete cellulases as shown by Halo *et al*. (2019). Stosz *et al*. (1996), Madi *et al*. (1997) and Luo *et al.* (2021) used different approaches, but all used the CF to determine enzyme bioassays, while antagonism and mycoparasitism were tested by dual cultures or in sandy soil placed in Petri dishes by calculating the percentage of colonized sclerotia, or inoculating pots with the diseased crop.

The metabolites released and causing electrolyte leakage in *Ceratocystis radicicola* and *Fusarium solani* and the SEM images prove the efficacy of *Aspergillus terreus* and *Talaromyces* new species in inhibiting pathogenic fungi by antibiosis and mycoparasitism. Fungal isolation from roots and rhizosphere (Al Naemi *et al*., 2016) indicate that *Aspergillus* species is common in the rhizosphere of date palm trees, and therefore may provide protection of date palm roots against some pathogenic fungi. Future studies should focus on 1) SEM imaging of dual culture inhibition zones at the first few days from inhibition and media pigmentation; 2) SEM imaging the effect of metabolites on the pathogens; 2) extraction of the metabolites secreted by each antagonistic fungus and identification of the chemical through bioassays and culturing the fungi on specialized media; 3) re-investigating the electrolyte leakage with longer time periods and with using CF discs on isolates of the pathogens.

Chapter 5

General discussion

Date palms are the principal crop in Oman and the Arabian Peninsula, linked to the heritage, culture and life style of the Omani people. The main pathogen of date palm, causing wilt, root and trunk rot, and black scorch is *Ceratocystis radicola* Bliss. It was reported as the most common and aggressive root pathogen in a survey in Oman by Al Saidi *et al.* (2012b). The *C. radicola* population in Oman has been shown to have moderate genetic diversity indicating that it has been present for a considerable amount of time (Al Saidi *et al.,* 2013). Wilt and yellowing, caused by *Fusarium solani,* has also been reported in date palm (Yasiri *et al.,* 2016). In Oman, it is considered as a secondary pathogen of date palm (Al Saidi *et al.,* 2012b). In this doctoral study, the aim was to determine the fungal diversity between feral and cultivated date palms from different locations. The second aim was to identify endophytes from the rhizosphere and roots of the cultivated and feral date palms and test their potential as antagonistic fungi against the date palm pathogens *C. radicola* and *F. solani.*

Exploitation of microbial communities promotes development of a disease suppressive soil environment. Examples include *Fusarium* suppressed by the presence of nonpathogenic *Fusarium* and fluorescent pseudomonad communities, *Rhizoctonia* by *Trichoderma* and *Burkholderia* species, and Take-all in wheat affected by fluorescent pseudomonad communities and *Trichoderma* (Mazzola, 2002).

Endophytic fungi have received increased research attention in the past decade as potential new biological and safe management methods for pests and diseases. Nishad *et al.* (2020) emphasized the importance of researching and using indigenous biocontrol agents as the best ways to prevent issues of invasiveness from non-native bioagents. For example, Redda *et al*. (2018) identified 21 species from 380 strains of *Trichoderma* isolated from Inner Mongolia grasslands, in which 195 strains were powerful antagonists inhibiting more than 50% of the pathogens *Fusarium oxysporum*, *Rhizoctonia solani* and *Botrytis cinerea*.

In our study, the analysis of fungal diversity in soil samples from date palm sampling sites indicated no effect on fungal diversity regardless of the locations or cultivation systems. This may be due to the uniqueness of the date palm rhizosphere system in which certain fungal species may preferentially grow. A study by Al-Sadi *et al.* (2012) showed that many of the fungi associated with root system in 111 date palm trees were common to different regions in Oman, whilst in Qatar, 182 isolates were recorded during a survey of rhizosphere soil from healthy and diseased date palms to identify pathogens and biocontrol agents (Nishad *et al.*, 2020). The most common nonpathogenic genera were *Aspergillus*, *Rhizopus*, *Trichoderma* and *Fusarium*. Pathogenic fungi isolated from various date diseases (black leaf scorch, trunk rot, inflorescence blight, offshoot diplodia and root rot) were *Neodeightonia phoenicum*, *Thielaviopsis punctulata*, *Fusarium brachygibbosum*, *Fusarium equiseti* and *Fusarium solani* (Nishad *et al.*, 2020). In this study, the detected fungal classes were similar to the classes reported by Kazerooni *et al.* (2017). Date palm endophyte fungal diversity was shown by Ben Chobba *et al*. (2013) to be high from leaves and

roots, and also that the endophytic population varies depending on the plant part investigated. This study demonstrated the diversity of cultivable and uncultivable endophytes in date palm.

Soil analysis showed the variability of organic matter levels and other nutrients between the soil samples with no effect of location or cultivation type on soil fertility. This is expected, since Oman is an arid region with low rain fall and crop cover, and the resultant soil texture affects the amount of nutrients attained in the soils. This may also be due to the fact the date palms are still fertilized in the traditional methods of organic manures (Al Yahyai *et al.*, 2015). PCA analyses has shown the lack of clustering of fungal species based on cultivation systems and locations. This indicates an absence of any effect from cultivation systems or locations on fungal species distribution. The study shows for the first time that fungal diversity in date palms is not affected by locations or cultivation systems. Fungal diversity is primarily associated with date palm roots and there is no influence from locations or cultivation systems on them.

Investigating the antagonistic activity of different fungal species on *Ceratocystis* and *Fusarium* species indicated that *Aspergillus* had a greater antagonistic effect than *Talaromyces* species. This may be due to the fact that the *Talaromyces* species was a mix of 3 new isolates so the effect was not from one isolate at a time. Previous studies (Halo *et al.*, 2018; Halo *et al.*, 2019; Kazerooni *et al.*, 2019; Al Shibli *et al.*, 2019; Karunasinghe *et al.*, 2020) all indicated that *Aspergillus* species and *Talaromyces* species, obtained from desert plants, mangrove, sea purslane, cucumber and tomato, resulted in morphological abnormalities in the mycelium of

Pythium species and *Rhizoctonia* species and suppressed damping-off. Findings from this study showed that some fungal species isolated from date palm roots may help protect dates against some pathogenic fungi, including the *Ceratocystis* and *Fusarium* species that are known to result in wilt diseases (Al-Sadi *et al.,* 2012).

Several reports have reported *Talaromyces* species to be antagonistic to plant pathogens. For example, *Talaromyces* from the Yap Trench in the Pacific Ocean were antagonistic to the cucumber wilt pathogen *Fusarium equisiti* (Luo *et al.*, 2021), whilst *Talaromyces flavus* has been shown to control *Verticillium dahliae* and *Sclerotia rolfsii* (Stosz *et al.,* 1996; Madi *et al.,* 1997). *Aspergillus* species have also been reported to have many uses in industry and as BCAs, with antagonistic effects on plant pathogens. *Aspergillus terreus* was shown to control several wilt diseases of crops caused by *Sclerotinia sclerotiorum* (Malo *et al.,* 2006), and *A. terreus* also showed suppression of *Fusarium oxysporum* f.sp. *lycopersici* causing tomato wilt and the bacterium *Dickeya chrysanthemi* causing potato soft rot (Choi *et al.,* 2022). Suppression of *Rhizoctonia solani,* causing damping off disease, occurred when *A. terreus* was added to diseased crops of beans and broad beans (Ahmed *et al.,* 2023).

In our study, molecular and morphological identification revealed the presence of three potential new species of *Talaromyces* isolated from the Omani date palm rhizosphere. This is a first report on the new potential *Talaromyces* species. The identification and the constructed phylogenetic tree of the potential new *Talaromyces* species showed it was in Section *Trachyspermi*. This was in line with the findings of Wei *et al.* (2021), who showed by molecular phylogenetic

investigations that the species in *Penicillium* subgenus *Biverticillium* are in the same clade as *Talaromyces* rather than other species of *Penicillium.* This supported the nomenclature revisions to use a single name for a single species. Also, Samson *et al.* (2011) listed 72 species in *Talaromyces*, which Yimaz *et al.* (2014) resolved into 7 sections, *Bacillispori, Helici, Islandici, Purpurei, Subinflati, Talaromyces* and *Trachispermi.* According to Wei *et al.* (2021), *Talaromyces* is a common soil inhabitant, with many other species that are not readily isolated in pure culture. This may be due that *Talaromyces* does not acclimatize to artificial media and environments, thus they show very slow growth. Also, some species are rare and endemic and are seldomly encountered, and isolation methods require improvement and modifications. Even when pure cultures are obtained, some prove challenging to identify via morphological means, especially in degenerated ones. This was encountered in this study during the maintenance in pure culture, where two isolates were distinguished in their colony morphology and abundance of red pigmentation.

SEM images provided evidence along with the electrolyte leakage experiments on the efficacy of *Aspergillus* species and *Talaromyces* species in suppressing and degrading pathogenic *Ceratocystis* and *Fusarium* species by antibiosis and mycoparasitism. This was in line with previous findings (Al Naemi *et al.*, 2016; Melo *et al.*, 2006; Luo *et al.*, 2021; Stosz *et al.*, 1996; Madi *et al.*, 1997). Electrolyte leakage experiments showed the opposite results to the studies of Halo *et al.* (2018; 2019), Kazerooni *et al.* (2019), Al Shibi *et al.* (2019) and Kumarasinghe *et al.* (2020). This can be explained by the fact that *C. radicola* and *F. solani* might require

different approaches for the measurement of the effect of their metabolites along with more time to measure the effects.

This research in date palms, especially the use of feral palms for exploring new endophytic fungi and using them as biocontrol agents is a new and potentially valuable area of study. Future studies should continue to investigate the potential endophytic fungi from the rhizosphere and the date palm roots and fronds in suppressing date palm pathogens with consideration of safety and applicability to the field. In addition, investigations could be made on the biochemical compounds which the fungi and date palms activate or produce to inhibit pathogens. Electrolyte leakage analysis should be modified to use culture filtrate discs embedded in the pathogen isolate culture, and trying different media for isolation of antagonistic fungi to obtain culture filtrates. Another approach could be extracting the metabolites and identifying their chemical nature and stability. A second future prospect could be to use better, well-defined SEM imaging and the sampling of dual cultures at the onset of antagonism and pigment production, or sampling from the pathogen culture exposed to the culture filtrate or the metabolite secreted by the antagonistic fungi.

In a third future area of study, the morphological identification and parameters for the potential new *Talaromyces* species should be repeated and completed by using the recommendations of Wei *et al.* (2021), of media compositions and molecular analysis and sequencing. Further molecular identification is also required with the use of other sequencing primers recommended in publications, to enable the recording of new species for Oman, and allow further research to flow through.

A fourth and final future prospect is to test the applicability of these antagonists to suppress date palm wilt under normal environmental conditions. A pathogenicity test to find the most effective concentrations and application methods of the pathogens should be used to achieve the closest replication of natural field conditions and stresses. Also, the required application to achieve the desired establishment of the antagonist in the soil and the required concentration (spore/ml) of the pathogen to achieve infection should be established. Finally, the best method of application to the diseased date palms in the field should be determined. These future prospects will result in a more detailed investigation on the most effective and sustainable biocontrol approach for the management of date palm wilt.

References

Abdelaziz, A.O., El Wakil, D.A., Hashem, A.H., Al Askar, A.A., Abd Elgawad, H. and Attia, M.S. (**2023**). Effcient role of endophytic *Aspergillus terrus* in biocontrol of *Rhizoctonia solani* causing damping-off disease of *Phaseolus vulgari* and *Vicia faba*. *Microoraganisms* 11: 1487.

Agriculture and Fisheries Development Fund (AFDF), Unpublished Report for Project "Survey and Diagnosis of Panama Disease in Oman Phase 1".

Aguilar-Trigueros, C.A. and Rillig, M.C. (**2016**). Effect of different root endophytic fungi on plant community structure in experimental microsims. *Ecology and Evolution* 6: 8149-8158.

Ahmad, T., Moosa, A. and Abdul Rehman (**2020**). In vitro efficacy of microbial antagonists, botanical extracts and synthetic chemicals against mango quick wilt pathogen *Ceratocystis manginecans*. *International Journal of Fruit Science* 20: 705-719.

Al-Bulushi, I. M., Bani-Uraba, M.S., Guizani, N.S., Al-Khusaibi, M.K. and Al-Sadi, A.M. (**2017**). Illumina MiSeq sequencing analysis of fungal diversity in stored dates. *BMC Microbiology* 17: 72.

Al Adawi, A.O., Deadman, M.L., Al Rawahi, A.K., Al Maqbali, Y.M., Al Jahwari, A.A., Al Saadi, B.A., Al Amri, I.S. and Wingfield, M.J (**2006**). Aetiology and causal agents of mango sudden decline disease in the Sultanate of Oman. *European Journal of Plant Pathology* 116: 247–254.

Al Naemi, F.A., Ahmed, T.A., Nishad, R. and Radwan, O (**2016**). Antagonistic effects of *Trichoderma harzianum* isolate against *Ceratocystis radicicola*: pioneering a biocontrol strategy aginst black scorch disease of date palm trees. *Journal of Phytopathology* 164: 464-475.

Al-Raisi, Y.M., B'Chir, M.M. Al-Mandhari, A.M., Deadman, M.L. and Gowen, S.R. (**2011**). First report of *Ceratocystis radicicola* associated with date palm disease in Oman. *New Disease Reports* 23**:** 23.

Al-Sa'di, A.M., Drenth, A., Deadman, M., de Cock, A.W.A.M. and Aitken, E.A.B. (**2007**). Molecular characterization and pathogenicity of *Pythium* species associated with damping off in greenhouse cucumber (*Cucumis sativus* L.) in Oman. *Plant Pathology* 56**:** 140-149.

Al-Sadi, A.M., Al-Said, F.A., Al-Jabri, A.H., Al-Mahmooli, I.H., Al-Hinai, A.H. and de Cock, A.W.A.M. (**2011a**). Occurrence and characterization of fungi and oomycetes transmitted via potting mixtures and organic manures. *Crop Protection* 30**:** 38-44.

Al-Sadi, A.M., Al-Said, F.A., Al-Kiyumi, K.S., Al-Mahrouqi, R.S., Al-Mahmooli, I.H. and Deadman, M.L. (**2011b**). Etiology and charcterization of cucumber vine decline in Oman. *Crop Protection* 30**:** 192-197.

Al-Sadi, A.M., Al-Hilali, S.A., Al-Yahyai, R.A., Al-Said, F.A., Deadman, M.L., Al-Mahmooli, I.H. and Nolasco, G. (**2012a**). Molecular characterization and potential sources of Citrus Tristeza Virus in Oman. *Plant Pathology* 61**:** 632-640.

Al-Sadi, A.M., Al-Jabri, A.H., Al-Mazroui, S.S. and Al-Mahmooli I.H. (**2012b**). Characterization and pathogenicity of fungi and oomycetes associated with root diseases of date palms in Oman. *Crop Protection* 37**:** 1-6.Al-Sadi, A.M., Al-Moqbali, H., Al-Yahyai, R., Al-Said, F. and Al-Mahmooli, I. (**2012c**). AFLP data suggest a potential role for the low genetic diversity of acid lime (*Citrus aurantifolia*) in Oman in the outbreak of witches' broom disease of lime. *Euphytica* 188**:** 285-297.

Al-Sadi, A.M., AL-Wehaibi, A.N., Al-Shariqi, R.M., Al-Hammadi, M.S., Al-Hosni, I.A., Al-Mahmooli, I.H. and Al-Ghaithi, A.G. (**2013**). Population genetic analysis reveals diversity in

Lasiodiplodia species infecting date palm, Citrus, and mango in Oman and the UAE. *Plant Disease* 97**:** 1363-1369.

Al-Sadi, A.M. (**2013**). Phylogenetic and population genetic analysis of *Ceratocystis radicicola* infecting date palms. *Journal of Plant Pathology* 95**:** 47-55.

Al-Sadi, A.M., Al-Ghaithi, A.G., Al-Fahdi, N. and Al-Yahyai, R.A. (**2014**). Characterization and pathogenicity of fungal pathogens associated with root diseases of citrus in Oman. *International Journal of Agriculture and Biology* 16**:** 371-376.

Al-Sadi, A.M., Al Owaisi, F.A., Edwards, S., Al Nadabi, H. and Al Fahdi, A.M. (**2015**). Genetic analysis reveals diversity and genetic relationship among *Trichoderma* isolates from potting media, cultivated and uncultivated soil. *BMC Microbiology* 15: 147.

Al-Sadi, A.M., Al-Masoodi, R.S., Al-Ismaili, M. and Al-Mahmooli, I.H. (**2015**). Population structure and development of resistance to hymexazol among *Fusarium solani* populations from date palm, Citrus and cucumber. *Journal of Phytopathology,* in press.

Al Shibli, H., Dobretsov, S., Al Nabhani, A., Maharachchikumbura, S.S.N. and Al Sadi, A.M. (**2019**). *Aspergillus terrus* obtained from mangrove exhibits antagonistic activities against *Pythium aphanidermatum* – induced damping off of cucumber. *PeerJ7*: e7884 DOI 10.7717/peerj.7884.

Anderson, M.J. (**2017**). Permutational multivariate analysis of variance (PERMANOVA). Wiley Stats Ref: Statistics Reference Online

Anees, M., Tronsmo, A., Edel-Hermann, V., Hjeljord, L.G., Heraud, C. and Steinberg C. (**2010**). Characterization of field isolates of *Trichoderma* antagonistic against *Rhizoctonia solani*. *Fungal Biology* 114: 691-701.

Al Wardi, M .and Choudri, B.S. (**2018**). Spatial assessment and variability of soil properties on the Saiq plateau, Oman. *Journal of Materials and Environmental Sciences* 9: 528-535.

Al-Yahyai, R. and Khan, M.M. (2015). Date palm status and perspective in Oman (Ch 6) In:, Date Palm Genetic Resources and Utilization:Volume 2: Asia and Europe, J.M. Al-Khayri et al. (eds.) Springer Science+Business Media Dordrecht.

Al-Yahyai, R., Khan, I., Al Sadi, A., Al Wahaibi, A. and Deadman, M. (2012). Status of *Citrus aurantifoilia* infected with witches' broom disease of lime in Oman. *Conference Acta Horticulturae* 928: 375-381.

AlYasiri, I.I., Saad, N.A., Ismail, A.I. and Nasser, A.R. (**2016**). Identification and diagnosis of some pathological phenomena on the date palm caused by Fusarium species in Iraq. *International Journal of Current Microbiology* 5: 692-700.

Al Yahyai, R. and Khan, M.M. (2015). Date palm status perspective in Oman. In: Date Palm Genetic Resources and Utilization. Vol.2, Asia and Eorope. Ed. J.M.Al Khayri.

Bhattacharya, R., Saha, S., Kostina, O., Muravink, L. and Mitra, A. (**2020**). Replacing critical point drying with a low-cost chemical drying provides comparable surface image quality of glandular trichomes from leaves of *Millingtonia hortensis* L.f. in scanning electron micrographs. *Applied Microscopy* 50: 15.

Barnett, H.L. and Hunter, B.B. (**1998**). *Illustrated genera of imperfect fungi,* Minnesota, USA, APS Press.

Ben Choba, I., Elleuch, A., Ayadi, I., Khannous, L., Namsi A., Cerqueira, F., Drira, N., Gharsallah, N. and Vallaeys, T. (**2013**). Fungal diversity in date palm (*Phoenix dactylifera*) revealed by culture dependent and culture in-dependent approaches. *Journal of Zhejiang University-Science B (Biomed and Biotechnol)* 14: 1084-1099.

Berg, G., and Smalla, K. (**2009**). Plant species and soil type cooperatively shape the structure and function of microbial communities in the rhizosphere. *FEMS Microbial Ecology* 68: 1-13.

Bouizgarne, B., Brault, M., Pennarun, A.M., Rona, J.P., Ouhdouch, Y., El Hadrami, I. and Bouteau, F. (**2004**). Electrophysiological responses to fusaric acid of root hairs from seedlings of date palm-susceptible and -resistant to *Fusarium oxysporum* f. sp. *albedinis*. *Journal of Phytopathology* 152**:** 321–324.

Deng, Y., Umbach, A.K. and Neufeld, J. (**2024**). Nonparamatic richness estimates Chao1 and ACE must not be used with amplicon sequence variant data. *The ISME Journal* 18: wrar 106.

Cabrera, O.G., Molano, E.P.L., José, J., Álvarez, J.C. and Pereira, G.A.G. (**2016**). Ceratocystis wilt pathogens: history and biology—highlighting *C. cacaofunesta*, the causal agent of wilt disease of cacao. In: Bailey, B., Meinhardt, L. (eds) Cacao Diseases. Springer, Cham.

Caldwell, D. and Iyer-Pascuzzzi, A.S. (**2019**) A scanning electron microscopy technique for viewing plant-microbe interactions at tissue and cell-type resolution. *Phytopathology* 109: 1302-1311.

Chao, C.C.T. and Kruueger, R.R. (**2007**). The date palm (*Phoenix dactylifera* L.): overview of biology, uses and cultivation. *HortScience* 42: 1077-1082.

Chauhan, P., Sharma, N., Tapwal, A., Kumar, A., Verma, G.S., Meena, M., Seth, C.S. and Swapnil, P. (**2023**). Soil microbiome: diversity, benefits and interactions with plants. *Sustainability*: 14643.

Chavan, A., Barkah, H.J.E. and Lokesh, S. (**2020**). Effect of angiospermic epiphytes on the relative status of ergosterol and electrolyte leakage in fungal pathogens. *International Journal of Current Pharmaceutical Research* 12: 111-113.

Choi, H.W. and Ahsan, S.M. (**2022**). Biocontrol activity of *Aspergillus terrus* ANU-301 against two distinct plant diseases, tomato *Fusarium* wilt and potato soft rot. *Plant Pathology Journal* 38: 33-45.

Conaway, W.S. and MacHardy, W.E. (**1977**). Distribution and growth of *Fusarium oxysporum* f.sp. *lycopersici* race 1 or race 2 within tomato plants resistant or susceptible to wilt. *Phytopathology* 68: 938-942.

de Beer, Z.W., Duong, T.A., Barnes, I., Wingfield, B.D. and Wingfield, M.J. (**2014)**. Redefining *Ceratocystis* and allied genera. In: Studies in Mycology, Volume 79, Number 1, pp. 187-219 (33). Publisher: Westerdijk Fungal Biodiversity Institute.

El Mardi, M.O., Al Said, F., Sakit, C.B., Kharusi, L.A., Rahbi, I.N. and Mahraz, K.A. (**2007**). Effect of pollination method, fertilizer and mulch treatments on the physical and chemical characteristics of date palm (*Phoenix dactylifera* L.) fruit 1: physical characteritics. *ACTA Horticulture* 736: 317-328.

El-Modafar, C., (**2010**). Mechanisms of date palm resistance to Bayoud disease: current state of knowledge and research prospects. *Physiological and Molecular Plant Pathology*, 74**:** 287-294.

Fakruddin, MD., Mazumdar, R.M., Chowdhury, A., Hossain, M.N., Mahjan, S. and Islam, S. (**2013**). Pyrosequencing - a next generation sequencing technology. *World Applied Science Journal* 24: 1558-1571.

Farhat, A.A. (**2019**). Easy way to count spores and prepare spore suspension by hemocytometer. http://www..researchgate.net/publication/337772212.

FAO. FAOSTAT. In., FAO, (**2020**).

Freeman, S. and Maymon, M. (**2000**). Reliable detection of the fungal pathogen *Fusarium oxysporum* f.sp. *albedinis*, causal agent of Bayoud disease of date palm, using molecular techniques. *Phytoparasitica* 28: 1-12.

Frisvad, J.C., Yilmaz, N., Thrane, U., Rasmussen, K.B., Houbraken, J. and Samson, R.A.(**2013**). *Talaromyces astrorseus* a new species efficiently producing industrially relevant red pigments. *PLOS V8* Issue 12: e84102.

Gao, J., Weng, H., Zhu, D., Yuan, M., Guan, F, and Xi,Y. (2008). Production and charaterisation of cellulolytic enzymes from the thermoacidophilic fungal *Aspergillus terrus* M11 under solid-state cultivation of corn stover. *Biosource Technology* 99: 7623-7629.

Gao, Y., Xiujun, W., Xianglan, L., Jiaping, W., Minggang, X. and Dongwei, L. (**2016**). Dynamics of soil organic and inorganic carbon in the cropland of upper yellow river delta, *China Scientific Reports* 6: 36105.

George, E., Rolf, S. and John, R. (**2013**). Methods of soil, plant and water analysis. A management for the west Asia north African region. 3rd Edition. International Center for Agriculture Research in the Dry Areas (ICARDA).

Goes, L.B., Lima da Costa, A.B., Freire, L.L. and Tinti de Oliveira, N. (**2002**). Randomly Amplified Polymorphic DNA of *Trichoderma* isolates and antagonism against *Rhizectonia solani*. *Brazilian Archives of Biology and Technology* 45: 151-160.

Goh, Y.K., Marzuki, N.F., Pa, T.N.F., Goh,T.K., Kee, Z.S., Goh, Y.K., Yusof, M.T., Vujanovic, V. and Goh, K.J. (**2020**). Biocontrol and plant-growth-promoting traits of *Talaromyces apiculatus* and *Clonostachys rosea* consortium against Ganoderma basal stem rot disease of oil palm. *Microorganisms* 8:1138.

Golding, C.G., Lamboo, L.L., Beniac, D.R. and Booth, T.F. (**2016**). The scanning electron microscope in microbiology and diagnosis of infectious diseases. *Scientific Reports* 6: 26516.

Goldstein, J. (**2003**). Scanning electron microscopy and X-Ray microanalysis. 3rd ed. New York: Kluwer Academic/Plenum Publishers.

Gros-Balthazard, M., Galimberti, M., Kousathanas, A., Newton, C., Ivorra, S., Paradis, L., Vigouroux, Y., Carter, R., Tengberg, M., Battesti, V., Santoni, S., Falquet, L., Pintaud, C., Terral, J.F. and Wegmann, D. (**2017**). The discovery of wild date palms in Oman reveals a complex domestication history involving centers in the Middle East and Africa. *Current Biology* 27: 221-2218.

Gros-Balthazard, M., Newton, C., Ivorra, S., Pierre, M.H., Pintaud, C. and Terral, J.F. (**2016**). The domestication syndrome in *Phoenix dactylifera* seeds: toward the identification of wild date palm populations. *PLoS One* 11: e0152394.

Gutiérrez-Santa, A., Carrillo-Cerda, H.A., Rodriguez-Campos, J., Valázquez-Fernández, J.B., Patrón-Soberano, O.A. and Contreras-Ramos, S.M. (**2020**). Dynamics of volatilomes emitted during cross-talking of plant-growth-promoting bacteria and the phytopathogenic *Fusarium solani*. *World Journal of Microbiology and Biotechnology* 36: 152.

Harrington, T.C. (**2013**). Ch.11, *Ceratocystis* Diseases. In: Infectious Forest Diseases, CAB International. Eds. P. Gonthier and G. Nicholotti.

Hafizi, R., Salleh, B. and Latiffah, Z. (**2013**). Morphological and molecular characterization of *Fusarium solani* and *F. oxysporum* associated with crown disease of oil palm. *Brazilian Journal of Microbiology* 44: 959-968.

Halo, B., Al Yahyai, R. and Al Sadi, A.M. (**2018**). *Aspergillus terrus* inhibits growth and induces morphological abnormalities in *Pythium aphanidermatum* and suppresses *Pythium*-induced damping-off of cucumber. *Frontiers in Microbiology* 9: 95.

Halo, B., Al Yahyai, R., Maharachchikumbura, S.S.N. and Al Sadi, A.M. (**2019**). *Talaromyces variabilis* interferes with *Pythium aphanidermatum* growth and suppresses *Pythium* induced damping-off of cucumbers and tomatoes. *Scientific Reports* 9: 11255 http://doi.org/10.1038/s41598-019-47736-x.

Han, P.-J., Sun, J.-Q. and Wang, L. (**2022**). Two new sexual *Talaromyces* species discovered in estuary soil in China. *Journal of Fungi* 8: 36.

Hashim, M., Al Amiri, S., Shatha, A., Al Rumman, S,A. and Moustafa, M.E.M. (**2016**). Supression of phytopathogenic fungi by plant extracts of some weeds and the possible mode of action. *British Microbiology Research Journal* 15: 1-13.

Haydari, A. and Pessaraki, M. (**2010**). A review on biological control of fungal plant pathogens using microbial agents. *Journal of Biological Sciences* 10: 273-290.

Higgs, M. (**2024**). The latest developments in sequencing technologies. In: Frontline Genomics, The Sequencing Buyers Guide, 6th Edition. Ch 3 and Ch 9.

Hoshino, Y.T. and Matsumoto, N. (**2005**). Skimmed milk improves the efficacy of DNA extraction from andisol, a volcanic ash soil. *JRAQ* 39: 247-252.

Houssien, A.A., Ahmed, S.M. and Ismail, A.A. (**2010**). Activation of tomato plant defence response against *Fusarium* wilt disease using *Trichoderma harzianum* and salicylic acid under greenhouse conditions. *Research Journal of Agriculture and Biological Sciences* 6: 328-338.

Howard, J., Hoyt, S., Isensee, K., Telszewski, M. and Pidgen, E. (**2014**). Field sampling of soil carbon pools in coastal ecosystems. In: Coastal Blue Carbon: Methods for assessing carbon stocks and emissions factors in mangroves, tidal marshes and seagrass meadows. Publisher: Conservation International, Intergovernmental activity of *Pseudomonas fluorescens* and *Trichoderma viride* against selected species of fungal pathogens. *Asian Research Journal of Agriculture* 1: 1-7.

Huang, X., Liu, L., Wen, T., Zhu, R. and Zhang,J. (**2015**). Illumina Miseq investigation on the changes of microbial community in the *Fusarium oxysporum* f.sp. *cubense* infected soil during and after reductive soil disinfestaion. *Micobiological Research* 181: 33-42.

Hurriso, T.T., Moebius-Clune, D.J., Culman, S.W., Moebius-Clune, B.N., Thies. J.E. and van Es, M. (**2018**). Soil protein as a rapid soil health indicator of potentially available organic nitrogen. *Agricultural and Environmental Letters* Research letter.

Ijaz, M., Afza, R., Zafar, M., Hamayun, M., Khan, S.M., Ahmed, Z., Ahmed M., Khan, S.A., Shah, R. and Yahya, M. (**2022**). Taxonomic investigation of selected rust fungi using scanning electron microscopy from Khyber Pakhtunkwa, Pakistan. *Microscopy Research and Technique* 85: 755-766.

Jiang, X.-Z., Yu, Z.-D., Ruan, Y.-M. and Wang,L. (**2018**). Three new species of *Talaromyces* sect, *Talaromyces* discovered from soil in China. *Scientific Reports* 8: 4932.

Kamoun, S., Furzer, O., Jones, J.D.G., Judelson, H.S., Ali, G.S., Dalio, R.J.D., Roy, S.G., Schena, L., Zambounis, A., Panabiéres, F., Cahil, D., Ruocco, M., Figueiredo, A., Chen, X-R., Hulvey, J., Stam, R., Lamour, K., Gijzen, M., Tyler, B.M., Grűnwald, N.J., Mukhtar, M.S.,Tomé, DFA., Tör, M., Ackerveken ,GvD., McDowell, J., Daayf, F., Fry, W.E., LindQvist-Kreuze, H., Meijer, H.J.G., Petre, B., Ristaino, J., Yoshida, K.,Birch, P.R.J. and Govers, F. (**2015**). The top 100 oomycete pathogens in molecular plant pathology. *Molecular Plant Pathology* 16: 413-434.

Karunasinghe, T.G., Maharachchikumbura, S.S.N., Rethinasamy, V. and Al Sadi, A.M. (**2020**). Antagonistic activity of endophytic and rhizosphere fungi isolated from sea purslane (*Sesuvium portulacastrum*) against *Pythium* damping off of cucumber. *Plant Disease* 104: 2158- 2167.

Kazerooni, E.A. and Al-Sadi, A.M. (**2016**). 454-pyrosequencing reveals variable fungal diversity across farming systems. *Frontiers in Plant Science* 7**:** 314.

Kazerooni, E.A., Rethinasamy, V. and Al-Sadi, A.M. (**2019**). *Talaromyces pinophilus* inhibits *Pythium* and *Rhizoctonia*-induced damping-off of cucumber. *Journal of Plant Pathology* 101: 277-383.

Kwon, C.Y., Rasmussen, J.B., Francl, L.J. and Meinhardt, S.W. (**1996**). A quantitative bioassay for necrosis toxin from *Pyrenophora tritici-repentis* based on electrolyte leakage. *Biochemistry and Cell Biology, Phytopathology* 86: 1360-1363.

Lahlahi, R., Ezrari, S., Radouane, N., Kenfaoui, J., Esmaeel, Q., El Hamss, H., Belabess, Z. and Brark, E.A. (**2022**). Biological control of plant pathogens: a global perspective. *Microorganisms* 10: 596.

Lou, M., Chen,Y., He, J., Tang, X., Wu, X. and Xu, C. (**2021**). Identification of a new *Talaromyces* strain DYM25 isolated from the Yap trench as a biocontrol agent against Fusarium wilt of cucumber. *Microbiological Research* 251: 126841.

Madi, L., Katan, T., Katan, J. and Henis, Y. (**1997**). Biological control of *Sclerotium rolfsii* and *Verticillium dahliae* by *Talaromyces flavus* is mediated by different mechanisms. *Phytopathology* 87: 1054-1060.

Mazzola, M. (**2002**). Mechanism of natural soil suppressivness to soilborne diseases. *Antonie van Leeuwenhoek* 81: 557-564.

McGowen, J. and Fitzpatrick, D. (**2020**). Chapter 5: Recent advances in oomycete genomics. In: Advances in Genetics, Vol. 105, Ed. Dhavendra Kumar. P.2-2382020. Elsvier Inc.

Melo,I .S., Faull, J.L. and Nascimento, R.S. (**2006**). Antagonism of *Aspergillus terrus* to *Sclerotinia sclerotiorum*. *Brazilian Journal of Microbiology* 37: 417-419.

Miao Miao, C.P., LiMi, Q., GuoQiao, X., Kun Zheng, Y., Wei Chen, Y., Hua Xu, L., Lin Guan, H. and Xing Zhao, L. (**2016**). Rhizospheric fungi of *Panax notoginseng*: diversity and antagonism to host phytopathogens. *Journal of Ginseng Research* 40: 127-134.

Manoch, L. and Dethoup, T. (**2011**). A potential use of *Talaromyces* species as biological agents against plant pathogenic fungi. *Thai Journal of Agricultural Sciences* 44: 81-91.

Mansoori, B. and Kord, M.H. (**2006**). Yellow death; a disease of date palm in Iran caused by *Fusarium solani*. *Journal of Phytopathology* 154**:** 1257-1127.

Marzachi, C., Veratti, F. and Bosco, D. (**1998**). Direct PCR detection of phytoplasmas in experimentally infected insects. *Annals of Applied Biology* 133: 45-54.

Miao, C.-P., Mi, Q.-L., Qiao, X.-G., Zheng, Y-.K., Chen, Y.-K., Xu, L.-H., Guan, H.-L. and Zhao, L.-X. (**2015**). Rhizospheric fungi of *Panax notoginseng*: diversity and antagonism to host phytopapathogens. *Journal of Ginseng Research* 40: 127-134.

Naraghi, L., Haydari, A., Rezaee, S., Razavi, M. and Afshari-Azad, H. (**2010**). Biological control of *Verticillium* wilt of greenhouse cucumber by *Talaromyces flavus*. *Phytopathology Mediterranean* 49: 321-329.

Naasko, K., Martin, T., Mammana, C., Murray, J., Mann, M. and Sprunger, C. (**2023**). Soil protein: a key indicator of soil health and nitrogen management. Soil Science Society of American Journal, Soil Nutrient Management and Soil and Plant Analysis 1-20.

Nishad, R. and Ahmed, T.A. (**2020**). Survey and identification of date palm pathogens and indigenous biocontrol agents. *Plant Disease* 104: 2498-2508.

Omara, A.E-D. and El Maghraby, F.M.(**2023**). Novel bioinformatics with *Trichoderma lixii* to improve the growth dynamics and biocontrol of the cowpea damping-off disease. *Microbial Research* 14: 2041-2066.

Plaats-Niterink, A.J.V. (**1981**). Monograph of the genus *Pythium*. *Studies in Mycology* 21**:** 1-242.

Ploetz, R. (**2006**).*Fusarium*-induced diseases of tropical, perennial crops. Symposium: Annual Meeting of The American Phytopatholgical Society August 1, 2005, Austin TX. *Phytopathology* 96 No. 6.

Ploetz, R., Freeman, S., Konkol, J., Al-Abed, A., Naser, Z., Shalan, K., Barakat, R. and Israeli, Y. (**2015**). Tropical race 4 of Panama disease in the Middle East. *Phytoparasitica* 43: 283–293.

Praveen-Kumar, J.C., Tarafdar, D.K., Painuli, P., Raina, M.P., Singh, R.K., Beniwal, M.L., Santra, P. and Shamsuddin, M. (**2009**). Variability in arid soil characteristics, trends in arid zone research in India (Eds. Amal Kar, B.K. Garg, M.P. Singh and S. Kathju), Central Arid Zone Research Institute, Jodhpur, 78-112 pp.

Purwati, R.D., Hidayah, N. and Sujindro (**2008**). Inoculation methods and conidial densities of *Fusarium oxysporum* f.sp *cubenes* in Abaca. *Hayati Journal of Biosciences* 15: P1-7.

Rabiey, M., Hailey, L.E., Roy, S.R., Grenz, K., Al Zadjali, M., Barett, G.A. and Jackson, R.W. (**2019**). Endophytes vs tree pathogens and pests: can they be used as biological control agents to improve tree health? *European Journal of Plant Pathology* 155: 711-729.

Ramos, M.C., Lizaga, I., Gaspar, L. and Navas, A. (**2022**). The impacts of exceptional rainfall on phosphorus mobilization in a mountain agroforestry catchment (NE, Spain). *Catena* 216: 106-407.

Ravi, R.K., Walto, K. and Khosroheidari, M. (**2018**). Miseq: next generation sequencing platform for genomic analysis. Ch.12, PP 223-232 In: Benchtop Next Generation Sequencing: Methods in Molecular -Disease Gene Identification Biology. Ed. Di Stifano,J.K

Redda, E.T., Ma, J., Mei, J., Li, M., Wu, B. and Jiang, X. (**2018**). Antagonistic potential of different isolates of *Trichoderma* against *Fusarium oxysporum*, *Rhizoctonia solani* and *Botrytis cinerea*. *European Journal of Experimental Biology* 8: 12.

Roncero, M.I.G., Hera, C., Ruiz-Rubio, M., Maceira, F., Madrid, M.P., Caracuel, Z., Calero, F., Delgado-Jarana, J., Rodrıguez, R., Martınez-Rocha, A.L., Velasco, C., Roa, J., Martın-Urdiroz, M., Cordoba, D. and Di Pietro, A. (**2003**). *Fusarium* as a model for studying virulence in soilborne plant pathogens. *Physiological and Molecular Plant Pathology* 62: 87–98.

Saleh, A.A., Sharafaddin, A.H.,El_Komy, M.H., Ibrahim,Y.E., Hamad, Y.K. and Molan, Y.Y. (**2017**). *Fusarium* species associated with date palm in Saudi Arabia. *European Journal of Plant Pathology* 148: 367–377.

Sempere, F., and Santamarina, M.P. (**2011**). Cryo-scanning electron microscopy and light microscopy for the study of fungal interactions. *Microscopy Research and Techniques* 74: 207-211.

Sharma, A., Batra, N.G. and Sharma, H. (**2014**). Physical and chemical analysis of the rhizosphere soil of *Phoenix dactylifera* L. in semi arid regions of Jaipur District. *International Research Journal of Pharmaceutical and Applied Sciences (IRJPAS)* 4: 9-15.

Shrestha, A., Park, S.H., Shrestha, B., Kim, K., Chae, J.C. and Lee, K.J. (**2014**). Biological control of oomycetous plant pathogens: A Review. *Nepal Journal of Science and Technology* 15: 157-166.

Sreeshama, P.S. and Jose, V. (**2016**). Comparison of antagonistic activity of *Pseudomonas fluorescens* and *Trichoderma viride* against selected species of fungal pathogens. *Asian Research Journal of Agriculture* 1: 1-7.

Stone, J.K., Polishook, J.D. and White, J.F (**2004**). Endophytic fungi (ch12) in: Biodiversity of fungi. Elsevier Academic Press pp: 241-270.

Stosz, S.K., Fravel, D. and Roberts, D.P. (**1996**). In vitro analysis of the role of glucose oxidase from *Talaromyces flavus* in biocontrol of the plant pathogen *Verticillium dahliae*. *Applied and Environmental Microbiology* 12: 3183-3186.

Suleman, P., Al-Musallam, A. and Menezes, C.A. (**2002**). The effect of biofungcide Mycostop on *Ceratocystis radicicola*, the casual agent of black scorch on date palm. *Biocontrol* 47**:** 207-216.

Suprapta, D.N (**2012**). Potential of microbial antagonist as biocontrol against plant fungal pathogens. *Journal ISSAAS* 18::1-8.

Su, H.J., Hogenhout, S.A. Al-Sadi, A.M. and Kuo, C.H. (**2014**). Complete chloroplast genome sequence of Omani lime (*Citrus aurantiifolia*) and comparative analysis within the Rosids. *PLoS ONE* 9**:** e113049.

Verma, M., Braret, S.K., Tyagi, R.D., Surampalli, S.Y. and Valero, J.R. (**2007**). Antagonistic fungi *Trichoderma* spp.: Panoply of biological control. *Biochemical Engineering Journal* 37: 1-20.

Vinale, F., Sivasithamparam, K., Ghisalberti, E.L., Marra, R., Woo, S.L. and Lorito, M. (**2008**). *Trichoderma* –plant-pathogen interaction. *Soil Biology and Biochemistry* 40: 1-10.

Volossiouk, T., Robb, J. and Nazar, R. (**1995**). Direct DNA extraction for PCR-mediated assays of soil organisms. *Applied and Environmental Microbiology* 61: 3972-3976.

Wei, S., Xu, X and Wang, L. (**2021**). Four new species of *Talaromyces* section *Talaaromyces* discovered in China. *Mycologia* 113: 492-508.

White, T. J., Bruns, T., Lee, S. and Taylor, J. (**1990**). "Amplification and direct sequencing of fungal ribosomal RNA genes for phylogenetics," in PCR protocols: A Guide to Methods and Applications, eds M. A. Innis, D. H. Gelfand, J. J. Sninsky and T. J. White (New York, NY: Academic Press), 315–322.

Yaish, M.W., Al Harrasi, I., Al Ansari, A.S., Al Yahyai, R. and Glick, B.R. (**2016**). The use of high throughput DNA sequence analysis to assess the endophytic microbiome of date palm roots grown under different levels of stress. *International Microbiology* 19:143-155.

Yi, Z., Zhao, P. and Axmacher, J.C. (**2023**). Estimating total species richness: fitting rarefaction by asymptomatic approximation. *Ecosphere* 14: e4363.

Zaid, A., de Wet, P.F., Djerbi, M. and Oihabi, A. (**2002**). Diseases and pests of date palms. In: Zaid, A. (ed), Date Palm Cultivation Rome, Italy., FAO.

Zhang, J., Cook, J., Nearing, J.T., Zhang, J., Raudonis, R., Glick, B.R., Langille, M.G.I and Cheng, Z. (**2021**). Harnessing the plant microbiome to promote the growth of agricultural crops.

Zhang, Z., Luo, L., Tan X., Kong, X., Yang, J., Wang, D., Zhang, D., Jin, D. and Liu, Y. (**2018**). Pumpkin powdery mildew disease severity influences the fungal diversity of the phyllosphere. *PeerJ* DOI 10.7717/peerj.4559.

Annex 1

Sample collection and labelling per Area.

Ser	Area (State)	Location	Root samples and label	Rhizosphere soil samples and label
1	Samail (Governorate of Dhakiliyah) May 2018 Image 3 to 6	Feral 1	SR1/SR2/SR3/SR4	SS1/SS2/SS3/SS4
		Feral 2	SR1/SR2/SR3/SR4	SS1/SS2/SS3/SS4
		Total	16	16
		Farm 1	SR9/SR10/SR11/SR12	SS9/SS10/SS11/SS12
		Farm 2	SR13/SR14/SR15/SR16	SS13/SS14/SS15/SS16
		Total	16	16
2	Swaiq (Governorate of North Batinah) May 2018 Image 7and8	Farm 1	QR1/QR2/QR3/QR4	QS1/QS2/QS3/QS4
		Farm 2	QR5/QR6/QR7/QR8	QS5/QS6/QS7/QS8
		Total	8	8
3	Hoqain (Governorate of North Batinah) May 2018	Farm 1	HR1/HR2/HR3/HR4	HS1/HS2/HS3/HS4
		Feral 1	HR5/HR6/HR7/HR8	HS5/HS6/HS7/HS8
		Total	8	8

Annex 2

Soil Chemical Analysis Raw Data (ND is for Not Detected)

	SAMPLE ID	As 193.696 (ppm)	Zn 206.200 (ppm)	P 213.617 (ppm)	Pb 220.353 (ppm)	Cd 228.802 (ppm)	Ni 231.604 (ppm)	Fe 238.204 (ppm)	Hg 253.652 (ppm)	Cr 267.716 (ppm)	Mg 285.213 (ppm)	Ca 317.933 (ppm)	Cu 327.393 (ppm)	Al 396.153 (ppm)	Na 589.592 (ppm)	K 766.490 (ppm)
1	SS1	ND	17.52	50.62	ND	ND	278.67	9379.03	ND	57.73	33663.79	43194.32	48.91	10231.53	669.96	814.83
2	SS2	ND	25.15	80.76	ND	ND	404.18	17570.54	ND	95.23	52940.22	58106.81	70.15	20662.96	1003.30	1267.10
3	SS3	ND	25.30	59.34	ND	ND	336.12	14234.86	ND	75.88	46530.36	44693.80	85.33	17726.93	872.35	1416.23
4	SS4	ND	20.80	62.23	ND	ND	325.52	13689.28	ND	72.52	46315.53	47146.17	70.19	17141.57	1229.66	1563.49
5	SS5	ND	12.66	49.31	ND	ND	246.21	9469.69	ND	56.19	35394.07	30264.98	79.07	11044.01	505.62	786.80
6	SS6	ND	19.11	150.95	ND	ND	358.94	16708.30	ND	90.18	56281.49	44029.53	62.37	25287.98	1712.18	2245.75
7	SS7	ND	22.68	94.81	ND	ND	391.38	19435.39	ND	100.03	59141.93	39137.93	63.43	25956.21	1059.28	498.39
8	SS8	ND	19.12	69.42	ND	ND	332.26	13921.93	ND	78.31	48042.20	35501.24	92.84	16721.19	707.24	1036.06
9	SS9	ND	18.40	59.81	ND	ND	349.24	13674.18	ND	74.29	48471.65	47579.14	66.50	15741.25	1141.71	705.21
10	SS10	ND	28.28	143.51	ND	ND	367.61	17570.70	ND	90.64	53143.98	57087.77	58.32	24462.10	1516.47	722.33
11	SS11	ND	25.63	243.75	ND	ND	354.11	16305.08	ND	85.03	49050.44	56061.97	49.45	20584.69	1154.24	759.92

12	SS12	ND	21.65	8.78	ND	ND	328.05	13871.10	ND	73.40	45881.19	54848.67	140.27	17885.26	946.76	487.48
13	SS13	ND	34.49	1033.79	ND	ND	130.95	5639.42	ND	32.42	23545.33	37450.36	45.67	6225.05	589.26	799.78
14	SS14	ND	64.78	1218.28	ND	ND	315.73	16248.19	ND	99.63	53968.86	66469.09	78.58	20297.28	1128.06	1311.09
15	SS15	ND	49.45	753.11	ND	ND	145.71	9600.06	ND	56.40	29428.61	46229.02	57.88	14907.26	649.72	704.47
16	SS16	ND	21.86	519.50	ND	ND	161.73	8525.67	ND	46.88	32393.07	49866.21	64.80	11012.32	575.61	582.77
17	HS 1	ND	25.96	421.50	ND	ND	247.57	8858.28	ND	55.63	38606.53	69333.30	50.94	5525.93	331.09	494.75
18	HS 2	ND	40.81	470.68	ND	ND	204.54	6284.79	ND	42.57	30159.29	63630.74	43.94	3856.48	449.02	463.68
19	HS 3	ND	23.80	285.56	ND	ND	315.31	11595.71	ND	76.16	50033.90	69577.17	48.78	7037.94	382.21	493.49
20	HS 4	ND	54.14	635.72	ND	ND	292.28	10204.08	ND	64.60	44237.08	71246.21	43.02	5639.46	488.16	478.64
21	HS 5	ND	32.97	545.77	ND	ND	167.96	3996.48	ND	32.37	27452.28	69141.27	44.07	3175.67	514.77	340.31
22	HS 6	ND	21.09	483.15	ND	ND	273.53	8490.98	ND	56.07	43884.67	68653.36	39.92	5014.92	656.82	455.21

	SAMPLE ID	As 193.696 (ppm)	Zn 206.200 (ppm)	P 213.617 (ppm)	Pb 220.353 (ppm)	Cd 228.802 (ppm)	Ni 231.604 (ppm)	Fe 238.204 (ppm)	Hg 253.652 (ppm)	Cr 267.716 (ppm)	Mg 285.213 (ppm)	Ca 317.933 (ppm)	Cu 327.393 (ppm)	Al 396.153 (ppm)	Na 589.592 (ppm)	K 766.490 (ppm)
23	HS 7	ND	40.71	845.87	ND	ND	330.00	11943.77	ND	77.13	52596.87	73886.00	58.69	7507.81	918.83	956.10
24	HS 8	ND	28.81	620.20	ND	ND	330.06	11421.87	ND	77.90	50781.44	68831.71	56.69	7862.93	632.45	555.66
25	QS 1	ND	36.66	581.94	ND	ND	375.90	10351.79	ND	100.48	49012.43	58594.50	42.80	4144.44	1669.78	506.58
26	QS 2	ND	30.20	211.93	ND	ND	506.96	16539.14	ND	137.06	67308.56	46796.75	53.95	7738.28	361.27	450.84
27	QS 3	ND	24.64	255.70	ND	ND	527.20	16525.12	ND	159.95	69419.16	53019.31	51.97	7068.16	443.02	385.65
28	QS 4	ND	22.58	272.79	ND	ND	412.57	14508.03	ND	112.14	58605.58	62881.84	40.00	7384.35	1583.92	2164.95
29	QS 5	ND	22.86	180.68	ND	ND	478.13	11949.52	ND	106.26	56569.81	34413.02	49.91	6009.74	502.21	398.50
30	QS 6	ND	25.08	251.76	ND	ND	329.07	7990.98	ND	73.08	38971.67	30760.87	24.15	4854.88	373.14	595.74
31	QS 7	ND	16.26	137.71	ND	ND	446.03	12356.90	ND	102.34	55072.75	27558.02	33.36	7221.12	453.89	388.38
32	QS 8	ND	16.86	246.25	ND	ND	435.59	13117.22	ND	105.69	56697.60	31910.69	34.13	8314.98	553.14	675.97

Annex 3

Extraction of DNA of Soil Borne Fungi

Directly from Soil (Modified from Volossiouk et al. (1995))

1. Allow the soil to dry then remove large debris and rocks by sieving the soil in 1-2 mm sieve
2. Grind the soil with liquid nitrogen in a pestle and morter for 5 min
3. Place grinded soil in a 50ml sterile centrifuge tube
4. For Extraction weigh out 0.05g of the sample into a 2ml sterile eppendorff tube
5. Add 500 µl of skimmed milk solution
6. Voretex to mix well
7. Incubate in water bath at 60°c for 1 hour, invert every 15 minutes.
8. Centrifuge for 10 min at 13000 rpm at 4°c
9. Transfer supernatent by using 1000 µl pipette to 1.5 ml sterile eppendorff tube.
10. Add 500 µl SDS extraction buffer , invert tube twice .
11. In the fume hood ,add 1 volume (500 µl) of phenol:choloroform:isomyl alcohol (25:24:1)
12. Centrifuge for10 min13000 rpm at 4°c (or 20 min 4 rpm at 21°c)
13. Transfer supernatent (upper aqueus phase don't disturb interphase, leave behind some upper phase to avoid chloroform contamination) into .5 ml sterile eppendorff tube
14. Add 0.6 volume (400 µl) of cold isopropanol and 10 µl of sodium acetate NaAc. Invert gently , Incubate at -20°c over night
15. As soon as tubes are removed from freezer, centrifuge for 10 min at 13000 rpm at 4°c
16. Discard supernatent, wash pellet with 400 µl 70% ethanol
17. Centrifuge for 4 min at 13000 rpm at 4°c
18. Vacuum Centrifuge at 60°c for 10 min
19. Add 100 µl of deionized sterile distilled water
20. Assess the quality of DNA by using Nanao drop spectrophotometer (Thermo scientific,USA)

- Skim Milk Solution (0.1 g skim milk powder in 25 ml SDW)
- SDS Extraction Buffer:
    1. Weigh 0.3 g/100ml of 0.3% SDS
    2. Weigh 0.818g/ 100ml of 0.14 M NaCl
    3. Add to 100 ml bottle
    4. Pippette 1000+670 µl=1670 µl) 0.05 M NaOAc Sodium acetate
    5. Add distilled water up to volume 100 ml
    6. Stir and mix with magneti stirrer till all substances dissolve
    7. Adjust the pH to 5.0 by adding HCl

Annex 4

Microbiome Analysis Report

Author: Matthew R. Fox M.S.

March 28, 2019

Methods

1. Diversity was examined from two perspectives. First, overall richness (i.e., number of distinct organisms present within the microbiome), was expressed as the number of operational taxonomic units (OTUs), and was quantified using the Chao1 richness estimator.

$$S_{chao1} = S_{obs} + \frac{n_1(n_1-1)}{2(n_2+1)}$$

where ni is the number of OTUs with abundance i.

Second, overall diversity (which is determined by both richness and evenness, the distribution of abundance among distinct taxa) was expressed as Shannon Diversity. Shannon diversity (H0) is calculated using:

$$H' = -\sum_{i=1}^{R} p_i ln(p_i)$$

where R is richness and pi is the relative abundance of the i^{th} OTU.

2. Measures of diversity were screened for group differences using an analysis of variance (ANOVA). Sampling site and extraction method (i.e., group), as well as their interaction, were considered fixed effects. Repeated measures from the same mouse were the random effects factor.
3. Multivariate differences among groups were evaluated with "Permutational Multivariate Analysis of Variance Using Distance Matrices," function adonis [1]. For ADONIS, distances among samples first were calculated using unweighted or weighted UniFrac, and then an ANOVA-like simulation was conducted to test for group differences
4. Sequence data were processed using a Research and Testing pipeline that is described at: http://www.researchandtesting.com/docs/Data_Analysis_Methodology.pdf.

All analyses were conducted in R [1], using the vegan [1], labdsv [3], and phyloseq [4] packages.

References

[1] Jari Oksanen, F. Guillaume Blanchet, Roeland Kindt, Pierre Legendre, R. B. O'Hara, Gavin L. Simpson, Peter Solymos, M. Henry H. Stevens, and Helene Wagner. vegan: Community Ecology Package, 2011. R package version 1.17-8.

[2] R Development Core Team. R: A Language and Environment for Statistical Computing. R Foundation for Statistical Computing, Vienna, Austria, 2011. ISBN 3-900051-07-0.

[3] David W. Roberts. labdsv: Ordination and Multivariate Analysis for Ecology, 2010. R package version 1.4-1.

[4] Paul J. McMurdie and Susan Holmes. phyloseq: An R package for reproducible interactive analysis and graphics of microbiome census data. PLoS ONE, 8(4):e61217, 2013.43

Annex 5

Maximum Likelihood tutorial, for Maximum Parsimony and Bayesian Inference phylogeny

Phylogenetic Analyses

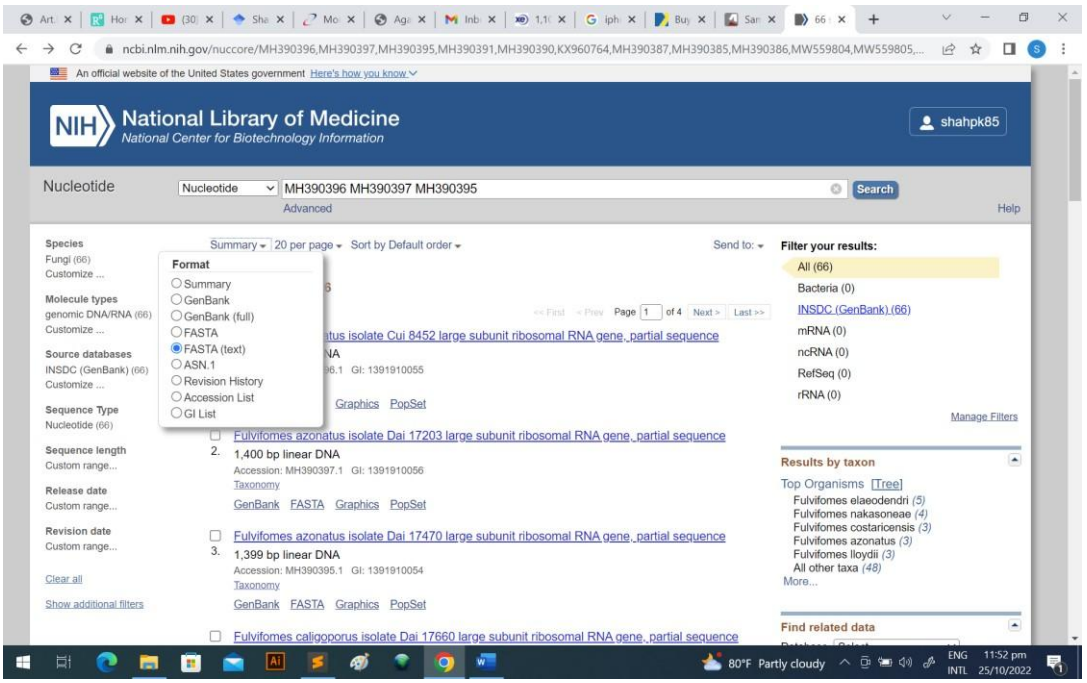
Three methods are used for Phylogenetic analyses of sequence data, and for each method, specific input data format is required.

1. Maximum Likelihood method (FASTA format)
2. Maximum Parsimony method (NEXUS format with specific command code)
3. Bayesian Inference method (NEXUS with MrBayes command code or XML format)

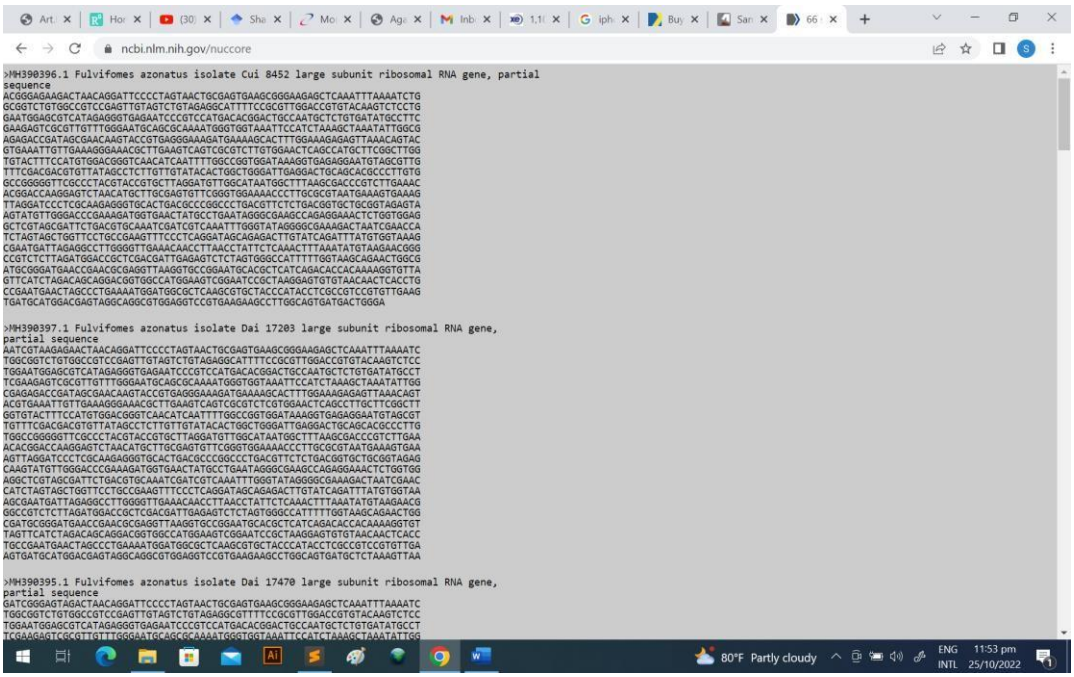
Maximum Likelihood analysis

To make a FASTA alignment input file……

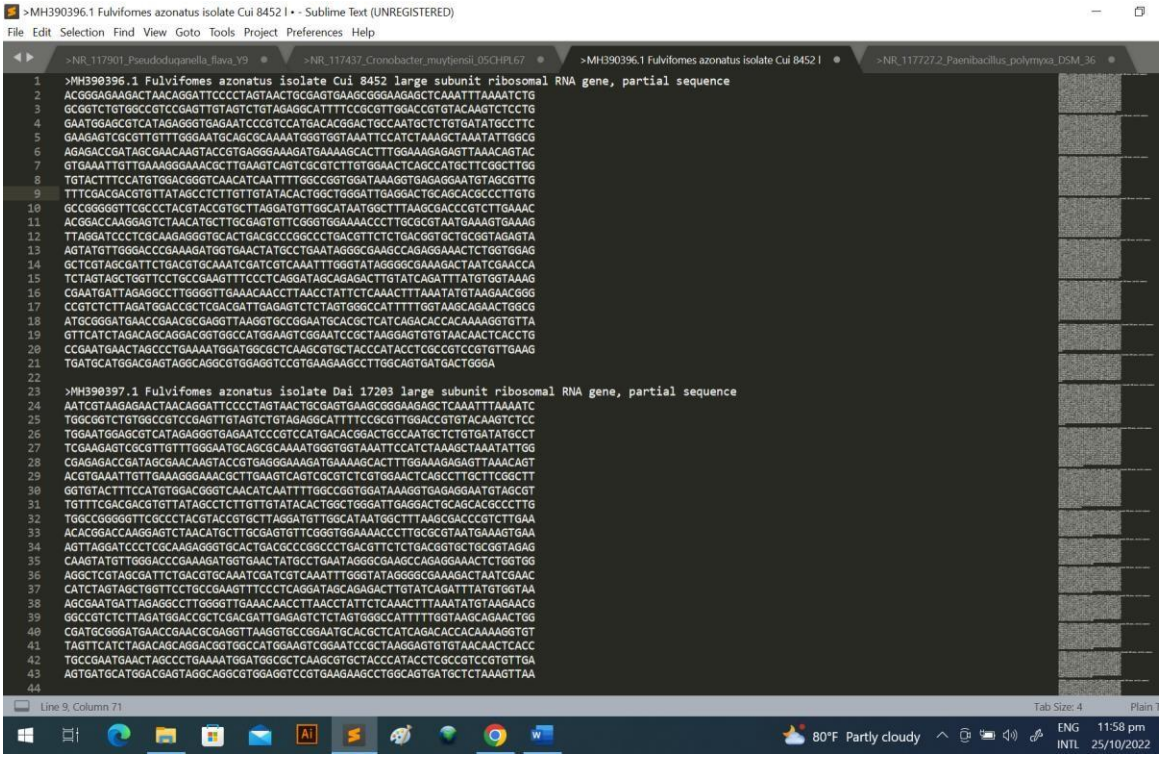
i. Download reference sequences from GenBank by pasting the accession numbers (space separated) to search box, with nucleotide option, summary with FASTA (text) and click the search



ii. Sequences will be shown as below

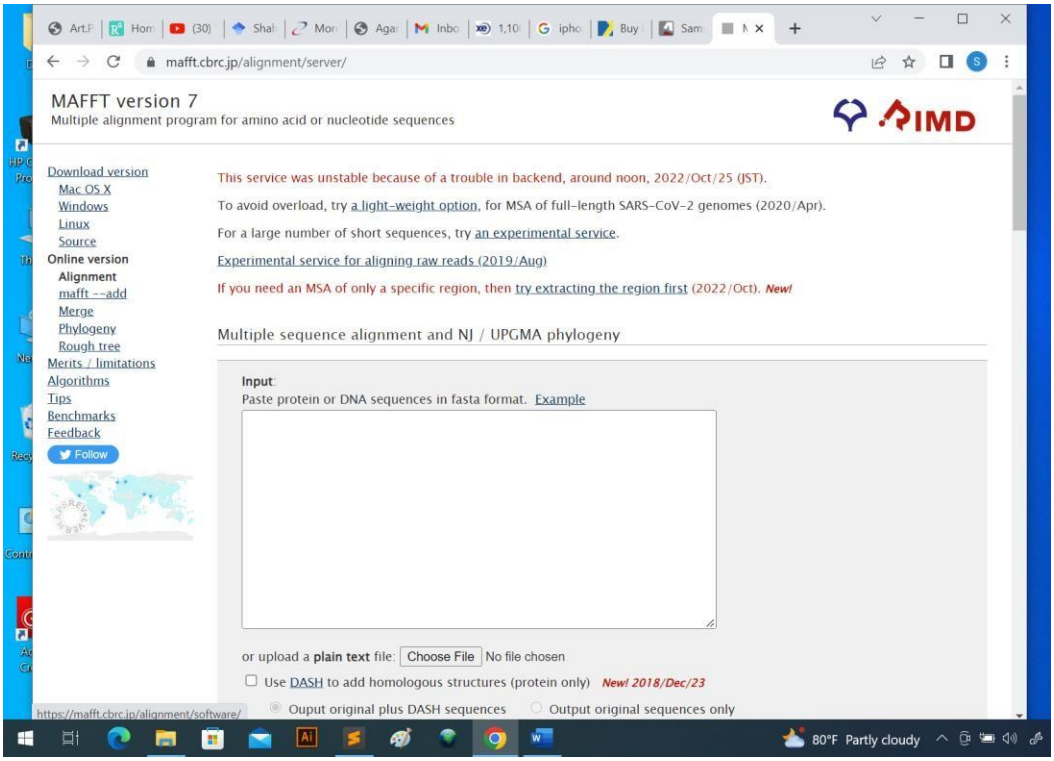


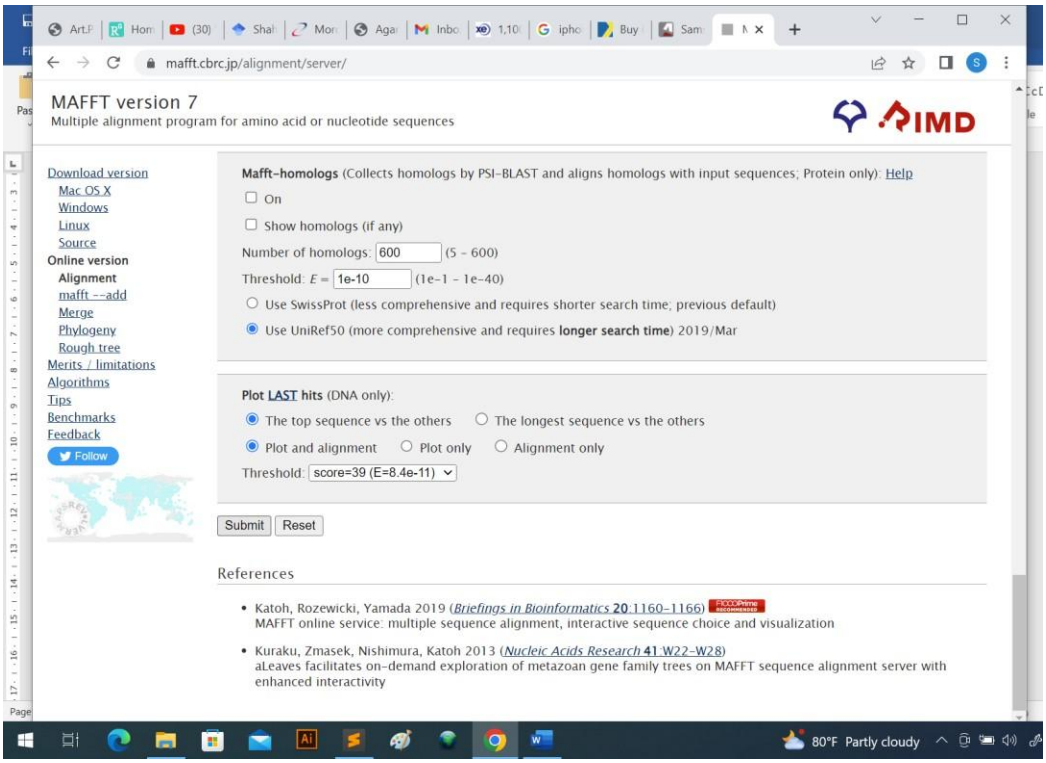
iii. Copy and Paste the sequences in Sublime Text Editor 3, remove the extra text information from the sequence ID, only keep the *accession number*, *taxon name*, *strain/isolate/voucher number* etc. Make sure to delete the punctuation marks, e.g. , : , ; , / , ? , (,) etc. as well. Also add your query sequences to Sublime



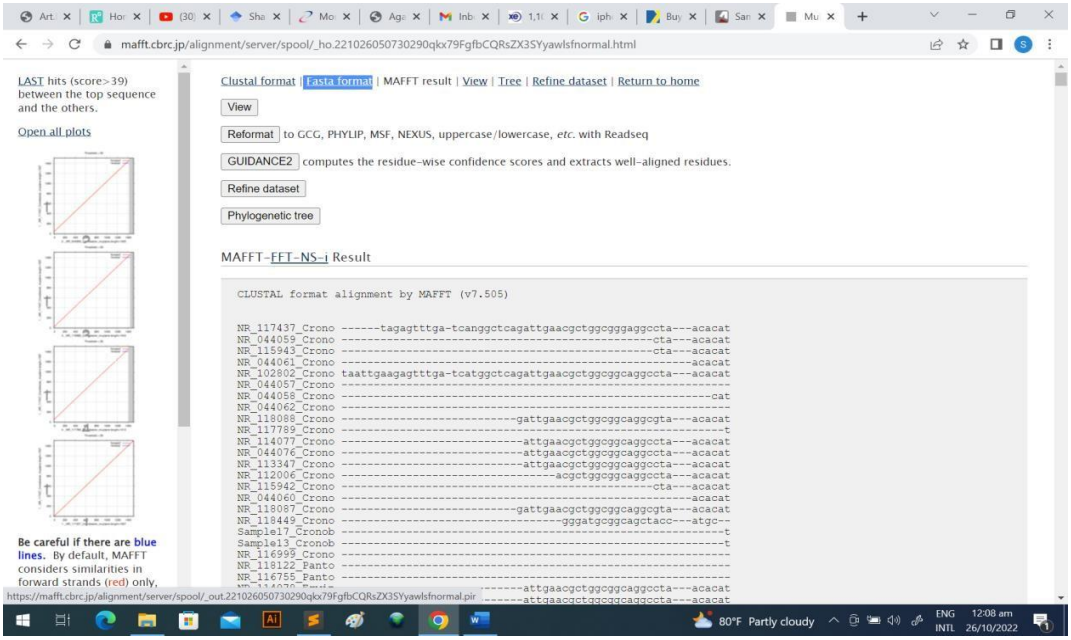
iv. Select all sequences by *Contl. A* and *Contl. C*

v. Alignment can be done online using different browsers, such as MAFFT (afft.cbrc.jp/alignment/server/), PRANK (https://www.ebi.ac.uk/goldman-srv/cgi-bin), MUSCLE (https://www.ebi.ac.uk/Tools/msa/muscle/) etc. Open any browser and paste the selected sequences in window box, using mafft e.g. Paste the sequences in the window and scroll down and click the submit button as shown below

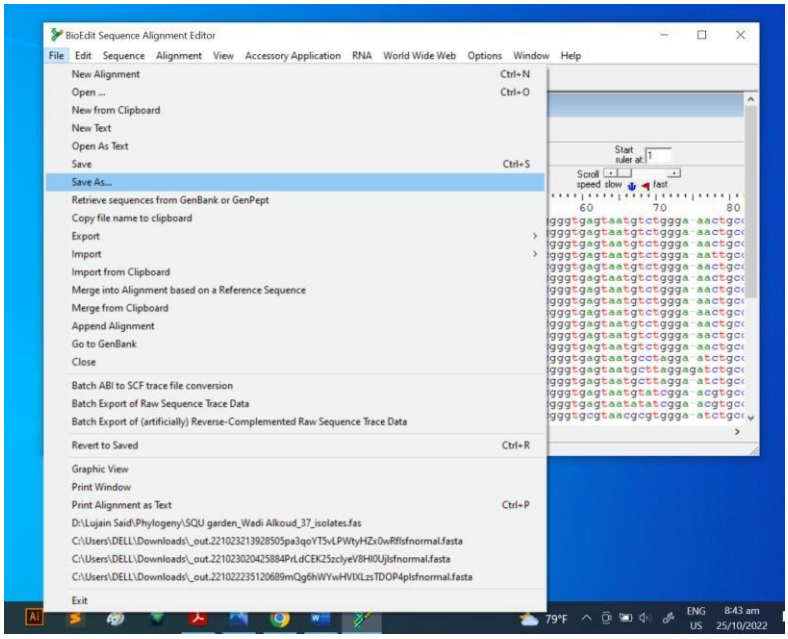




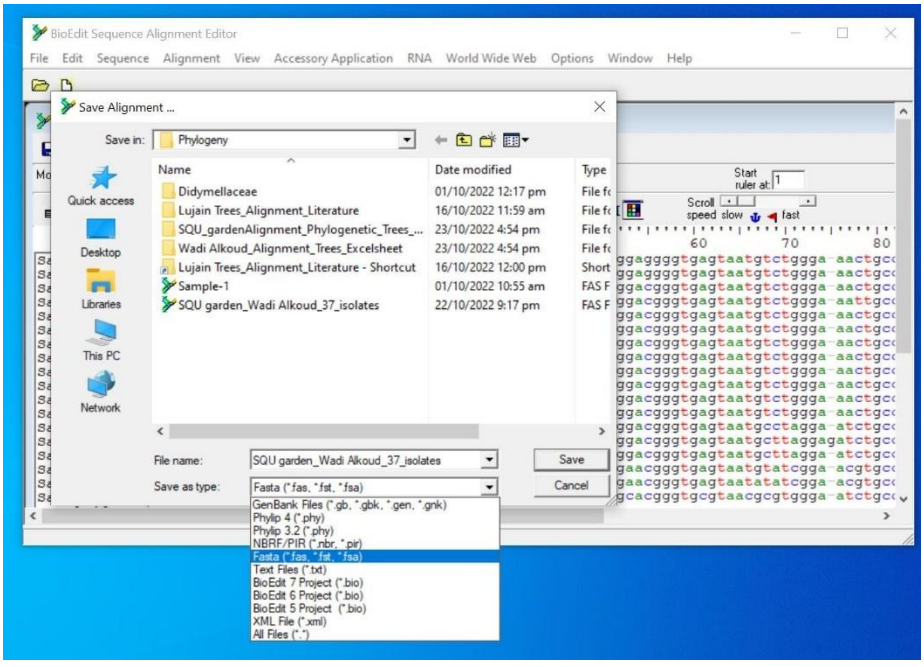
vi. A new window will be pup up, click the FASTA format in the new window to download the alignment file in fasta format



vii. Open the alignment file in BioEdit, click the FILE button and goes down to SAVE AS



viii. Write the File name and select the FASTA (*.fas, *.fst, *.fsa) option in the Save as type below….



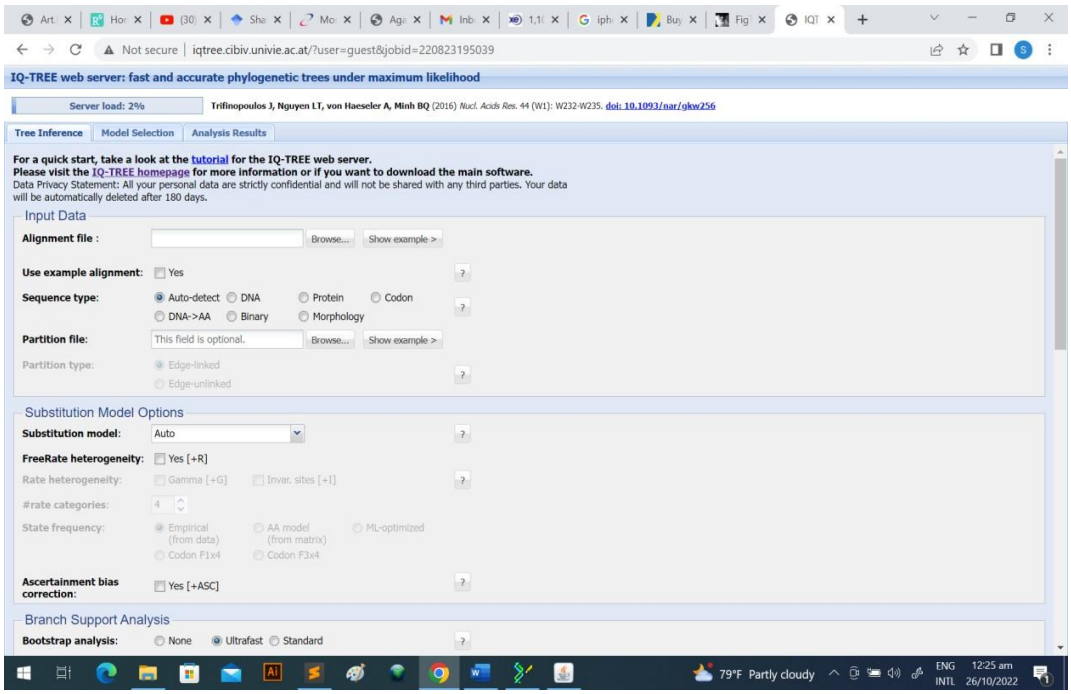
Before starting the analyses, you should install FigTree 1.4.4 (http://tree.bio.ed.ac.uk/software/figtree/)

Maximum likelihood analysis can be done using a number ways, either online browsers or installed packages. Installed software usually take longer time to complete, online pipeline completed much faster.

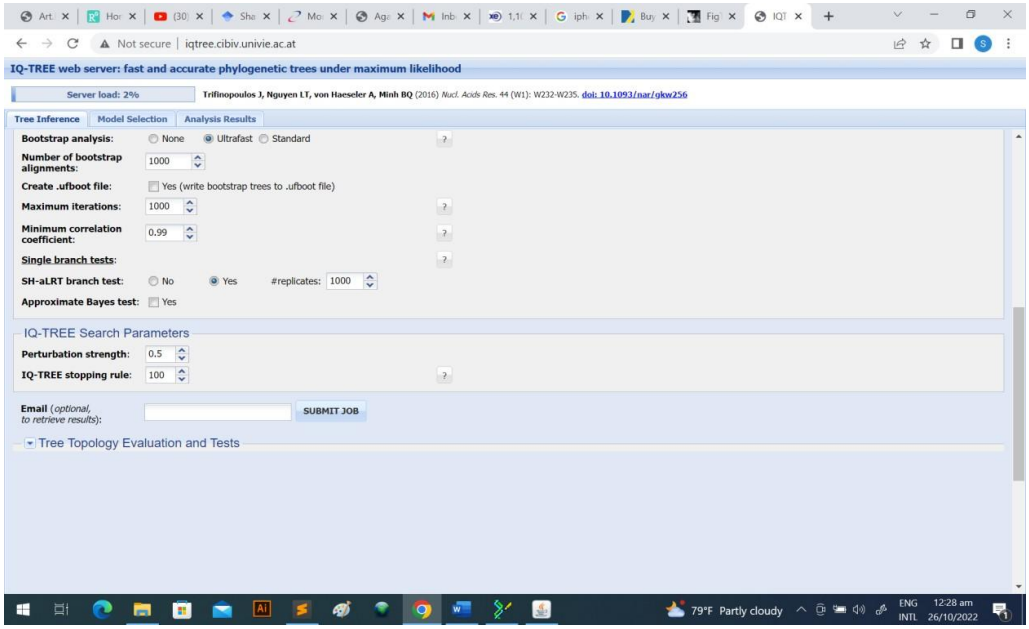
I. The most simple and common software is the **MEGA 6/7/X**, in this package user can do multiple tasks, such as Multiple Sequence Alignment, Maximum Likelihood Phylogeny, Maximum Parsimony etc. To do ML (Maximum Likelihood) phylogeny
   Open MEGA, go TEST Phylogeny, select Maximum Likelihood TEST, and just go with default settings.

II. IQ Tree web browser (http://iqtree.cibiv.univie.ac.at/). Here, you can do multiple analyses related to phylogenetic study, e.g. ML analysis.

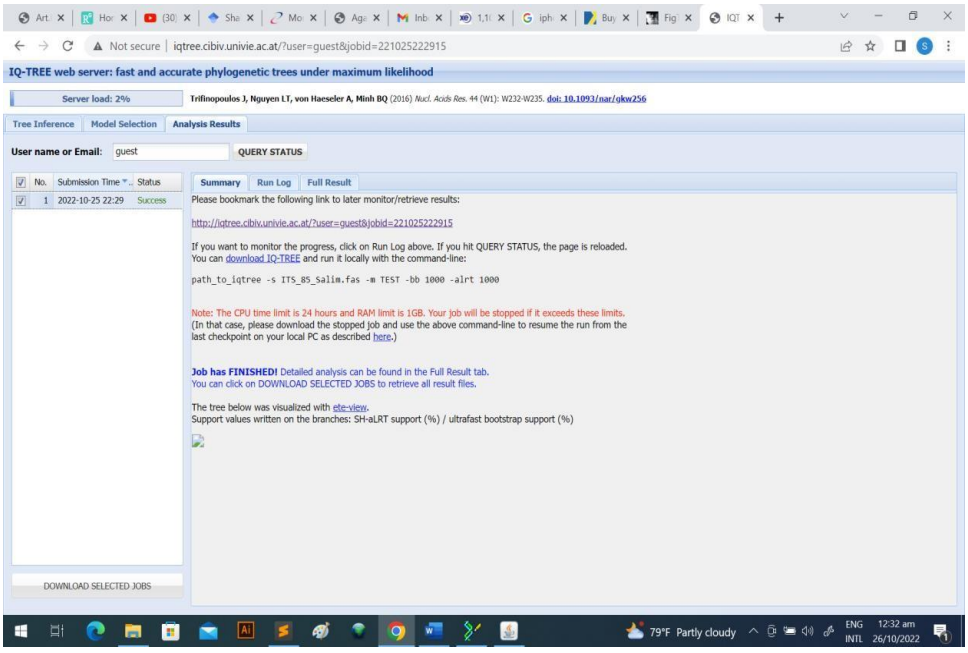
1. open the website http://iqtree.cibiv.univie.ac.at/



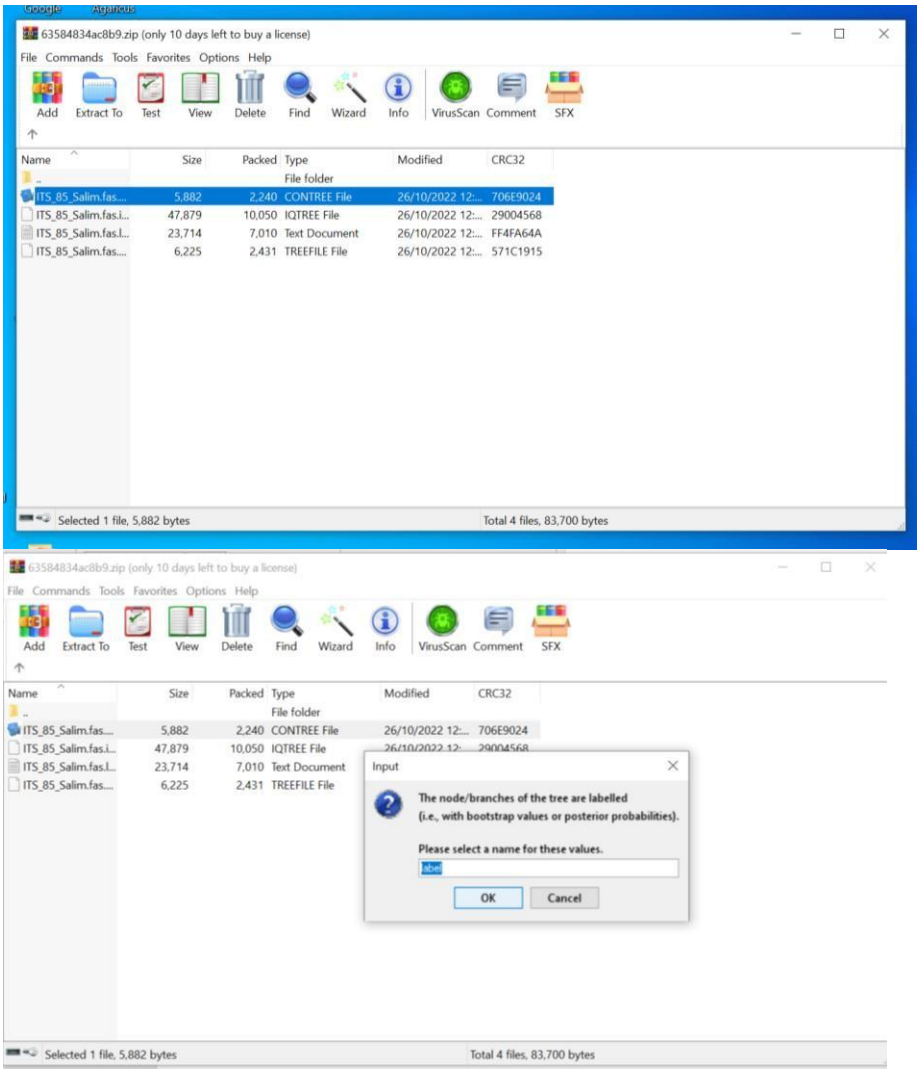
2. Click on the Brows button to upload the FASTA File and scroll down and click the submit button



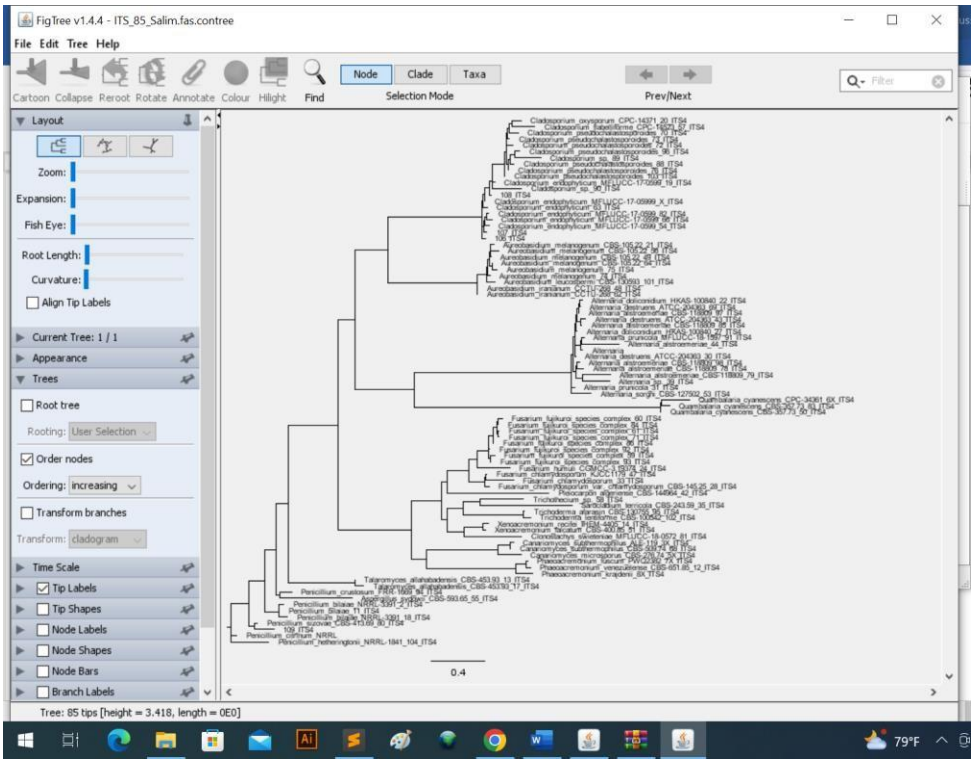
3. A new window will open where you can see the STATUS which will be shows running, you can refresh the website, after sometimes (a minute or so) status will be changes to SUCCESS



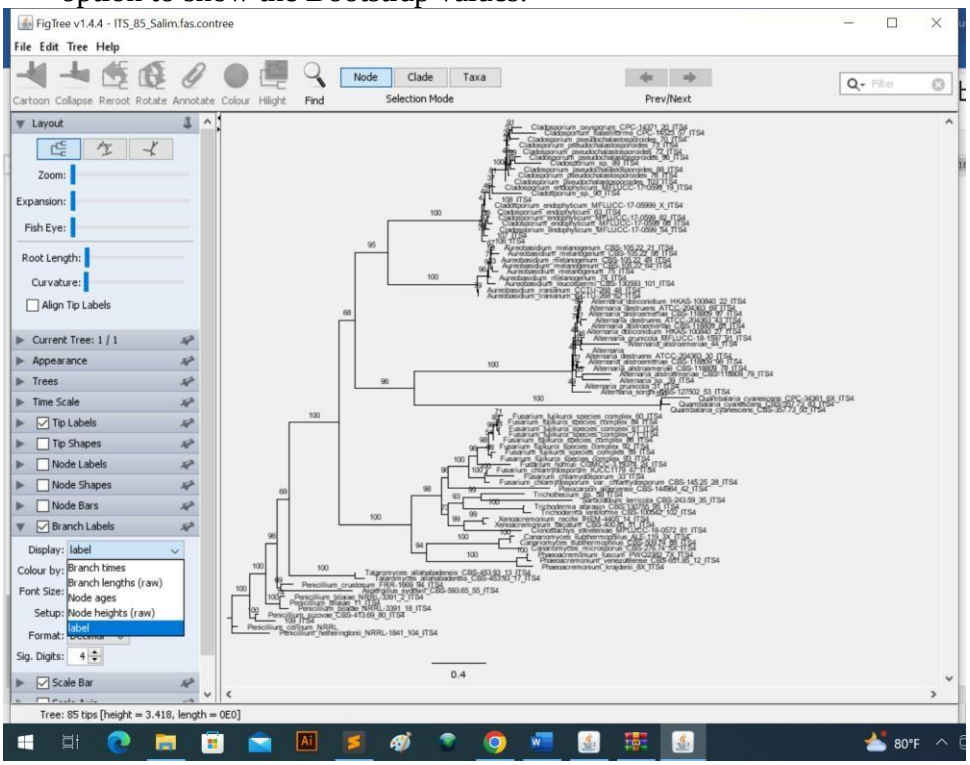
4. Click on the download success jobs, and open the COUNTREE file in FigTree



5. Click OK and the tree will be open in FigTree



6. On the left side of the FigTree window, there are different options, Tip Labels (manage font size of the taxa), Branch Labels (shows the bootstrap values). Select Branch Labels and select Labels in Display option to show the Bootstrap values.



7. Click on File at top left corner of the window to save the tree file in different output format, e.g. PDF

III. RAxML phylogeny using Cipres Science Gateway (https://www.phylo.org/portal2/)

(this is most common method of ML analysis, I will make the RAxML tutorial soon) IV. PHyML phylogeny (http://www.atgc-montpellier.fr/phyml/)

Annex 6

Colony Diameter of *Talaromyces* spp. with different media (Average colony dimeter per plate and Total average colony diameter for all replicates)

	Isolate C11 a Colony Diameter (cm)									
	Replicate	25°C dark 7 days	Average / plate	Total Average /media	37°C dark 7 days	Average / plate	Total Average/ media	37°C dark 7 days +30°C dark 7 days	Average/ plate	Total Average / media
CYA	1	Slow growth rate			Slow growth rate			1.8/1.7/2	1.83	1.533
	2	Slow growth rate			Slow growth rate			2/2.1/1.8	1.97	
	3	Slow growth rate			Slow growth rate			0.8/1/0.6	0.8	
YESA	1	1.5/1/1.8	1.43	1.80	No Data			No Data		
	2	2.4/2.2/2	2.2		No Data			No Data		
	3	1.3/2/2/	1.76		No Data			No Data		
CDA	1	1.3/1.5/1.5	1.43	1.48	No Data			No Data		
	2	1.4/1.5/1.5	1.46		No Data			No Data		
	3	2/1.3/1.4	1.56		No Data			No Data		
MEA	1	2/2.1/1	1.7	1.78	1.5/2/1.2	No Data	1.77	No Data		
	2	2.2 /2.4/1.4	2		1.7/1.6/1.8	No Data		No Data		
	3	1.8/1.8/1.35	1.65		2.3/2/1.9	No Data		No Data		
OA	1	1.6/1.5/1.5	1.53	1.70	No Data			No Data		
	2	1.7/2.5/2.2	2.13		No Data			No Data		
	3	1.3/1.4/1.6	1.43		No Data			No Data		
CMA	1	1.4/1.9/1.5	1.6	1.24	No Data			No Data		
	2	1.4/1.5/1.1	1.33		No Data			No Data		
	3	1/0.6/0.8	0.8		No Data			No Data		

	Isolate C11 b Colony Diameter (cm)									
	Replicate	25°C dark 7 days	Average / plate	Total Average /media	37°C dark 7 days	Average / plate	Total Average/ media	37°C dark 7 days +30°C dark 7 days	Average/ plate	Total Average / media
CYA	1	Slow growth rate			Slow growth rate			2/2/1.8	1.93	1.78
	2	Slow growth rate			Slow growth rate			1.5/1.6/1.7	1.6	
	3	Slow growth rate			Slow growth rate			1.8/1.6/2	1.8	
YESA	1	2.2/1.8/2	2	2.13	No Data			No Data		
	2	2/2.5/1.8	2.1		No Data			No Data		
	3	2.2/2.4/2.3	2.3		No Data			No Data		
CDA	1	1.4/1.3/1	1.23	0.99	No Data			No Data		
	2	0.8/0.6/1	0.8		No Data			No Data		
	3	0.9/1.3/0.6	0.93		No Data			No Data		
MEA	1	2.1/2/2/	2.03	1.88	1.6/2.4/1.8	1.93	1.56	No Data		
	2	1.5/1.5/2	1.66		1.2/1/0.9	1.03		No Data		
	3	2.1/1.5/2.3	1.96		1.5/1.7/2	1.73		No Data		
OA	1	2/2/2.3	2.1	1.92	No Data			No Data		
	2	1.5/1.7/2	1.73		No Data			No Data		
	3	1.8/2/2	1.93		No Data			No Data		
CMA	1	1.5/1.2/1.2	1.3	1.33	No Data			No Data		
	2	1.4/1.4/1.6	1.46		No Data			No Data		
	3	1.4/1.5/0.8	1.23		No Data			No Data		

	Isolate C12b Colony Diameter (cm)									
	Replicate	25°C dark 7 days	Average / plate	Total Average /media	37°C dark 7 days	Average / plate	Total Average/ media	37°C dark 7 days +30°C dark 7 days	Average/ plate	Total Average / media
CYA	1	Slow growth rate			Slow growth rate			2.6/2/2.4	2.33	2.3
	2	Slow growth rate			Slow growth rate			2/3/2.8	2.27	
	3	Slow growth rate			Slow growth rate			No data		
YESA	1	2.2/2.2/2	2.13	1.93	No Data			No Data		
	2	1.8/2.5/1.7	2		No Data			No Data		
	3	2/1.7/1.3	1.66		No Data			No Data		
CDA	1	1.3/0.8/1.3	1.13	0.91	No Data			No Data		
	2	0.6/1/0.8	0.8		No Data			No Data		
	3	0.8/0.7/0.9	0.8		No Data			No Data		
MEA	1	2.2/2.5/1.3	2	1.89	1.8/1.4/1.3	1.5	1.49	No Data		
	2	2/1.5/1.4	1.63		1.5/2.3/1.3	1.7		No Data		
	3	2.1/2/2	2.03		1/1.2/1.6	1.26		No Data		
OA	1	1.8/2/2	1.93	1.93	No Data			No Data		
	2	1.8/1.5/2	1.76		No Data			No Data		
	3	2.3/2/2	2.1		No Data			No Data		
CMA	1	1.5/1.1/0.8	1.13	1.20	No Data			No Data		
	2	1/1/1.0	1		No Data			No Data		
	3	1.7/1.4/1.3	1.46		No Data			No Data		

Annex 7

Electrolyte leakage (mV) and pH measurement for *Ceratocystis radicicola and F.solani* after application of *Talaromyces* spp. culture filtrate CF at 0, 2 and 24 hours.

Talaromyces X *C. radicicola*						
	0 hr		2hr		24hr	
Replicate	pH	mV	pH	mV	pH	mV
1	4.01	170.86	4.95	117.14	5.02	113.14
2	4.01	170.86	4.96	116.57	5.16	105.14
3	4.01	170.86	4.98	115.43	5.08	109.71
Control	4.01	170.86	4.01	170.86	4.01	170.86
Talaromyces	4.01	170.86	4.01	170.86	4.01	170.86
CF (avg)	4.01	170.86	4.01	170.86	4.01	170.86
Talaromyces X *F. solani*						
	0 hr		2hr		24hr	
Replicate	pH	mV	pH	mV	pH	mV
1	4.01	170.86	4.01	170.86	4.06	168
2	4.01	170.86	4.01	170.86	4.22	158.86
3	4.01	170.86	4.01	170.86	4.14	163.43
Control	4.01	170.86	4.01	170.86	4.01	170.86
Talaromyces	4.01	170.86	4.01	170.86	4.01	170.86
CF	4.01	170.86	4.01	170.86	4.01	170.86

Electrolyte leakage (mV) and pH measurement for *C. radicicola and F.solani* after application of *Aspergillus terreus* culture filtrate CF at 0, 1 and 24 hours

A. terreus X *C. radicicola*						
	0 hr		1hr		24hr	
Replicate	pH	mV	pH	mV	pH	mV
1	4.33	146.86	4.33	150.29	4.34	152
2	4.28	155.43	4.34	152	4.32	153.14
3	4.22	158.86	4.38	149.71	4.35	151.43
Control CF	4.20	160	4.20	160	4.17	161.71
A.terrus	4.19	160.57	4.21	158.86	4.17	161.71
	4.19	160.57	4.21	158.86	4.18	161.14
A. terreus X *F. solani*						
	0 hr	1hr	24hr			
Replicate	pH	mV	pH	mV	pH	mV
1	4.35	151.43	4.30	154.29	4.30	168
2	4.43	146.86	4.46	145.14	4.52	158.86
3	4.29	154.86	4.41	148	4.45	163.43
Control CF	4.20	160	4.20	160	4.17	161.71
A.terrus	4.19	160.57	4.21	158.86	4.17	161.71
	4.19	160.57	4.21	158.86	4.18	161.14


تم بحمد الله